ON THE HEME SENSING SYSTEM OF GRAM-POSITIVE BACTERIAL PATHOGENS

By

Devin L. Stauff

Dissertation

Submitted to the Faculty of the

Graduate School of Vanderbilt University

in partial fulfillment of the requirements

for the degree of

DOCTOR OF PHILOSOPHY

in

Microbiology and Immunology

May, 2009

Nashville, Tennessee

Approved:

Dana Borden Lacy

Richard N. Armstrong

Dean W. Ballard

Timothy L. Cover

Doug S. Kernodle

David W. Wright

Eric P. Skaar

To my wife, Amy

pone me ut signaculum super cor tuum

ut signaculum super brachium tuum

quia fortis est ut mors dilectio

dura sicut inferus aemulatio

lampades eius lampades ignis atque flammarum

ACKNOWLEDGMENTS

First and foremost, I would like to acknowledge and gratefully thank my mentor, Eric Skaar. You have been all that a student can hope for from a mentor. Over the past few years, I've benefited immensely in my scientific apprenticeship from your energy and your relentless hard work on my behalf. Moreover, knowing that you care about the people in your lab, that you are committed to my fulfillment and that of my family, has been by itself a great motivation for me.

I also am indebted to the friends I've made in the Skaar lab, past and present. I first thank Victor Torres for the immense amount of input and advice he has generously provided me throughout my graduate education. Those who know Victor know that he is indefatigably hard-working, a source of insightful and constructive criticism, and above all a wonderful and caring friend. Furthermore, Victor himself contributed directly to the work herein (especially studies of HrtAB function and virulence properties of *S. aureus* Δ*hrtA*). I have acknowledged his contributions and those of other direct contributors mentioned here in the figure legends where appropriate (VJT, Victor Torres). I thank fellow graduate students (Michelle Reniere, Gleb Pishchany [GP, who also contributed directly to the work presented here], Indriati Hood), postdocs/fellows (Brian Corbin, Jeff Mason, Ahmed Attia), undergraduates (Susan Dickey, Rose Joyce [RJ]), and research assistants (Olusegun "Sheg" Aranmolate [OA, by far the most uplifting and jubilant member of the Skaar lab, who contributed immensely and invaluably to all work searching for small molecule activators of HssRS] Keith Adams, Amanda McCoy, Danielle Bagaley [DB, another direct contributor], Melissa Crowder).

I thank the many collaborators that have directly contributed to the work presented here. David Friedman (DBF) and Corbin Whitwell (CW) from the Vanderbilt University Department of Biochemistry contributed immensely to the work described in

Chapter II, performed all mass spectrometry presented herein, and taught me a number of invaluable facts about and/or tricks related to work with proteins and mass spectrometry. Paul Dunman and his laboratory (Kelsi Anderson and Lisa Kuechenmeister) also contributed greatly, performing or assisting us with all microarray experiments.

I also must thank my rather large committee (Borden Lacy, Richard Armstrong, Dean Ballard, Timothy Cover, Doug Kernodle, David Wright, and Eric Skaar). Thank you for the time you've spent guiding my lines of investigation and providing much-needed advice over the last year. I also sincerely thank the Chairman of the Department of Microbiology and Immunology, Jacek Hawiger, for his care for and hard work on behalf of the students of the Department in general, and myself in particular, and for his helpful comments during my Departmental Research in Progress talks.

I acknowledge the extraordinary support provided by the Department of Microbiology and Immunology staff. Specifically, I thank Jean Tidwell and Helen Chomicki for all of the assistance they provided to me during the scheduling of my Defense. I also thank Mark Hughes and Matt Bruckse for all their assistance surrounding meetings I attended during my stay in the Department. I was supported by the Immunobiology of Blood and Vascular Systems training grant, NIAID, NIH Grant T32 HL069765. My work was supported by United States Public Health Service Grants 5 U54 AI057157-06 (SERCEB), AI69233 and AI073843-01A2 from the NIAID, National Institutes of Health.

Above all, I thank my family for supporting me throughout my days as a graduate student. I thank my wife, Amy, for her endless patience and all the sacrifices that she has made for me and for our family. You remain a faithful companion and a true friend. I also thank my children, Isaiah Russell and Owen Ezra. You are what I look forward to at the end of every day.

TABLE OF CONTENTS

LIST OF TABLES

LIST OF FIGURES

LIST OF ABBREVIATIONS

2D-DIGE	two-dimensional difference gel electrophoresis
ABC	ATP-binding cassette (ABC transporter)
BHI	brain-heart infusion broth
DIP	2,2'-dipyridyl
IPTG	isopropyl-β-D-thiogalactopyranoside
IVIS	*in vivo* imaging system
LB	Luria broth
MRSA	methicillin-resistant *Staphylococcus aureus*
MS	mass spectrometry
PCR	polymerase chain reaction
PCR-SOE	PCR-sequence overlap extension
TB	terrific broth
TCA	trichloroacetic acid
TF	transferrin
TSA	tryptic soy agar
TSB	tryptic soy broth
TCS	two-component system

CHAPTER I

INTRODUCTION

Bacterial pathogens: a scourge to human health

From the dawn of recorded history, human beings have had an intimate association with a wide range of bacterial pathogens. Ancient accounts contain detailed descriptions of and instructions for the treatment of lepers and those exhibiting signs of skin and soft tissue infections (1, 2):

> Or if there be any flesh, in the skin whereof there is a hot burning, and the quick flesh that burneth have a white bright spot, somewhat reddish, or white; then the priest shall look upon it: and, behold, if the hair in the bright spot be turned white, and it be in sight deeper than the skin; it is a leprosy broken out of the burning: wherefore the priest shall pronounce him unclean: it is the plague of leprosy (3).

In 430 BC, war with Sparta precipitated an unprecedented influx of refugees into Athens, leading to an outbreak of plague (likely caused by a bacterial pathogen of the genus *Rickettsia*). This was one contributing factor to the downfall of the great Greek State (4). In 125 AD, an anthrax outbreak killed tens of thousands of Romans, one of many plagues to affect the Roman Empire (4). Numerous plague outbreaks (at least in part attributable to *Yersinia* subspecies) devastated what later became Europe throughout the following two millennia, killing the great Emperor and Stoic philosopher Marcus Aurelius in 166 AD, literally decimating Europe in 1104-10 AD, and killing a third of Europeans from 1345-51 AD (4).

Following the advent of modernity, a devastating blow was struck to the march of the prokaryotic contagion when, in 1927, Scottish bacteriologist G. Alexander Fleming

serendipitously discovered a contaminating mold that inhibited the growth of *Staphylococcus aureus* on agar plates (14). This mold was found to produce a highly effective antibacterial agent, later named penicillin (14). Following the development of penicillin into an effective drug, penicillin was quickly implemented in the treatment of Allied soldiers wounded in the line of combat in the second World War (4). Penicillin quickly became mass produced, yet its discovery and production merely foreshadowed the implementation of a wide range of antibacterial agents that many thought would close the book on infectious disease.

In spite of much optimism surrounding the discovery of safe, effective antibacterial pharmacologic agents, it quickly became apparent that the infamous reputation of bacterial pathogens as a scourge to human health would not remain in question for long. In the early 1960s, strains of *Staphylococcus aureus* resistant to the β-lactam antibiotic methicillin were first isolated; these strains, known as methicillin-resistant *S. aureus* (MRSA) quickly became prevalent in hospital settings as the cause of invasive infections (51, 67). Though drug resistance was initially confined to clinical settings, the spread of MRSA merely foreshadowed the emergence of community-acquired infections caused by multiple drug resistant bacterial pathogens (59, 93). By the beginning of the 21st century, it has become apparent that the rate of discovery of new antibacterial agents is in many cases easily rivaled by the rate of acquisition of resistance mechanisms on the part of the targeted pathogens. Because of resistance in pathogens targeted by antibacterial agents as well as other limitations to antibiotic therapy, it is now clear that bacterial infections are not a phenomenon of the distant past, conquered by the ingenuity of man.

Staphylococcus aureus antibiotic resistance and pathogenesis

The quintessential example of a bacterial pathogen that continues to match the pace of drug discovery with drug resistance mechanisms is the Gram-positive human pathogen *Staphylococcus aureus*. The first bacterial pathogen found to have acquired penicillin resistance mechanisms was *S. aureus* (92). Currently, staphylococcal strains that are resistant to most commonly available antibiotics are prevalent (71, 103). Furthermore, strains have emerged that are resistant to one of the few remaining antibiotics that inhibits the growth of MRSA strains, namely vancomycin (167).

S. aureus is a commensal of the skin and anterior nares, colonizing approximately 25% of humans (178). In this context, *S. aureus* is relatively harmless; however, serious diseases can occur when *S. aureus* breaches host epithelial barriers. Following invasion of the host, *S. aureus* is capable of infecting virtually any tissue of the human body, leading to diseases including skin and soft tissue infection, endocarditis, pneumonia, and osteomyelitis. In addition, *S. aureus* toxins are capable of inducing several severe intoxications including toxic shock syndrome and other sepses that can rapidly lead to death. The inherent capacity of *S. aureus* to cause severe infections is compounded by widespread antibiotic resistance on the part of this species. For these reasons, *S. aureus* can be regarded as one of the most significant threats to human health worldwide (71).

Host defenses against *S. aureus*: the role of iron

Any bacterial pathogen that invades host tissues must overcome or circumvent mechanisms of innate and adaptive immunity. One strategy utilized by the mammalian innate immune system to prevent bacterial proliferation is known as nutritional immunity. Nutritional immunity refers to the host-mediated sequestration of nutrients essential for the growth or fitness of a pathogen (19). Metal ions are an example of a class of

nutrients that is maintained within host tissues at concentrations too low to support the growth of most bacteria (30, 38). Specifically, mammalian tissues contain very low concentrations of bio-available iron, a nutrient required by almost all bacterial pathogens (30). Free iron is maintained at low levels through host iron-binding proteins (including transferrin and lactoferrin) and through maintenance of physiologic pH, in which iron is sparingly soluble (30, 40).

S. aureus is unable to proliferate in normal, physiologic iron concentrations typical of mammalian tissues, and iron therefore has an influence on staphylococcal virulence (65). This is because numerous biochemical processes of prokaryotes (including DNA synthesis, avoidance of reactive oxygen species, and aerobic respiration) critically depend on iron (30, 85). Consequently, growth in low iron is a stressful state for *S. aureus* as well as other bacteria that require iron, and thus elaborate iron acquisition systems are expressed under conditions of iron deprivation (40).

The canonical strategy for iron acquisition employed by bacteria involves the secretion of iron-chelating small molecules known as siderophores. Siderophores bind free iron ions with remarkably high affinities, removing iron atoms from bacterial surroundings. Siderophore-iron complexes then bind siderophore receptors on the bacterial surface; from here, chelated iron is imported into the bacterial cytoplasm for release and incorporation into iron-binding proteins. *S. aureus* is able to produce siderophores upon iron starvation; furthermore, siderophore-mediated iron acquisition may influence the outcome of the host-pathogen interaction (41).

Although *S. aureus* is capable of acquiring iron though siderophore-mediated uptake pathways, which are also capable of targeting transferrin and lactoferrin, free iron and transferrin/lactoferrin-bound iron represents only a fraction of the total iron within the human body. Most host iron is found in the form of the heme molecule (44). This is due

to the fact that heme is the cofactor of hemoglobin and myoglobin, the oxygen-shuttling and oxygen-storing proteins of human blood and muscle tissue, respectively. Although abundant in the human body, iron in the form of heme is subject to more layers of sequestration than any other iron source: in heme, iron cannot by itself dissociate from the porphyrin ring. Furthermore, heme is stably associated with hemoglobin or myoglobin, and hemoglobin and myoglobin are both sequestered within mammalian cells.

Heme capture by *S. aureus*

S. aureus is able to access heme-iron from the host through the concerted actions of a set of cell wall-anchored, membrane-bound, and cytoplasmic proteins known collectively as the iron-regulated surface determinants (Isd). An emerging paradigm is beginning to explain how the *S. aureus* Isd machinery functions to acquire heme during the association between staphylococci and host tissues rich in heme (112, 134, 151). *S. aureus* is capable of lysing erythrocytes by secreting pore-forming toxins including alpha toxin, causing the release of hemoglobin (18, 87). Upon hemoglobin release, cell wall-anchored IsdB and IsdH are able to bind hemoglobin (168), allowing IsdA (which is also anchored to the cell wall) to remove heme from hemoglobin (187). IsdA passes heme to IsdC, an Isd protein embedded deeply within the cell wall (187). Heme is then passed from IsdC to the membrane-localized transport system IsdDEF, which shuttles heme into the cytoplasm. Here, the heme monooxygenases IsdG and IsdI degrade heme to release free iron, which is capable of satisfying the nutrient needs of *S. aureus* (133, 149). The importance of heme acquisition to pathogenesis is highlighted by virulence defects observed in strains inactivated for members of the Isd family (133, 150, 168). It appears that *S. aureus* can circumvent nutritional immunity by tapping into an abundant source of host iron inaccessible to all but a few microorganisms.

Furthermore, it is possible that interfering with the ability of *S. aureus* to acquire iron from heme during infection represents a potentially fruitful avenue for the development of effective anti-staphylococcal therapeutic agents.

Control of iron acquisition by the ferric uptake regulator

Through siderophore-mediated iron uptake and Isd-dependent heme capture, *S. aureus* is able to satisfy its nutrient iron requirement. However, it is possible that *S. aureus* may encounter environments (such as the skin) that are not iron-restricted; in such environments, it would be metabolically wasteful to elaborate systems devoted to iron acquisition. Furthermore, if iron acquisition systems are expressed in conditions of iron abundance, too much iron may be imported into bacterial cells. This would be disadvantageous to a bacterium, as iron by itself is toxic to biological systems at high concentrations due to its capacity to catalyze the formation of reactive oxygen species (7). Therefore, most bacteria tightly regulate the expression of iron acquisition systems, only allowing their expression under conditions of iron starvation (40).

In most bacteria (including *S. aureus*) genes encoding iron acquisition systems are tightly controlled by a repressor called the *f*erric *u*ptake *r*egulator (Fur). A ferroprotein, Fur chelates iron under conditions of iron abundance and binds to well-defined sequences upstream of genes for iron acquisition systems, repressing their expression (52). Under conditions of iron paucity, Fur dissociates from iron, decreasing its affinity for operator regions within the genes it represses, and allowing expression of iron uptake machinery (52). This prevents the cellular stress that would accompany iron overload, and avoids the equally stressful condition of iron starvation through the regulated expression of iron uptake systems. In *S. aureus*, the importance of Fur to the fitness of *S. aureus* is highlighted by virulence defects observed for *S. aureus* lacking a functional *fur* gene (80, 183). Furthermore, Fur-mediated control of gene expression

overlaps with heme acquisition in *S. aureus*, as the Isd system is directly regulated by Fur (112, 133).

Metalloporphyrin toxicity: the heme paradox

Just as iron levels must be tightly regulated within a bacterial cell to avoid the twin problems of iron overload and iron starvation, heme homeostasis must be monitored closely to achieve a balance between paucity and toxicity. This is because heme is a powerful catalyst that can induce the formation of reactive oxygen species (53). Furthermore, heme is lipophilic, and tends to insert into membranes, interrupting membrane fluidity and leading to lipid damage. For this reason, biological systems that synthesize heme or associate with high amounts of exogenous heme must take steps to avoid heme toxicity (9, 134, 188). Furthermore, a few bacterial pathogens express systems that are required for the avoidance of heme toxicity (20, 21, 127). Such systems are likely to be of particular importance for bacteria that acquire heme exogenously from their host during infection (162). More specifically, *S. aureus* and other pathogens that acquire heme have been shown to be rapidly killed by heme-like molecules brought into the bacterial cell due to the elaboration of heme uptake systems (20, 21, 162).

Although mechanisms of iron uptake by siderophores and heme uptake by the Isd system have been extensively investigated in *S. aureus*, comparatively little attention has been devoted to understanding the mechanisms of iron homeostasis on a global level in this bacterium. Genes under Fur-mediated control in *S. aureus* can be predicted *in silico*; however, no studies have addressed the response of *S. aureus* to either iron starvation or deregulation of the Fur regulon. Furthermore, no studies have addressed the "other side of the coin" of heme capture by *S. aureus*: the problem of heme toxicity.

Herein, we report the cytoplasmic Fur, iron and heme regulons of *S. aureus*. These studies reveal an iron starvation-induced metabolic shift leading to the release of iron from host iron-sequestering proteins. This may represent a strategy for increasing the amount of iron available to staphylococci. In addition, we demonstrate a mechanism whereby *S. aureus* and related Gram-positive pathogens avoid heme toxicity by sensing heme through a novel two-component system, which controls expression of a transport system responsible for heme detoxification. This scheme of heme detoxification is conserved in *Bacillus anthracis*, the causative agent of anthrax and an evolutionary relative of *S. aureus*. We show that perturbation of heme detoxification alters staphylococcal virulence, and that heme is sensed during the association of *B. anthracis* with vertebrate tissues. Last, we begin to elucidate the mechanism of activation of a novel heme-sensing histidine kinase utilizing a small molecule library screen. These findings reveal that Gram-positive organisms exquisitely balance heme acquisition with the avoidance of heme toxicity by sensing and responding to heme.

CHAPTER II

EFFECTS OF IRON STARVATION AND DISRUPTION OF THE FERRIC UPTAKE REGULATOR ON THE *STAPHYLOCOCCUS AUREUS* CYTOPLASMIC PROTEOME

Introduction

Low iron is a stressful condition to *Staphylococcus aureus*. Accordingly, *S. aureus* requires iron to successfully colonize the host (30). However, elevated levels of iron or iron-containing compounds actively acquired by *S. aureus* (such as heme) are also toxic (162). To ensure efficient uptake and metabolism of host iron sources, *S. aureus* uses Fur to control expression of a variety of genes in response to the level of available iron (183). Importantly, a global analysis of Fur and iron-regulated proteins in this important human pathogen has not been reported. In addition, although numerous studies have focused on the mechanism of heme capture by *S. aureus*, no studies have addressed the response of *S. aureus* to growth in levels of heme that are stressful to staphylococci.

Based on the demonstrated role for iron, Fur, and heme in staphylococcal pathogenesis, we sought to evaluate changes in global protein regulation in response to alterations in bacterial iron status (chelation of iron, disruption of *fur*, and addition of heme) using two-dimensional difference gel electrophoresis (2D-DIGE). 2D-DIGE enables quantitative differential display analysis with statistical confidence, and is based on 2D gel separations whereby thousands of protein features can be resolved based on isoelectric point and by apparent molecular mass. It uses spectrally resolvable fluorescent dyes to pre-label samples that are then multiplexed onto the same gel, allowing for direct quantification of each resolved protein feature between the three dye channels without analytical (gel-to-gel) variation. Multiple samples from a complex experiment can be analyzed across several 2D-DIGE gels through the inclusion of an

internal standard comprised of every sample present in the experiment, which is included in each multiplexed gel (5, 60, 63). Within each gel, quantitative measurements are made for each resolved protein feature relative to the cognate signal from the internal standard, which is then used to normalize the intra-gel ratios between gels in a coordinated experiment. Thus, 2D-DIGE enables multiple conditions with repetition to be quantitatively analyzed with statistical confidence. Proteins of interest are then identified using mass spectrometry (MS) and database interrogation. Algorithms such as unsupervised hierarchical clustering can be applied to 2D-DIGE datasets to enable analysis of global expression patterns. Combining multivariable 2D-DIGE/MS with multivariate statistical analyses clusters cellular protein responses across distinct environmental conditions based on total expression profiles. These technologies can be combined to identify expression changes in coordinated biochemical pathways. Such data can be used to predict phenotypic changes predicted to be the outcome of shifting from one metabolic pathway to another.

Here, we utilize 2D-DIGE to reveal the subset of cytoplasmic proteins regulated by iron, Fur, and heme in *S. aureus*. We show that *S. aureus* alters the abundance of a set of proteins upon conditions of heme exposure, possibly leading to heme detoxification. We also show that *S. aureus* undergoes a dramatically different response to growth in low iron or to disruption of Fur, both of which perturb staphylococcal iron homeostasis. This latter response alters the abundance of key enzymes involved in staphylococcal central metabolism, leading to the production of acidic metabolic end products. The commensurate decrease in pH accompanying iron status perturbation and release of acidic metabolic products triggers the release of iron from the host iron-sequestering protein transferrin. This represents a potential strategy for iron acquisition whereby *S. aureus* senses low iron, alters the pH of its surroundings, and acquires iron released from host proteins. Results obtained from this study identify a novel strategy

used by *S. aureus* to increase iron availability, and begin to define the iron-, Fur-, and heme-dependent regulons of *S. aureus*.

Methods

Bacterial strains and growth conditions - *S. aureus* clinical isolate Newman was used in all experiments. Prior to preparation of cytoplasmic extracts, bacteria were grown in tryptic soy broth (TSB) for 15 hours at 37^{o} C with shaking at 180 RPM. Iron starvation was achieved by addition of 1 mM 2,2' dipyridyl (DIP) to the growth cultures prior to inoculation. Heme treatment was achieved by addition of 10 μM heme to the growth cultures prior to inoculation. All cultures were harvested at comparable optical densities during early stationary phase. Newman Δ*fur* was created through transduction of the previously created Δ*fur* allele from RN4220 (113) to strain Newman with the transducing phage Φ-85 as previously described (149).

Preparation of cytoplasmic fractions - Cytoplasmic extracts were prepared upon completion of 15 hours of bacterial growth. Cells were pelleted by centrifugation at 6000 g for 15 minutes. Pellets were re-suspended in TSM (100 mM Tris, pH 7.0, 500 mM sucrose, 100 mM $MgCl_2$) and incubated at 37^{o} for 45 minutes in the presence of 1 mg of lysostaphin. Following cell wall digestion, protoplasts were isolated by centrifugation at 13,700 g and washed once and re-suspended in 20 ml of buffer (50 mM Tris, pH 7.5, 150 mM NaCl, 100 μM phenylmethylsulfonylfluoride). To lyse the protoplasts, samples were subjected to two rounds of French Press mediated lysis at 20,000 psi. Insoluble material was removed by ultracentrifugation at 100,000 g for 45 minutes. The collected supernatant, representing the cytoplasmic fraction, was used in subsequent analyses.

2D-DIGE/MS - Quadruplicate samples from the four conditions were independently prepared as described below. For each sample, 0.25 mg protein was separately precipitated with methanol and chloroform (179) and re-suspended in 30 μl lysis buffer (7M urea, 2M thiourea, 4% CHAPS, 30 mM Tris, 5 mM magnesium acetate). The NHS-ester dyes Cy2/3/5 were used for the minimal labeling protocol using an internal standard (5, 60, 63). Briefly, one-third of each sample (10 μl, 83 μg) was removed and

combined into a single tube to comprise the pooled-sample internal standard (1330 µg total). The remaining two-thirds of each individual sample (20 µl, 167 µg) was individually labeled with 200 pmol of either Cy3 or Cy5, while the pooled-sample was labeled *en masse* with 1600 pmol Cy2. The samples were quenched with 10 mM lysine (2 µl for each 200 pmol) for 10 minutes on ice, followed by the addition of equal volume 2x rehydration buffer (7M urea, 2M thiourea, 4% CHAPS, 4 mg/ml DTT). Pairs of Cy3/Cy5-labeled samples were mixed with an equal aliquot of the Cy2-labeled internal standard according to the schema in Figure 1B. Tripartite samples were brought up to 450 µl with 1x rehydration buffer (same as 2x buffer but with 2 mg/ml DTT) and passively rehydrated into 24 cm 4-7 immobilized pH gradient (IPG) strips for 24 hrs (total of 500 µg per gel).

All 2D-DIGE-associated instrumentation was manufactured by GE Healthcare/Amersham Biosciences (Piscataway, New Jersey). First-dimensional separations were performed on a manifold-equipped IPGphor first-dimension isoelectric focusing unit, and second-dimensional 12% SDS-PAGE was carried out using hand-cast gels that had one plate pre-silanized (to ensure subsequent accurate robotic protein excision) using an Ettan DALT 12 unit, both according to the manufacturer's protocols. Cy2/3/5-specific 16-bit data files were acquired at 100 µm resolution separately by dye-specific excitation and emission wavelengths using a Typhoon 9400 Variable Mode Imager, and the gels were stained for total protein content with SyproRuby (Molecular Probes/Invitrogen) per the manufacturer's instructions.

The DeCyder v6.5 suite of software tools (Amersham Biosciences/GE Healthcare) was used for 2D-DIGE analysis. The normalized volume ratio of each individual protein spot-feature from a Cy3- or Cy5-labeled sample was directly quantified relative to the Cy2-signal from the pooled-sample internal standard corresponding to the same spot-feature. This is performed for all resolved features in a single gel where no

gel-to-gel variation exists between the three co-resolved signals. The individual signals from the Cy2-standard were then used to normalize and compare Cy3:Cy2 and Cy5:Cy2 abundance ratios across the 8-gel set, enabling statistical confidence to be associated with each change in abundance or charge-altering post-translational modification using Student's t-test and ANOVA analyses. Hierarchical clustering was performed using the DeCyder Extended Data Analysis (EDA) module.

Proteins of interest were robotically excised, digested into peptides in-gel with modified porcine trypsin protease (Trypsin Gold, Promega) and peptides applied to a stainless steel target using an integrated Spot Handling Workstation per the manufacturer's recommendations. Matrix assisted laser desorption/ionization, time-of-flight mass spectrometry (MALDI-TOF MS) and data-dependant TOF/TOF tandem MS/MS was performed on a Voyager 4700 (Applied Biosystems, Framingham MA). The resulting peptide mass maps and the associated fragmentation spectra were collectively used to interrogate *S. aureus* Mu50 sequences to generate statistically significant candidate identifications using GPS Explorer software (Applied Biosystems) running the MASCOT search algorithm (www.matrixscience.com). Searches were performed allowing for complete carbamidomethylation of cysteine, partial oxidation of methionine residues, and 1 missed cleavage. Molecular Weight Search (MOWSE) scores, number of matched ions, number of matching ions with independent MS/MS matches, percent protein sequence coverage, and correlation of gel region with predicted MW and pI were collectively considered for each protein identification.

Measuring medium/culture pH - Bacteria were grown in 10 ml of TSB in a 50 ml flask for 15 hours at 37^{o}C with 180 rpm shaking. Iron was chelated from the media by adding DIP to a final concentration of 1 mM. After 15 hours the cultures were centrifuged and the supernatants were collected. All pH values were measured using a S20 SevenEasy pH meter (Mettler Toledo).

Iron release from transferrin - Measuring the release of iron from transferrin (TF) was performed as previously described (72). Iron-bound TF exhibits an absorption peak at 470 nm. As iron dissociates from TF the intensity of the peak at 470 nm absorption decreases. Absorption at 470 nm was measured every 30 seconds for 15 minutes upon introduction of the samples. TF stock solutions of 400 μM were prepared by suspending human TF (Sigma) in distilled water. TF stock solutions were added at a final concentration of 40 μM to all samples. All absorption readings were measured using a Cary 100 UV-Vis spectrophotometer from Varian.

Results

2D-DIGE/MS analyses of the *S. aureus* cytoplasmic proteome upon alterations in iron status. To identify proteins that respond to alterations in iron availability or exposure to host iron sources, we performed differential expression analyses on *S. aureus* cultures grown under various conditions of iron exposure. Cytoplasmic proteins were prepared from *S. aureus* Δ*fur* grown under iron-replete conditions and from wild type grown under either iron-replete conditions, after iron starvation through treatment with DIP, or after exposure to heme. Protein extracts from each of the four conditions were independently isolated in quadruplicate to control for non-biological variation, and the resulting 16 extracts were simultaneously co-resolved across 8 2D-DIGE gels that were coordinated by a 16-mix pooled-sample internal standard as described in Methods (Figure1A).

2D-DIGE analysis combined with subsequent hierarchical clustering (Figure 1B) allowed for protein expression changes between these four conditions to be grouped into the following five classes: (I) proteins that are negatively regulated by iron and Fur (Table 1), (II) proteins that are positively regulated by iron and Fur (Table 2), (III) proteins that are regulated by iron independent of Fur (Table 3), (IV) proteins that are regulated by Fur independent of iron (Table 4), and (V) proteins that are regulated by heme independent of Fur or iron (Table 5). We identified 29 resolved protein features (representing 20 distinct proteins including isoforms) under iron-dependent negative regulation by Fur, 30 distinct features (25 proteins including isoforms) under iron-dependent positive Fur-mediated regulation, and 21 distinct proteins that respond exclusively to heme. This analysis revealed that exposure of *S. aureus* to heme results in a vastly different, and less severe, change in cellular protein expression as compared to altering the iron status of the bacterium (Figure 1B). Importantly, a novel, uncharacterized transport system with a potentially important role in staphylococcal

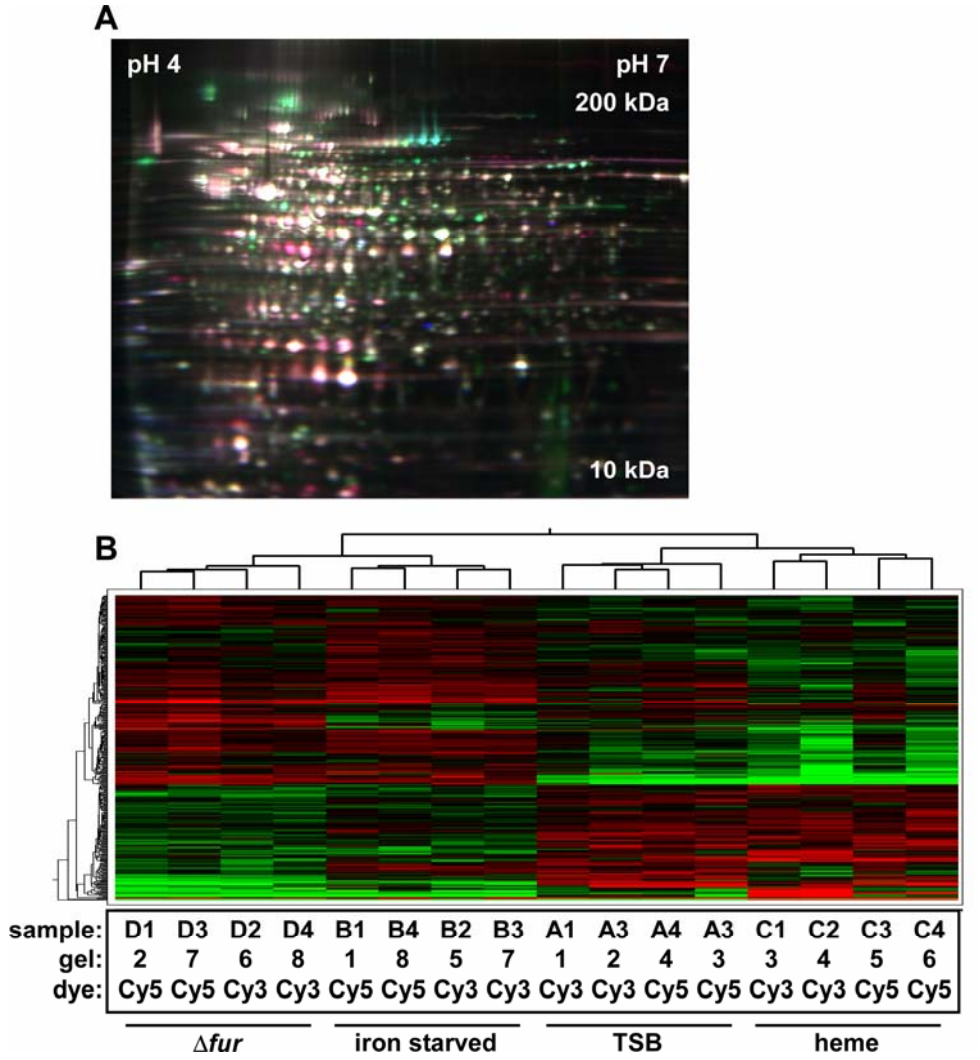

Figure 1. 2D-DIGE-based proteome analysis of *Staphylococcus aureus* following perturbation of iron status. ***A.*** False-colored representative gel from the 8-gel set containing three differentially labeled samples as described in Chapter II Methods. Cy2-labeled internal standard (*blue*), Cy3-labeled control #1 (*green*), and Cy5-labeled iron-starved #1 (*red*) are overlayed for illustrative purposes. ***B.*** Unsupervised hierarchical clustering of the 16 individual DIGE expression maps (groups, shown along top) and of individual proteins (shown on the left), with relative expression values for each protein displayed as a heat map using a relative scale ranging from -0.5 (green) to +0.5 (red). The gel number (1-8) and Cy3/5 dye labeling for each sample is listed below. Adapted from Friedman et al., 2006 (Ref. 61). Experiments were performed in collaboration with DBF and CW.

heme metabolism was dramatically increased in abundance under conditions of heme exposure. However, because iron- and Fur-dependent changes differ greatly from heme-dependent changes (Figure 1B), the remainder of this Chapter will address the affects of iron perturbation on the *S. aureus* proteome. Heme-dependent changes and the critical role of the heme-regulated transport system in staphylococcal heme metabolism will be discussed in the subsequent Chapters of this manuscript.

***S. aureus* proteins negatively regulated by iron and Fur.** Proteins that are up-regulated upon iron starvation or inactivation of *fur* (via release from repression) represent proteins negatively regulated by Fur in an iron-dependent manner, and hence comprise the canonical Fur regulon of the bacterium. We identified 29 distinct protein features comprising 20 unique cytoplasmic proteins that are up-regulated from 1.3-fold to over 14-fold in the absence of iron or Fur (Table 1). These results demonstrate a strong correlation between expression changes upon iron chelation *vs*. the absence of *fur*. As expected, iron acquisition systems previously shown to be iron-regulated *via* Fur are up-regulated under these conditions including proteins involved in siderophore synthesis (SbnE isoforms exhibiting over 3-fold increases in low iron or Δ*fur*,) (41) and transport (FhuA, over 8-fold increases) (145).

Five of 21 proteins that were negatively regulated by iron and Fur with mostly moderate changes in abundance (*ca*. 1.5-fold) are enzymes of the glycolytic pathway including fructose 1-P kinase (FruB), fructose bisphosphate aldolase (FbaA), triosephosphate isomerase (Tpi), glyceraldehyde 3-phosphate dehydrogenase (Gap), and transketolase (Tkt) (Table 1). This observation is consistent with a systemic up-regulation of glycolysis upon iron starvation, which would lead to a commensurate increase in pyruvate for subsequent use in either the TCA cycle, or as a substrate for fermentative metabolism.

TABLE 1
Proteins negatively regulated by Fur and iron

SAV locus[1]	gene name[2,3]	function[3]	fold regulation (-Fe)	*p* value[4]	fold regulation (*Δfur*)	*p* value[4]
0116	NA	cysteine synthetase	9.41	0.0012	9.98	0.00054
0116	NA	cysteine synthetase	3.00	0.00018	2.64	0.00056
0117	NA	ornithine cyclodeaminase	3.12	0.0038	3.83	0.00022
0117	NA	ornithine cyclodeaminase	14.13	0.0022	17.88	0.00086
0120	*sbnE*	siderophore synthesis	3.22	0.00044	4.13	0.00013
0120	*sbnE*	siderophore synthesis	4.47	0.0025	5.63	0.0011
0120	*sbnE*	siderophore synthesis	4.07	0.013	5.22	0.0067
0123	*sodM*	superoxide dismutase	1.57	0.033	2.13	0.0022
0123	*sodM*	superoxide dismutase	2.37	0.00032	2.07	0.0021
0255	*ispD*	2-C-methyl-D-erythritol-4 phosphate cytidyltransferase	1.73	0.0013	1.32	0.039
0513	*cysK*	O-acetylserine (thiol)-lyase	1.36	0.013	1.7	0.00095
0551	*hchA*	chaperone	1.99	0.00015	1.42	0.027
0647	*fhuA*	ferrichrome transport	8.19	0.0000012	8.34	0.0000016
0699	*fruB*	fructose 1-phosphate kinase	1.59	0.0097	1.43	0.031
0772	*gap*	glyceraldehyde 3-phosphate dehydrogenase	1.69	0.0054	2.27	0.0048
0772	*gap*	glyceraldehyde 3-phosphate dehydrogenase	1.53	0.014	1.66	0.0011
0772	*gap*	glyceraldehyde 3-phosphate dehydrogenase	1.51	0.036	1.44	0.022
0774	*tpi*	triosephosphatase isomerase	1.46	0.0068	1.52	0.0085
0968	NA	decarboxylase	1.57	0.0036	1.22	0.046
0984	NA	3-oxoacyl synthase	1.73	0.0038	1.3	0.021
1011	*fabI*	enoyl-[acyl carrier protein] reductase [NADH]	2.07	0.00046	1.42	0.026
1259	*frr*	ribosome recycling factor	1.49	0.00081	1.27	0.03
1342	*tkt*	transketolase	2.37	0.0000066	1.51	0.0013
1342	*tkt*	transketolase	2.59	0.000041	1.78	0.00078
1630	*aspS*	aspartyl-tRNA-synthetase	1.26	0.0034	1.31	0.015
2125	*fbaA*	fructose bisphosphate aldolase	1.53	0.00061	1.49	0.00016
2125	*fbaA*	fructose bisphospate aldolase	1.4	0.029	1.46	0.002
2125	*fbaA*	fructose bisphospate aldolase	5.19	0.00000098	5.93	0.000001
2125	*fbaA*	fructose bisphospate aldolase	3.66	0.0001	4.63	0.00005
2302	NA	D-octopine dehydrogenase	1.93	0.0028	1.33	0.042
2455	NA	endo 1,4 B-gluconase	1.94	0.0015	1.52	0.016

1. SAV number corresponds to position in the annotated *S. aureus* Mu50 genome.
2. Gene name corresponds to name listed in annotation of Mu50 genome. NA signifies no gene name listed.
3. Gene name and function were determined based on closest hit in a BLAST search with an e value of $< 10^{-10}$.
4. *p* values were calculated using Student's *t*-test.

***S. aureus* proteins positively regulated by iron and Fur.** Fur is traditionally considered a repressor of iron-regulated gene transcription. However, recent work has highlighted a role for Fur in the direct and/or indirect activation of a small subset of genes in *Helicobacter pylori* (97), *Vibrio cholerae* (115), *Neisseria meningitidis* (45), *Escherichia coli* (49, 111), and *Bacillus subtilis* (13). We identified 30 distinct protein features representing 25 unique proteins that were positively regulated by Fur in an iron-dependent manner as measured by decreased expression in the absence of Fur or upon iron starvation (Table 2).

Numerous regulatory factors were activated by Fur in an iron-dependent manner including RbsU. RbsU, down-regulated in Δ*fur* and iron-replete conditions, controls the expression of a variety of virulence genes and regulatory systems. Based on this pleotropy, small changes in RbsU expression may have profound effects on cellular metabolism. In particular, RbsU activates acetate catabolism; therefore, the Fur-dependent activation of RbsU is consistent with a down-regulation of the TCA cycle upon iron starvation or *fur* inactivation (154).

The value of iron to *S. aureus* is underscored by the Fur-mediated, iron-dependent activation of four separate proteins that are predicted to contain iron-sulfur clusters. Three of these proteins are the TCA cycle enzymes succinate dehydrogenase (SdhA), aconitate hydratase (CitB), and fumarate hydratase (CitG). A fourth TCA cycle enzyme, phosphoenolpyruvate carboxykinase (PckA), which coverts oxaloacetate to phosphoenolpyruvate during gluconeogenesis, was also down-regulated upon inactivation of *fur* or iron depletion. Two additional proteins associated with central metabolism and demonstrating this expression pattern are D-fructose-6-phosphate amidotransferase (GlmS) and glyceraldehyde 3-P dehydrogenase (GapB). GlmS converts fructose 6-P to glucosamine-6-P, and hence depletes substrate for phosphofructokinase in effect antagonizing glycolysis. GapB is a second glyceraldehyde

3-P dehydrogenase of *S. aureus* and based on its function in *Bacillus subtilis,* is predicted to possess GAPDH activity involved in gluconeogenesis (55). These results support the Fur-mediated up-regulation of glycolysis upon iron starvation, and suggest a commensurate systemic and regulated inhibition of the TCA cycle. Together, these findings support a model whereby in iron-starved *S. aureus,* excess pyruvate produced as a result of an up-regulation of the glycolytic pathway is shuttled into fermentative pathways as opposed to the TCA cycle. These results suggest that excess pyruvate produced as a result of increased glycolysis is converted to predicted products of staphylococcal fermentative metabolism.

***S. aureus* proteins regulated by iron independent of Fur.** In addition to Fur, *S. aureus* possesses the metal-dependent regulators Zur (102), PerR (79), and MntR (81), raising the possibility that factors other than Fur respond to changes in cellular iron content. We identified 22 unique proteins with changes in abundance upon iron starvation, but without detectable changes in response to inactivation of *fur* (Table 3). Three of these proteins are associated with cellular respiration including formate dehydrogenase (Fdh), Hpr Kinase (HprK), and NAD synthase (NadE). Thus, we have identified a significant pool of proteins that respond to iron independent of Fur, raising the possibility that an additional transcriptional regulator exists in *S. aureus* to monitor intracellular iron status. It should be pointed out that DIP binds divalent cations other than iron; this may in part explain for some of the expression changes that were observed.

TABLE 2
Proteins positively regulated by Fur and iron

SAV locus[1]	gene name[2,3]	function[3]	fold regulation (-Fe)	*p* value[4]	fold regulation (*Δfur*)	*p* value[4]
0018	*vicR*	response regulator	-1.39	0.03	-1.53	0.01
0226	*pflB*	formate acetyltransferase	-7.04	0.0022	-3.58	0.012
0226	*pflB*	formate acetyltransferase	-7.3	0.0043	-4.55	0.0094
0226	*pflB*	formate acetyltransferase	-6.67	0.0033	-4.46	0.0054
0519	NA	pyridoxine biosynthesis	-2.23	0.0078	-2.86	0.0025
0520	NA	SNO glutamine amidotransferase	-1.67	0.0083	-1.65	0.0044
0548	*tuf*	translation elongation TU	-4.07	0.036	-4.17	0.035
0605	*adh1*	alcohol dehydrogenase	-1.73	0.0046	-1.38	0.037
0605	*adh1*	alcohol dehydrogenase	-1.63	0.0074	-1.42	0.05
0938	NA	pyridine nucleotide disulfide oxidoreductase	-2.61	0.00003	-4.25	0.0000053
1139	*pheT*	Phe-tRNA synthetase	-1.19	0.043	-1.42	0.0039
1148	*sdhA*	succinate dehydrogenase	-3.8	0.00053	-6.42	0.0015
1178	NA	hypothetical protein	-1.61	0.00073	-1.4	0.041
1255	*codY*	transcriptional repressor	-1.49	0.0052	-2.35	0.0031
1350	*citB*	aconitate hydratase	-4.15	0.00013	-5.82	0.0000087
1492	*srrA*	staphylococcal respiratory regulator	-1.87	0.0011	-1.99	0.000012
1512	NA	tripeptidase	-1.22	0.0022	-1.54	0.0014
1687	*gapB*	glyceraldehyde 3-phosphate dehydrognenase 2	-6.1	0.000088	-14.48	0.00052
1729	*tyrS*	tyrosyl tRNA synthetase	-1.24	0.017	-1.26	0.033
1791	*pckA*	phosphoenolypyruvate carboxykinase	-1.77	0.037	-1.75	0.0023
1851	*citG*	fumarate hydratase	-2.47	0.00025	-3.78	0.000011
2067	*rbsU*	sigma B	-1.48	0.016	-2.12	0.0004
2136	*pdp*	pyridine-nucleoside phosphorylase	-1.77	0.0028	-2.34	0.00034
2154	*glmS*	D-fructose-6-phosphate amidotransferase	-1.53	0.024	-1.82	0.006
2154	*glmS*	D-fructose-6-phosphate amidotransferase	-1.42	0.007	-4.66	0.000011
2154	*glmS*	D-fructose-6-phosphate aminotransferase	-1.8	0.0038	-2.29	0.00063
2165	NA	MRP-like ATP-binding protein	-1.59	0.0052	-1.62	0.0026
2204	NA	hypothetical	-1.39	0.0044	-1.62	0.0001
2285	NA	butyryl-CoA dehydrogenase	-2.15	0.000057	-2.56	0.00002
2305	NA	glycerate dehydrogenase	-1.67	0.0073	-2.02	0.00067

1. SAV number corresponds to position in the annotated *S. aureus* Mu50 genome.
2. Gene name corresponds to name listed in annotation of Mu50 genome. NA signifies no gene name listed.
3. Gene name and function were determined based on closest hit in a BLAST search with an e value of $< 10^{-10}$.
4. *p* values were calculated using Student's *t*-test.

TABLE 3
Proteins regulated by iron independent of Fur

SAV locus[1]	gene name[2,3]	function[3]	fold regulation (-Fe)	*p* value[4]	fold regulation (*Δfur*)	*p* value[4]
0177	*fdh*	formate dehydrogenase	22.32	0.015	1.77	0.24
0226	*pflB*	formate acetyltransferase	2.03	0.045	-2.66	0.035
0380	*ahpF*	alkyl hydroxyperoxide reductase subunit F	-1.7	0.0036	2.05	0.00023
0381	*ahpC*	alkyl hycroxyperxide reductase subunit C	-1.73	0.00096	2.24	0.0000025
0551	*hchA*	chaperone	1.93	0.00099	1.32	0.06
0566	NA	hypothetical	1.55	0.0046	-1.09	0.5
0587	NA	hypothetical	1.27	0.0062	1.07	0.4
0760	*hprK*	Hpr kinase	1.14	0.05	-1.22	0.061
0844	NA	aminotransferase NifS homologue	1.22	0.05	1.11	0.15
0968	NA	decarboxylase	1.4	0.037	1.00	0.87
1088	NA	potassium transport	1.36	0.032	1.22	0.066
1533	NA	lipoate protein ligase	1.66	0.00071	1.05	0.62
1557	NA	endonuclease IV	1.53	0.0056	-1.08	0.61
1683	*thrS*	threonyl-tRNA synthetase	-2.61	0.0023	-1.61	0.069
1854	NA	hypothetical protein	1.28	0.05	-1.15	0.35
1912	*nadE*	NAD synthetase	-1.39	0.022	-1.2	0.19
1929	NA	hypothetical	1.26	0.019	1.0	0.93
2030	*groES*	GroES	1.75	0.0061	1.38	0.054
2124	*murZ*	UDP-N-acetylglucosamine carboxylvinyl transferase	1.56	0.0072	1.16	0.059
2229	*adk*	adenylate kinase	1.55	0.0013	1.26	0.069
2455	NA	endo 1,4 B-gluconase	1.33	0.036	-1.71	0.00022
2699	NA	N-hyroxyarylamine O-acetyltransferase	2.06	0.0016	1.14	0.47

1. SAV number corresponds to position in the annotated *S. aureus* Mu50 genome.
2. Gene name corresponds to name listed in annotation of Mu50 genome. NA signifies no gene name listed.
3. Gene name and function were determined based on closest hit in a BLAST search with an e value of $< 10^{-10}$.
4. *p* values were calculated using Student's *t*-test.

***S. aureus* proteins regulated by Fur independent of iron.** We also identified 24 unique proteins that changed expression upon inactivation of *fur* without any significant changes in iron availability status (Table 4). One such protein, GapR, is an activator of Gap expression and is up-regulated in the absence of Fur. This moderate increase in expression may contribute to the increase in Gap expression observed upon inactivation of *fur* (Table 1). Inactivation of *fur* leads to down-regulation of PckA and isocitrate dehydrogenase (CitC), consistent with our previous observation of Fur-mediated activation of the TCA cycle. Furthermore, acetoin reductase (ButA) is down-regulated by inactivation of *fur* implying a commensurate decrease in the production of 2,3-butanediol upon iron starvation. Taken together with results described above, this suggests that the major metabolic end-products of carbohydrate metabolism produced by iron-starved *S. aureus* are pyruvate, lactate and/or formate (Figure 2).

TABLE 4
Proteins regulated by Fur independent of iron

SAV locus[1]	gene name[2,3]	function[3]	fold regulation (-Fe)	*p* value[4]	fold regulation (*Δfur*)	*p* value[4]
0126	*butA*	acetoin reductase	-1.27	0.15	-1.55	0.024
0133	*sodM*	superoxide dismutase	-1.46	0.062	-2.33	0.0024
0139	*drm*	posphopentomutase	1.2	0.096	-1.47	0.0087
0226	*pflB*	formate acetyltransferase	1.75	0.065	-3.5	0.0053
0226	*pflB*	formate acetyltransferase	2.03	0.045	-2.66	0.035
0380	*ahpF*	alkyl hydroperoxide reductase subunit F	-1.7	0.0036	2.05	0.00023
0381	*ahpC*	alkyl hydroperoxide reductase subunit C	-1.73	0.00096	2.24	0.0000025
0491	NA	TatD related DNase	1.01	0.83	-1.76	0.033
0513	*cysK*	O-acetylserine (thiol)-lyase	1.3	0.093	1.42	0.025
0531	NA	tRNA/mRNA methyltransferase	1.13	0.26	1.51	0.00085
0771	*gapR*	glycolytic operon regulator	1.16	0.44	1.24	0.05
0842	NA	ABC transporter	-1.22	0.061	-1.4	0.0067
0957	*rocD*	ornithine-oxo-acid transaminase	-1.51	0.067	-3.14	0.0012
0958	*gudB*	NAD-glutamate dehydrogenase	-1.04	0.7	-1.42	0.013
0975	*clpB*	ClpB chaperone	1.29	0.09	2.06	0.0055
1339	*lexA*	transcriptional repressor	1.02	0.84	-1.59	0.026
1425	NA	hypothetical	-1.1	0.3	-1.55	0.000079
1694	*citC*	isocitrate dehydrogenase	-1.12	0.7	-2.8	0.018
1694	*citC*	isocitrate dehydrogenase	-1.4	0.12	-3.85	0.000048
1737	NA	3-deoxy-7-phosphheptulonate synthase	-1.02	0.76	-1.53	0.0053
1791	*pckA*	phosphoenolypyruvate carboxykinase	-1.35	0.12	-2.85	0.00039
2416	*pgm*	phosphoglycerate mutase	-1.06	0.96	-1.94	0.24
2416	*pgm*	phosphoglycerate mutase	1.27	0.093	-2.02	0.000075
2455	NA	endo 1,4 B-gluconase	1.33	0.036	-1.71	0.00022

1. SAV number corresponds to position in the annotated *S. aureus* Mu50 genome.
2. Gene name corresponds to name listed in annotation of Mu50 genome. NA signifies no gene name listed.
3. Gene name and function were determined based on closest hit in a BLAST search with an e value of $< 10^{-10}$.
4. *p* values were calculated using Student's *t*-test.

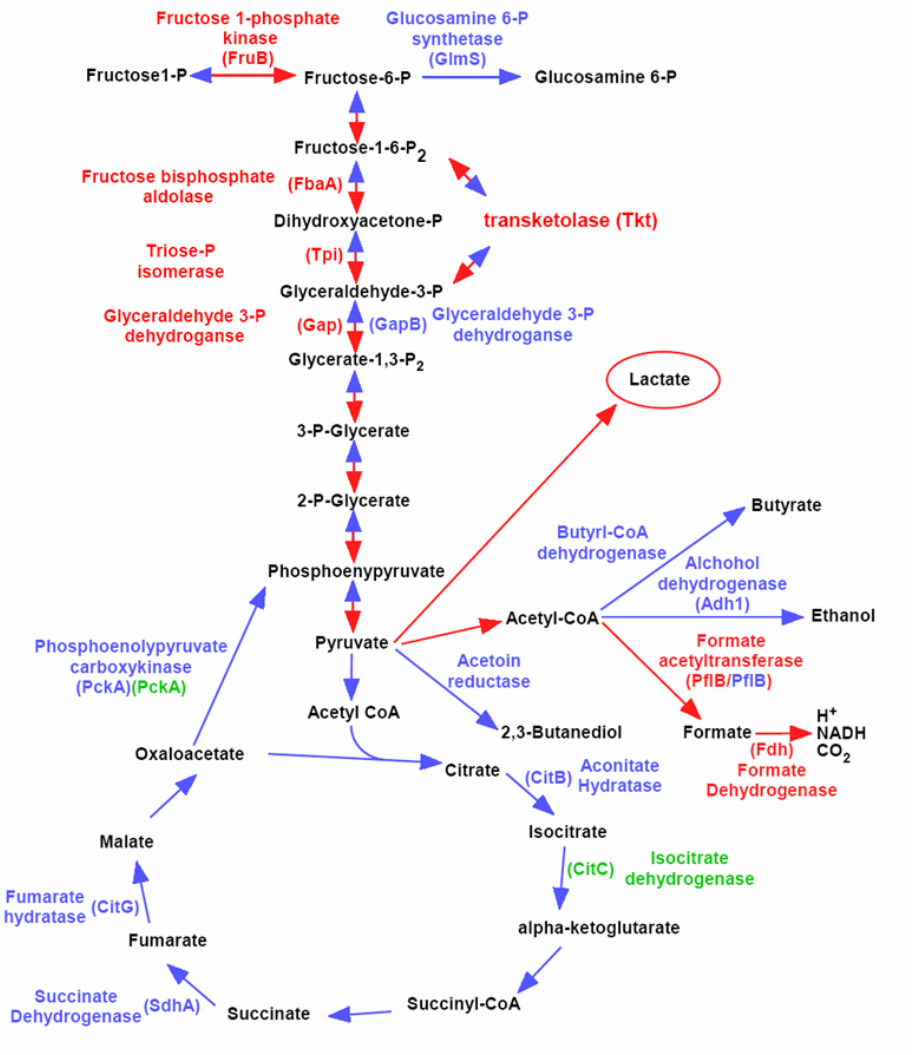

Figure 2. *S. aureus* shifts to fermentative pathways upon iron starvation. A subset of the predicted central metabolic reactions of *S. aureus* is shown. Proteins shown in red are up-regulated in the absence of iron or upon inactivation of *fur*. Proteins shown in blue are down-regulated in the absence of iron or upon inactivation of *fur*. Proteins shown in green are down-regulated in the absence of Fur independent of iron status. The red arrows predict the direction of reactions upon iron starvation, while the blue arrows predict reactions that are inhibited upon iron starvation. The red circle signifies one of the primary predicted metabolic end-products of iron-starved *S. aureus,* lactate. Adapted from Friedman et al., 2006 (Ref. 61).

Iron-starved *S. aureus* produce acidic metabolic end products leading to a decrease in local pH. Iron starved *S. aureus* are known to restrict oxidative capacity by oxidizing glucose with the accumulation of lactate, pyruvate, acetate, formate, and acetoin (165). The coordinated expression changes of the staphylococcal central metabolic pathways identified using 2D-DIGE/MS are summarized in Figure 2, and provide a mechanistic explanation for this observation. Our results suggest that iron starved *S. aureus* undergo a Fur-mediated redirection of central metabolic pathways leading to the production of acidic end products of fermentative metabolism.

To test this hypothesis, we measured the pH of medium from iron-replete, iron-deplete, and Δ*fur* cultures. These experiments demonstrated a drop in culture pH from 7.2 to 5.2 upon either iron starvation or *fur* inactivation. In contrast, iron-replete cultures increased pH to close to 8.0 in identical incubation conditions (Figure 3A). From these data, we conclude that *S. aureus* elaborates a Fur-mediated redirection of central metabolism under iron starvation leading to decreased pH of culture medium.

TF-iron represents a viable iron source to invading bacterial pathogens. In order to utilize TF-iron as a nutrient iron source, the iron must be dissociated from TF and transported into the bacterium. Free Fe^{3+} is more readily utilized as a nutrient source than TF bound iron, and iron is known to dissociate from TF upon changes in pH (126). We hypothesized that the Fur-dependent production of acidic metabolic end products by iron starved *S. aureus* facilitates the release of iron from TF through a decrease in local pH. To test this hypothesis, we measured iron release from TF mediated by spent medium from either iron-replete, iron-deplete, or Δ*fur* staphylococcal cultures. We found that medium from iron starved or Δ*fur* staphylococcal cultures significantly increased the rate of iron release from TF (Figure 3B). Taken together, these results demonstrate that the Fur-mediated production of acidic metabolic end products by iron starved *S. aureus* facilitates the release of iron from host iron-sequestering proteins.

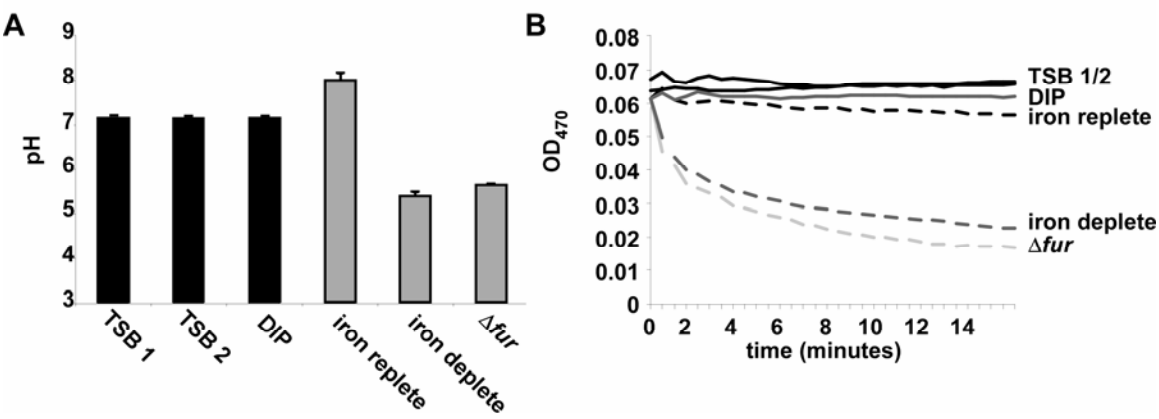

Figure 3. *S. aureus* produces acidic metabolic end products upon iron starvation or inactivation of *fur*. *A.* pH of media or culture supernatants following perturbation of iron status. pH readings were taken on triplicate flasks containing fresh TSB (TSB 1), TSB incubated at 37°C for 15 hours (TSB 2), TSB + 1 mM 2,2' dipyridyl (DIP) incubated at 37 °C for 15 hours, and 15-hour culture supernatants from *S. aureus* wild type grown in TSB (iron replete), TSB + 1mM DIP (iron deplete), and from *S. aureus* Δ*fur* grown in TSB (Δ*fur*). Averages are plotted; error bars correspond to one standard deviation from the mean. ***B.*** Iron release from transferrin in media (solid lines) or culture supernatants (dashed lines) following perturbation of iron status. Transferrin (40 μM) was added to media or culture supernatants described in *A*. Iron release was measured as a decrease in absorbance at 470 nm. Adapted from Friedman et al., 2006 (Ref. 61). Experiments were performed in collaboration with GP.

Discussion

We have analyzed changes in the cytoplasmic protein profile of *S. aureus* upon genetic (Δ*fur*) and biochemical (iron chelation, heme treatment) alterations in iron exposure. Using 2D-DIGE, we simultaneously surveyed the *S. aureus* proteome in response to these manipulations. Overall, 156 protein features of interest, specifying approximately 120 individual proteins (including changes in post-translational modification) were identified by mass spectrometry and placed into functional groups defining Fur-dependent and independent iron regulation as well as heme-responsive proteins. These studies begin to reveal regulatory mechanisms used by *S. aureus* to alleviate stress induced by changes in iron availability (genetic or biochemical) and exposure to elevated levels of host iron sources (heme).

Analysis of our 2D-DIGE data reveals a number of regulation patterns of potential importance to *S. aureus* physiology and pathogenesis. One noteworthy class of proteins identified in our study was down-regulated upon inactivation of *fur* in an iron-dependent manner, suggesting Fur-mediated positive regulation of these proteins. In Gram-negative bacteria, investigations have identified the small regulatory RNA (sRNA) Ryhb as being responsible for Fur-dependent protein activation in *E. coli* (110), *Pseudomonas aeruginosa* (180), *V. cholera* (42) and *Shigella flexneri* (125). The targets of Ryhb include some of the same genes identified in our study as being positively regulated by Fur, including the TCA cycle enzymes aconitase (*acnA*), fumarase (*fumA*), and succinate dehydrogenase (*sdhCDAB*) (111). This observation suggests that a similar mechanism of iron-dependent gene regulation is occurring in *S. aureus*; however, we were unable to identify any potential homologues to Ryhb in any Gram-positive bacterial genome using traditional BLAST analyses (data not shown). *S. aureus* has been reported to express at least 12 sRNAs with predicted roles in translational regulation through message stability (128). It is likely that an as-yet-undiscovered sRNA-mediated

regulatory system exists in *S. aureus* responsible for iron homeostasis through targeted mRNA degradation.

Our data indicate that iron starvation leads to the reversible inactivation (or down-regulation) of TCA cycle enzymes including aconitase, the down-regulation of which has been implicated as a survival response to oxidative stress induced during the host-pathogen interaction (152). In *S. aureus,* down-regulation of the TCA cycle through aconitase inactivation prevents maximal expression of the virulence factors lipase, staphylococcal enterotoxin C, and α and β hemolytic toxins, and therefore alters the interaction between *S. aureus* and the host (152). Additionally, inactivation of the TCA cycle or growth in iron deplete conditions leads to a decrease in production of formylated delta-toxin, a potent neutrophil attractant (153). Combined, these two factors have led to the suggestion that down-regulation of the TCA cycle may protect against host immune-mediated recognition of infecting *S. aureus* (153).

We propose a model whereby upon iron starvation, such as would be encountered inside the host, *S. aureus* up-regulates glycolysis through the release of Fur-mediated repression of glycolytic enzymes. Based on the simultaneous fur-mediated down-regulation of TCA cycle enzymes, pyruvate does not enter the TCA cycle, but instead is acted on by fermentative pathways. This is likely to funnel excess pyruvate primarily into acidic fermentative end products (Figure 2).

This shift to production of acidic metabolic end products is predicted to decrease the pH in the microenvironment surrounding infecting staphylococci, a hypothesis supported by the observation that the pH of the spent medium from iron starved or Δ*fur* staphylococci is significantly more acidic than that of spent medium from iron-replete cultures (Figure 3A). This overproduction of acidic end products and subsequent decrease in pH dissociates iron from host iron-sequestering molecules (Figure 3B). An

increase in local iron concentrations would significantly relieve the iron stress placed on the bacterium, and provide a growth advantage to invading staphylococci.

Our hypothesis is supported by published results showing that the uptake of iron (presented as $^{59}FeSO_4$) by *S. aureus* is twice as great at pH of 4.7 as it is at a pH of 7.4 (37) If correct, this model implies that under conditions of iron starvation, *S. aureus* alters its central metabolic pathways through Fur-mediated regulation of enzyme activity resulting in an increase in the local concentration of bio-available host iron. These fundamental changes in metabolic function potentially provide a survival advantage to *S. aureus* by preventing maximal activation of the immune system while bacteria struggle to alter their microenvironment to access host iron.

CHAPTER III

ROLE OF THE *STAPHYLOCOCCUS AUREUS* HEME-REGULATED TRANSPORTER IN OVERCOMING HEME TOXICITY

Introduction

Staphylococcus aureus is profoundly affected by conditions of iron scarcity. This is highlighted by the alterations seen in the cytoplasmic protein profile of staphylococci biochemically or generically perturbed in iron status (Chapter II). To combat iron starvation during infection, *S. aureus* utilizes heme as a source of scarce nutrient iron (112, 134, 150, 151). Furthermore, heme is the preferred source of iron for staphylococci (150). In *S. aureus* and related pathogens (including *Listeria monocytogenes* and *Bacillus anthracis*), heme acquisition is mediated by the iron-regulated surface determinants (Isd), which bind host hemoglobin released from lysed erythrocytes and remove, import, and degrade heme to release free iron. Isd family members are required for *S. aureus* to maintain full virulence, highlighting the importance of heme-iron acquisition to the outcome of the host-pathogen interaction (133, 168).

Although heme is a valuable source of nutrient iron for invading staphylococci, heme acquisition is a dangerous process. Heme, hemin (the oxidized, Fe^{3+} form of heme), and non-iron metalloporphyrins are toxic to biological systems due to their tendency to catalyze the formation of reactive oxygen species, which damage proteins, nucleic acids, and membrane lipids (53, 134, 161, 162, 169). It is therefore possible that during the invasion of host tissues rich in heme, *S. aureus* may encounter heme toxicity.

We have previously elucidated a subset of cytoplasmic proteins that undergo alterations in abundance upon exposure of staphylococci to heme (Chapter II). Although

a number of these proteins have known or probable roles in staphylococcal stress responses, a single protein feature corresponding to an uncharacterized transport system exhibited a dramatic change in abundance under conditions of heme exposure. This observation formed the basis of our foray into the response of *S. aureus* to heme, as we sought to (I) determine whether *S. aureus* succumbs to heme toxicity and (II) characterize the response of *S. aureus* to growth in high levels of heme.

Here, we show that while *S. aureus* is sensitive to heme toxicity, staphylococci are able to sense and adapt to exogenous heme by inducing the expression of a heme-detoxifying transport system, the *h*eme-*r*egulated *t*ransporter HrtAB. We show that HrtAB consists of a permease and ATPase component, the latter of which exhibits ATPase activity *in vitro* dependent on physicochemical conditions and conserved residues that are hallmarks of ABC transporter ATPases. Furthermore, HrtA catalytic activity is likely required for the resistance of *S. aureus* to heme toxicity. In the absence of HrtAB function, *S. aureus* exhibits perturbed virulence properties, pointing to a possible role for heme sensing in pathogenesis. These studies begin to shed light on a mechanism that allows *S. aureus* to avoid the lethal consequences of actively acquiring a toxic host molecule, and form the basis for the elucidation of a novel gene regulatory system conserved among Gram-positive bacteria (Chapters IV through VI).

Methods

Strains, mutants, and growth conditions - *S. aureus* strain Newman (50) and its derivatives were used in all experiments. For mutagenesis of *S. aureus*, a previously published protocol was followed (12). Briefly, sequences flanking *hrtA* were PCR amplified, assembled into pCR2.1 (Invitrogen) and recombined into pKOR1 (12). Inactivation of *hrtA* was achieved by allelic replacement with pKOR1Δ*hrtA* as described previously (12). TSB was used for the growth of *S. aureus*; for plasmid selection in *S. aureus*, chloramphenicol was used at a concentration of 10 μg/ml. Luria broth (LB, genetic manipulations) and terrific broth (TB, protein expression) were used for the growth of *Escherichia coli*; for plasmid selection in *E. coli*, ampicillin was used at a concentration of 100 μg/ml (138).

Genetic manipulations in S. aureus – All plasmids were first electroporated into the restriction deficient primary recipient RN4220 (124), after which they were electroporated into appropriate electrocompetent secondary recipients (139).

Complementation of S. aureus Δ*hrtA* - In the first PCR reaction, PCR-sequence overlap extension (PCR-SOE) primers were used to amplify the *hrtAB* promoter from *S. aureus* strain Newman genomic DNA. In the second PCR reaction, PCR-SOE primers were used to amplify the *hrtA* gene from Newman genomic DNA. The PCR products were purified (Qiagen gel extraction kit) and 1:300 dilutions of purified reaction 1 and reaction 2 PCR products were mixed and amplified using distal PCR primers. This yielded an amplicon in which the *hrtAB* promoter was fused to the *hrtA* gene. The *hrtAB* promoter-*hrtA* fusion was subcloned into pCR2.1 (Invitrogen). The insert was excised using restriction endonucleases EcoRI and BamHI and then ligated into pOS1 (143) cut with the same enzymes, generating p*hrtA*.

Growth curve assays and heme adaptation analysis – For adaptation assays, 15 hour cultures of *S. aureus* grown in the presence of 1 or 2 μM heme were diluted 1:75 into

150 µl of fresh medium containing 10 µM heme (Fluka BioChemika) in triplicate on a 96-well round-bottom cell culture plate. Cells were grown at 37 °C with shaking at 180 rpm and absorbance values were determined at the indicated times after inoculation. All spectrophotometry was performed using a Cary 50 MPR microplate reader coupled to a Cary 50 Bio UV-visible spectrophotometer (Varian, Inc.).

Purification of HrtA *and* HrtA *mutants* – The full-length *hrtA* open reading frame was inserted between the NdeI and BamHI sites of pET15b, creating pET15b.*hrtA* for the expression of an N-terminal hexahistidine-tagged HrtA. Pfu mutagenesis (176) was used to create expression constructs for the mutants HrtA:K45A, HrtA:R76A, HrtA:G145A, HrtA:G145T, and HrtA:E167Q. All mutants were verified by sequencing. For all protein expression, *E. coli* BL-21 (DE3) harboring each plasmid was subcultured 1:100 from 15 hour cultures into TB at 37 °C with shaking at 225 rpm until the 600 nm absorbance of the culture reached 0.4. Growth temperature was then switched to 16 °C for 1 hour and expression was induced by adding IPTG (0.25 mM). After an additional 20 hours of growth at 16 ˚C, bacteria were harvested and recombinant proteins were purified by nickel affinity chromatography using Ni-NTA Superflow (Qiagen) following the manufacturer's recommendations. Purified proteins were dialyzed against dialysis buffer (10 mM Tris, pH 7.5, 200 mM KCl, 0.5 mM EDTA, 1 mM DTT, 50% glycerol) overnight and stored at -20 °C. Protein concentration was determined by Bio-Rad Protein Assay (Bio-Rad). For removal of the N-terminal hexahistidine tag from HrtA, restriction grade Thrombin Protease (Novagen) was utilized according to the manufacturer's instructions and cleaved HrtA was stored at -20 °C.

ATPase activity assays – ATPase activities were determined using an Innova Biosciences colorimetric ATPase assay system according to the manufacturer's recommendations. Briefly, recombinant HrtA was diluted to a final concentration of 0.5 µM in 80 µl of 50 mM Tris (pH 7.5, or other pH as indicated), 2.5 mM $MgCl_2$ (or other

divalent cation if indicated), 0.5 mM ATP (or other concentration as indicated). All assays except the temperature-dependence assay were carried out at 20 °C for maximal ATPase activity. At 3, 10, and 20 minutes after the addition of ATP (or other time points as indicated), 20 µl of Innova Biosciences Gold Mix (1:100 dilution of Accelerator into P_iColorLock™ Gold) was added to the HrtA reaction mixture. Quenched reactions were incubated for 2 minutes, after which 10 µl of Stabilizer reagent was added. 650 nm absorbance readings were taken on a Cary 50 MPR microplate reader coupled to a Cary 50 Bio UV-visible spectrophotometer (Varian, Inc.).

Complementation constructs – A C-terminal c-*myc* tagged *hrtA* under the control of its native promoter was created by PCR amplifying *hrtA* from p*hrtA* using a 5' primer within the *hrtA* promoter and a 3' primer matching the 3' end of *hrtA* and including the coding sequence for the c-Myc epitope (EQKLISEEDL). Amplified DNA was inserted into the *E. coli*/*S. aureus* shuttle vector pOS1 (143), creating p*hrtA-myc*. The *hrtA-myc* K45A, R76A, G145A, G145T, and E167Q mutations were introduced as described above for the generation of *E. coli* HrtA mutant expression constructs, generating p*hrtA-myc*:K45A, p*hrtA-myc*:R76A, p*hrtA-myc*:G145A, p*hrtA-myc*:G145T, and p*hrtA-myc*:E167Q. Mutations were confirmed and secondary mutations were ruled out by sequencing. Expression of tagged HrtA and HrtA mutants in *S. aureus* was tested by preparing bacterial extracts and immunoblotting as follows. Fifteen ml cultures of bacteria grown in TSB + 5 µM heme for 15 hours were centrifuged and pellets were washed with wash buffer (50 mM Tris, pH 7.5, 150 mM NaCl). Bacteria were centrifuged again and re-suspended in TSM (100 mM Tris, pH 7.0, 500 mM sucrose, 10 mM $MgCl_2$) with 20 µg/ml lysostaphin, incubated at 37 °C for 30 minutes, and protoplasts were harvested by centrifugation. Protoplasts were re-suspended in 800 µl of lysis buffer (wash buffer containing 1 tablet complete EDTA-free protease inhibitor (Roche) per 10 ml) and were sonicated. Insoluble material was removed by centrifugation at 16000 x g for 20

minutes, and supernatant was analyzed. Thirty µg of supernatant material was subjected to SDS-PAGE, transferred to nitrocellulose, and blotted with sc-789 polyclonal rabbit anti-c-Myc primary (Santa Cruz Biotechnology, Santa Cruz, CA) and AlexaFluor-680-conjugated anti-rabbit secondary (Invitrogen) antibodies. Membranes were dried and scanned using an Odyssey Infrared Imaging System (LI-COR Biosciences, Lincoln, NE).

Results

***S. aureus* adapts to heme toxicity.** We first sought to test whether *S. aureus*, like other bacterial species, is sensitive to the toxicity of heme. We found that *S. aureus* inoculated into medium containing 10 μM heme fails to proliferate (Figure 4) due to a bactericidal activity that heme exerts on *S. aureus* cells. These data demonstrate that *S. aureus* succumbs to heme toxicity. During these experiments, we noticed that *S. aureus* is able to replicate in 10 μM heme at late time points following subculture (>12 hours), indicating that staphylococci are eventually able to overcome the toxicity of heme. We reasoned that *S. aureus* may be able to sense exogenous heme and adapt accordingly. We therefore tested whether *S. aureus* is able to adapt to heme toxicity by growing *S. aureus* in a low, sub-toxic heme concentration (2 μM), sub-culturing into 10 μM heme, and following *S. aureus* growth (Figure 4). We found that pre-exposure of *S. aureus* to 2 μM heme allows staphylococci to resist heme toxicity, an indication that staphylococci sense and respond to low levels of heme in a way that prepares bacterial cells for heme concentrations that would otherwise be lethal.

***S. aureus* expresses a potential heme detoxification system upon exposure to heme.** Adaptation to heme toxicity indicates that *S. aureus* may express a heme detoxification system in response to heme exposure. To identify potential heme-responsive proteins in *S. aureus*, we analyzed changes in the cytoplasmic proteome of *S. aureus* upon heme exposure by 2D-DIGE (experiment described in Chapter II). This experiment revealed a set of 21 proteins that undergo alterations in abundance upon heme exposure (Table 5). Importantly, not one of these proteins is altered upon iron starvation or inactivation of *fur*, an indication that perturbation of iron metabolism or availability induces a significantly different response than heme exposure (Figure 1B).

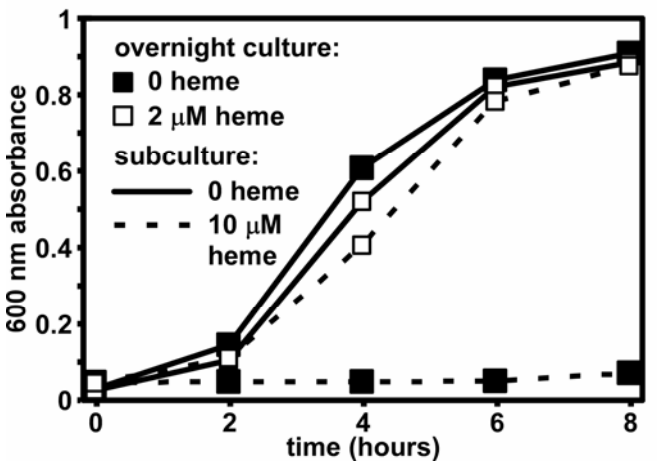

Figure 4. *S. aureus* adapts to heme toxicity. *S. aureus* wild type was grown overnight in medium without heme (solid squares) or medium containing 2 μM heme (empty squares). Overnight cultures were then subcultured into medium without heme (solid lines) or medium containing 10 μM heme (dashed lines). In all assays, 600 nm absorbance readings were taken on triplicate cultures at the indicated times after inoculation and averages +/- one standard deviation are shown (in most cases, error bars are too small to be seen).

TABLE 5

Proteins regulated by heme independent of iron and Fur

SAV locus[1]	gene name[2,3]	function[3]	fold regulation	*p* value[4]
0133	*sodM*	superoxide dismutase	-2.66	0.014
0211	*acpD*	acyl carrier protein phosphodiesterase	-1.51	0.0067
0390	*guaB*	inositol monophosphate dehydrogenase	-1.39	0.0024
0517	*lysS*	lysyl-tRNA synthetase	-1.72	0.0066
0519	*yaaD*	putative pyridoxal 5'-phosphate synthetase	3.78	0.000037
0550	*bioF*	7-keto-8-aminopelargonate synthase	-1.37	0.023
0551	*hchA*	hsp31 severe stress chaperone	-1.55	0.04
0706	*saeR*	response regulator	1.34	0.02
0844	*nifS*	pyridoxal phosphate-dependent aminotransferase	-1.14	0.027
0956	NA	putative NADH-dependent flavin oxidoreductase	-1.55	0.049
0970	*cdr*	coenzyme A disulfide reductase	-1.75	0.0025
1063	*folD*	methylenetetrahydrofolate dehydrogenase	-1.29	0.044
1446	NA	hypothetical protein	-1.25	0.0028
1475	*engA*	GTPase possibly involved in ribosome assembly/stability	-1.39	0.027
1732	*fhs*	formyltetrahydrofolate synthetase	-1.49	0.032
1854	NA	hypothetical protein	-1.41	0.024
2359	NA	putative ABC transporter	45.14	0.0000037
2514	*bcrA*	bacitracin ABC transporter	-3.63	0.00061
2524	*ddh*	D-specific D-2-hydroxyacid dehydrogenase	5.26	0.000067
2548	*clpL*	stress-responsive ATPase chaperone	1.58	0.033
2606	*fda*	fructose-bisphosphate aldolase	-1.66	0.018

1. SAV number corresponds to position in the annotated *S. aureus* Mu50 genome.
2. Gene name corresponds to name listed in annotation of Mu50 genome. NA signifies no gene name listed.
3. Gene name and function were determined based on closest hit in a BLAST search with an e value of $< 10^{-10}$.
4. *p* values were calculated using Student's *t*-test.

Proteins with changes upon heme exposure include potential stress-responsive factors (superoxide dismutase [SodM] and two stress-responsive chaperones [ClpL and HchA]) and enzymes involved in metabolism of the *S. aureus* low molecular weight oxidation/reduction buffer coenzyme A (coenzyme A disulfide reductase [Cdr], acyl carrier protein phosphodiesterase [AcpD]). Most proteins exhibited modest changes in abundance (1.2 – 5.3-fold); however, a single protein feature increased in abundance dramatically upon heme exposure (45.14-fold, $p<0.05$). Mass spectrometry-based protein identification followed by database interrogation was used to determine the gene encoding this heme-regulated protein. Known as SAV2359 (according to the *S. aureus* Mu50 genome annotation), this protein is predicted to be the ATPase component of a two-member ATP binding cassette (ABC) transport system. Ubiquitous amongst bacteria, ABC transporters couple the cleavage of ATP to the translocation of small molecules, ions, and other solutes across the bacterial membrane (24, 130, 186). In *S. aureus*, SAV2359 is predicted to be co-transcribed with SAV2360, the integral membrane permease component of this transport system (Figure 5A). BLAST-based searches reveal that SAV2359/60 is most closely related to ABC transporters with known roles in the export of small molecules from the bacterial cytoplasm. Importantly, no function has been ascribed to SAV2359/60; the genes remain hypothetical and their functions are predictions. We hypothesized that this protein may constitute a component of a *S. aureus* heme detoxification system. To reflect the heme-induced expression pattern of SAV2359, we named these genes the *h*eme-*r*egulated ABC *t*ransporter (*hrtAB*; *hrtA*, ATPase; *hrtB*, permease, Figure 5A).

The heme-regulated transporter is required for protection of *S. aureus* from heme toxicity. To test whether HrtAB protects *S. aureus* from heme toxicity, we generated a

mutant that lacks the *hrtA* gene and assessed the ability of the resulting strain to resist the inhibitory effects of high levels of heme. We found that *S. aureus* Δ*hrtA* is acutely sensitive to heme toxicity (Figure 5B), and intact *hrtAB* genes are required for the adaptation of *S. aureus* to heme (Figure 5C). Plate-based heme killing assays revealed that heme preferentially kills *S. aureus* Δ*hrtA* (Figure 5D). Furthermore, the heme sensitivity of this strain can be reversed by providing a full-length copy of *hrtA* under the control of its native promoter *in trans* to *S. aureus* Δ*hrtA* (Figure 5E). These data demonstrate that the heme-regulated transporter HrtAB is required for the resistance of *S. aureus* to heme toxicity.

HrtA exhibits *in vitro* ATPase activity. HrtA is predicted to be the ATPase component of HrtAB; however, no function for this protein has been demonstrated experimentally. To begin elucidating the function of HrtAB, we expressed and purified HrtA as a hexahistidine-tagged recombinant protein in *E. coli* (Figure 6A). To eliminate potential interference of the his(6) tag with HrtA enzymatic activity, we removed the tag by thrombin cleavage (Figure 6B). Next, we analyzed whether HrtA exhibits ATPase activity *in vitro* by testing whether it is capable of liberating inorganic phosphate from ATP. We found that HrtA, but not heat-inactivated HrtA, exhibits ATPase activity *in vitro* consistent with its predicted role as an ABC transporter ATPase (Figure 6C).

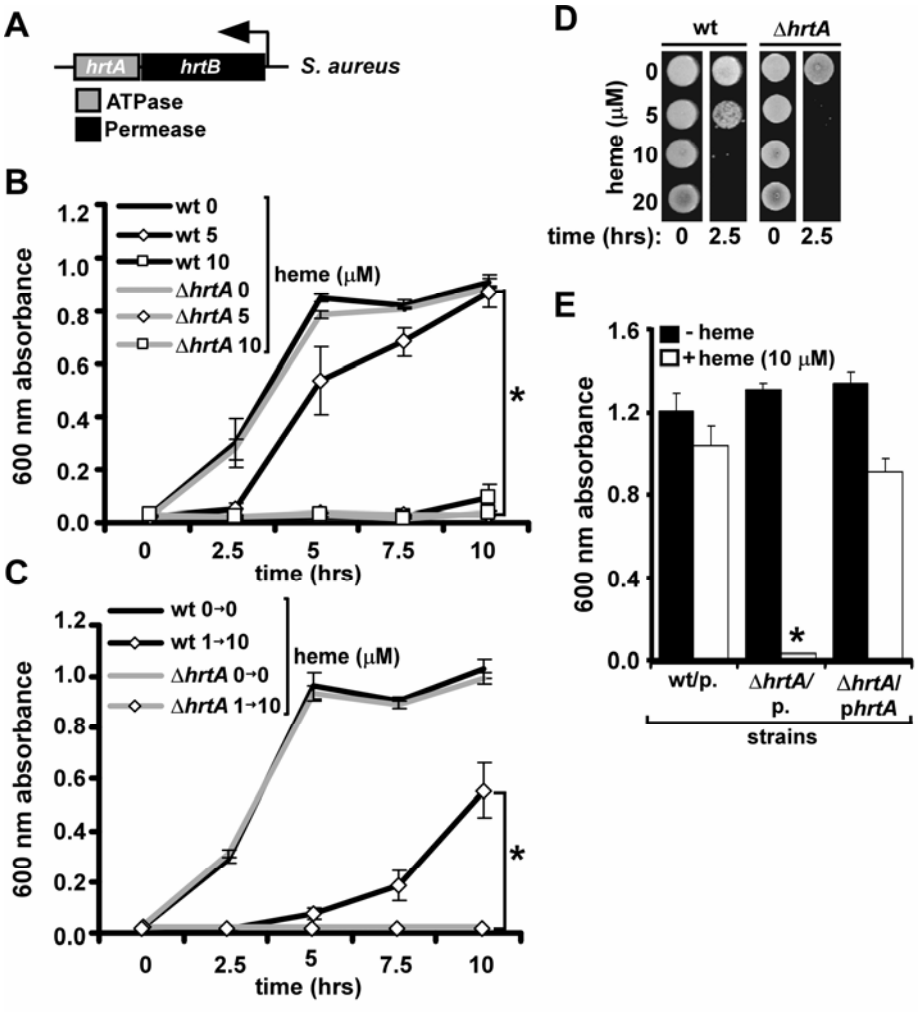

Figure 5. *S. aureus* requires HrtAB for resistance to heme toxicity. ***A.*** Genome locus of the *S. aureus* heme-regulated transporter *hrtAB*. Boxes represent open reading frames; arrow points in direction of transcription. ***B.*** Hrt is required for growth in heme. *S. aureus* wild type (wt, black lines) and Δ*hrtA* (grey lines) were cultured in no heme, 5 μM, or 10 μM heme and growth was tracked. ***C.*** Hrt is required for adaptation to heme toxicity. The experiment described in Figure 4 was repeated using *S. aureus* wild type and Δ*hrtA*. ***D.*** Hrt protects *S. aureus* from the bactericidal activity of heme. *S. aureus* wild type and Δ*hrtA* were exposed to the indicated heme concentration. Immediately after heme exposure and following 2.5 hours in heme, 10 μl of cells were plated on TSA. Shown are images of plates following 24 hours of growth. ***E.*** Complementation of Δ*hrtA*. *S. aureus* wild type harboring plasmid pOS1 (p.), Δ*hrtA* harboring pOS1, and Δ*hrtA* harboring pOS1 containing *hrtA* under the control of its native promoter (p*hrtA*) were cultured in medium containing no heme or 10 μM heme. Culture density 15 hours following subculture is shown. Data in panels *B, C,* and *E* represent averages of triplicate samples within the same experiment; error bars correspond to one standard deviation from the mean. Adapted from Torres et al., 2007 (Ref. 169). Experiments were carried out by VJT and DLS; GP constructed *S. aureus* Δ*hrtA*.

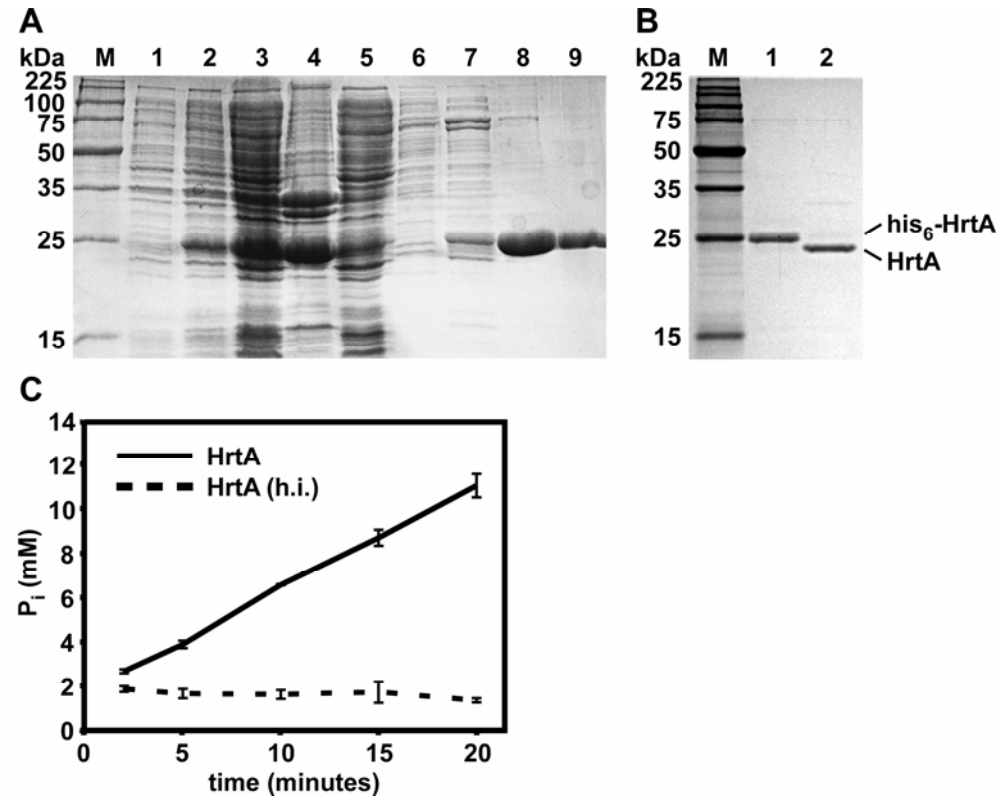

Figure 6. HrtA purification and ATPase activity. ***A.*** Coomassie blue-stained SDS-PAGE gel showing purification of *S. aureus* his_6-HrtA expressed in *E. coli*. Lanes: M, molecular weight ladder; 1, *E. coli* before IPTG induction; 2, *E. coli* after IPTG induction; 3, total cell lysate; 4, insoluble pellet obtained after French press and centrifugation; 5, soluble extract used for purification; 6-9, fractions obtained by elution of material bound to Ni-NTA with imidazole (10mM, 50mM, 100mM, and 500mM). ***B.*** SDS-PAGE showing removal of the hexahistidine tag from his_6-HrtA by thrombin protease. Lanes: M, molecular weight ladder; 1, 1 µg purified his_6-HrtA; 2, 1 µg HrtA with hexahistidine tag removed by thrombin cleavage. ***C.*** Time course analysis of ATP hydrolysis by HrtA. HrtA or heat inactivated HrtA (HrtA (h.i.)) were incubated at 20°C in the presence of ATP and release of inorganic phosphate was measured at the indicated time points. Adapted from Stauff et al., 2008 (Ref. 156). Experiments were performed in collaboration with DB.

HrtA enzymatic activity is influenced by ATP concentration, temperature, pH, and metal cofactor. ABC transporter ATPases have enzymatic activities that are influenced by multiple physicochemical conditions (78, 144). To assess the conditions under which HrtA displays maximum enzymatic activity and as a means of testing whether the activity of our HrtA preparations is sensitive to perturbations which would be expected to alter the activity of an ABC transporter ATPase, we tested the effects of ATP concentration, temperature, pH, and metal cofactor on the activity of HrtA.

We found that HrtA ATPase activity reaches a plateau at 0.25 mM ATP *in vitro* (Figure 7A). Interestingly and unexpectedly, the enzymatic activity of HrtA reaches a peak at 10-20°C and not 37°C (Figure 7B). This observation is not likely a result of enzyme instability at this temperature, as pre-incubation of HrtA at 37 °C for 20 minutes fails to alter the activity of this ATPase at 20 °C (Figure 7C). Therefore it is possible that HrtA displays an unusual temperature dependence *in vitro* that is not common to ABC transporter ATPases. HrtA reaches maximal catalytic activity within the range of pH 7.0-8.0 (Figure 7D), a range consistent with the near-neutral pH of the Gram-positive bacterial cytoplasm (39). Divalent metal cations are usually critical for the catalytic activity of ATPases. We found that magnesium (Mg^{2+}) and manganese (Mn^{2+}) both support the catalytic activity of HrtA at a number of tested concentrations, with Mn^{2+} supporting slightly elevated HrtA activity over Mg^{2+} at low concentrations (Figure 7E). In contrast, calcium (Ca^{2+}) does not support ATPase activity at any concentration tested (Figure 7E). These results demonstrate that HrtA is a Mn^{2+}/Mg^{2+}-dependent ATPase that functions at an optimal pH of 7.5-8.0 and displays unusual *in vitro* temperature sensitivity uncommon to ABC transporter ATPases.

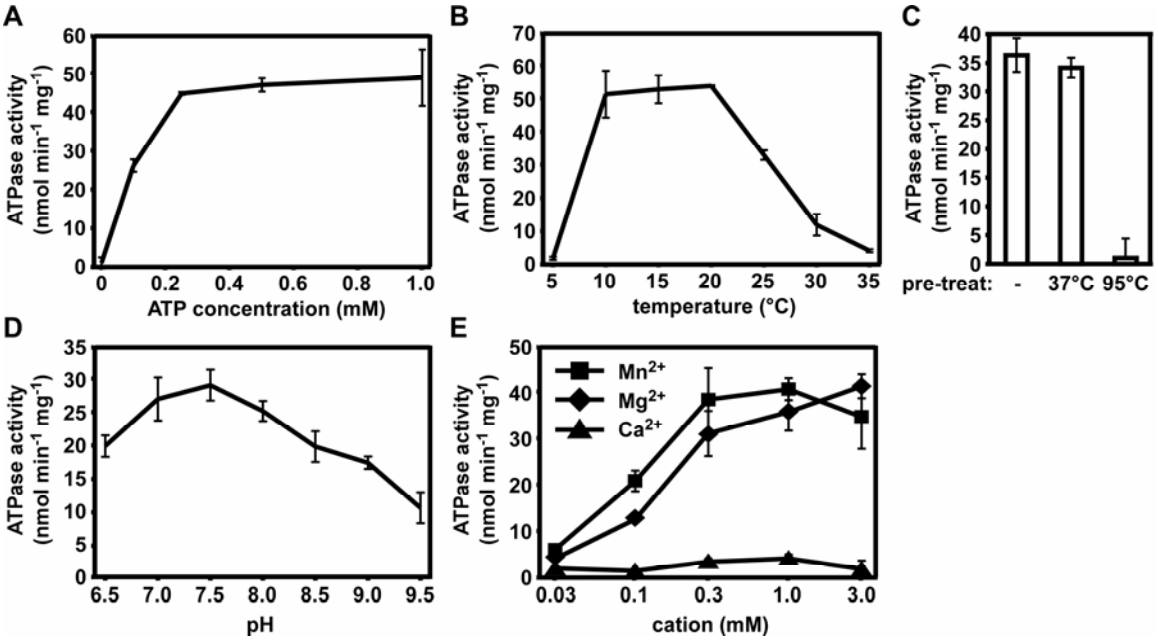

Figure 7. ATPase activity of HrtA is influenced by various physicochemical conditions. ***A.*** Concentration of ATP required for saturation of enzymatic activity. HrtA (0.5 μM) was incubated with increasing concentrations of ATP at 20°C and ATPase activity was measured. ***B.*** ATPase activity determination at different temperatures. ***C.*** Effect of temperature pre-treatment on HrtA activity. HrtA was incubated at the indicated temperature for 20 minutes and ATPase activity was determined at 20 °C. ***D.*** Influence of pH on HrtA ATPase activity. ***E.*** Effect of divalent metal cations on HrtA activity. HrtA ATPase activity was determined in the indicated concentration of $MnCl_2$, $MgCl_2$, or $CaCl_2$. For all experiments, the average of triplicate ATPase activities is indicated; error bars represent one standard deviation from the mean. Adapted from Stauff et al., 2008 (Ref. 156).

Predicted ATP binding and cleavage residues are required for *in vitro* HrtA ATPase activity. ABC transporter ATPases encode highly conserved sequence motifs involved in ATP binding and hydrolysis (78, 144). These include the Walker A motif (GxxGxGKS/T), the Walker B motif (DEP/AxxxLD), and the ABC signature sequence (LSGGxxQRV) (174). The signature motif is specific to nucleotide-binding domains of ABC-type transporter ATPases, while the Walker A and B Motifs are common to most ATPases and are involved in the binding and hydrolysis of nucleotides (104). Walker A Motifs bind ATP through a conserved lysine residue, while Walker B Motifs employ a conserved glutamic acid residue to hydrolyze ATP. In addition, the signature motif contains an absolutely conserved LSGGQ motif required for ATPase activity (104). In HrtA, all three sequence motifs can be detected (Figure 8A). To determine whether these sequences are critical for the ability of HrtA to bind and cleave ATP, highly conserved residues within each motif (K45 of Walker A, G145 of ABC signature, E167 of Walker B) as well as a residue outside of these motifs (R76) were individually mutated and HrtA mutants were purified and tested for ATPase activity (Figures 8B, 8C). Importantly, mutation of R76 reduces the rate of ATP cleavage by HrtA to about 50% of that observed for wild type HrtA, while mutation of residues K45, G145, or E167 eliminates the ability of HrtA to cleave ATP (Figure 8C). These data indicate that conserved residues within nucleotide-binding and hydrolysis motifs of HrtA are essential for ATP cleavage. The fact that mutation of a residue outside of the conserved nucleotide binding motif also alters the rate of ATP hydrolysis by HrtA suggests that non-conserved regions of HrtA are involved in catalysis *in vitro*.

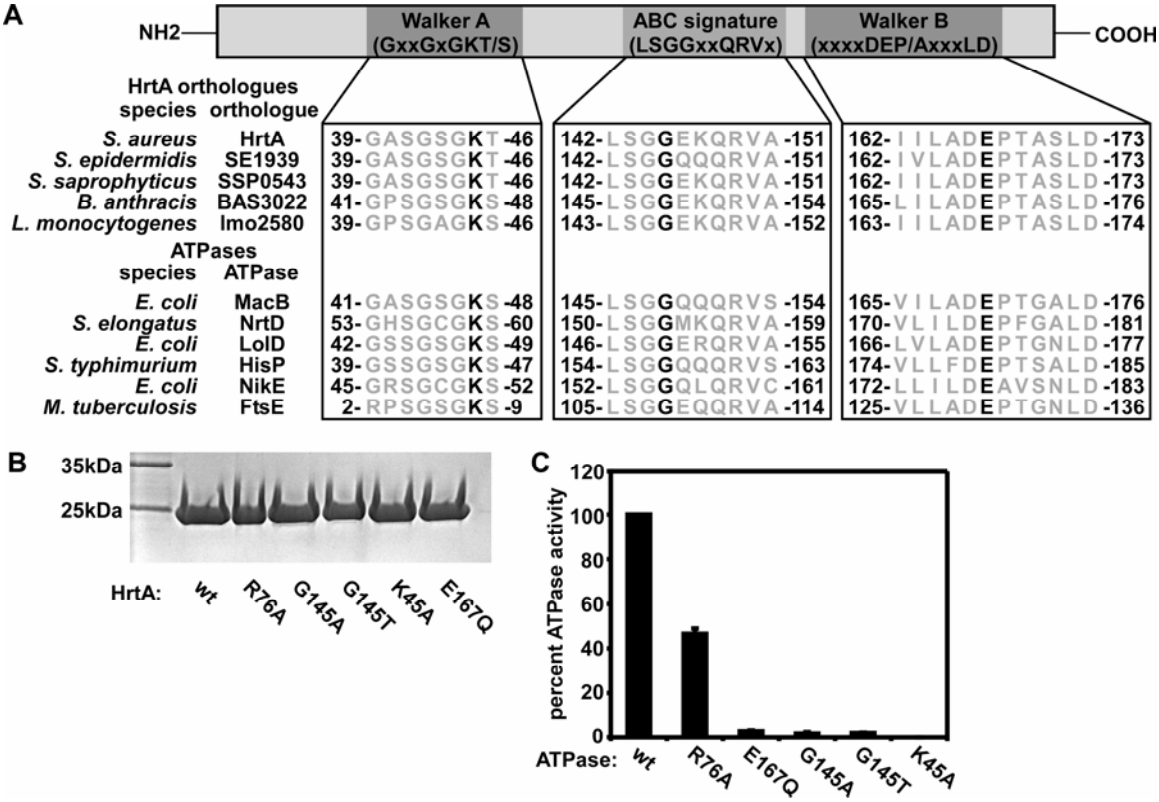

Figure 8. Residues essential for HrtA ATPase activity. ***A.*** Representation of a prototypical ABC transporter ATPase subunit and sequence alignment of conserved domains. Walker A, ABC signature, and Walker B motifs can be detected within HrtA orthologues and other characterized bacterial ABC transporter ATPases. Conserved residues selected for mutagenesis (Lys 45, Gly 145, and Glu 167 of *S. aureus* HrtA) are shown in black. ***B.*** Coomassie blue-stained SDS-PAGE gel showing recombinant purified wild type HrtA (wt) and HrtA mutants in residues within motifs predicted to be involved in nucleotide binding or hydrolysis (G145A, G145T, K45A, E167Q) or a residue outside of such motifs (R76A). ***C.*** Relative ATPase activity of HrtA mutants compared to wild type (wt). ATPase activities of recombinant HrtA and HrtA site mutants described in *B* were determined and are expressed as the percent of ATPase activity exhibited by wild type HrtA. The average percentage of triplicate ATPase activities is indicated; error bars represent one standard deviation from the mean. Adapted from Stauff et al., 2008 (Ref. 156). Experiments were performed in collaboration with DB.

Residues required by HrtA for *in vitro* ATPase activity are required for the resistance of *S. aureus* to heme toxicity. We next tested whether HrtA residues that are required for ATPase activity *in vitro* are required for the functionality of HrtAB *in vivo*. Full-length *hrtA* under the control of the *hrtAB* promoter was tagged with a C-terminal *c-myc* epitope tag, inserted into an *S. aureus* complementation vector, and independently mutated at the four residues analyzed for *in vitro* ATPase activity (Figure 9C). *S. aureus* Δ*hrtA* was then transformed with these plasmids and the resulting strains were analyzed for their ability to adapt to heme toxicity by growth curve analysis following subculture into 10 μM heme.

While *S. aureus* Δ*hrtA* cannot proliferate in 10 μM heme, *S. aureus* Δ*hrtA* expressing wild type HrtA-Myc can grow in 10 μM heme (Figure 9A, 9B). Significantly, none of the strains expressing HrtA-Myc point mutants that are unable to cleave ATP *in vitro* are able to rescue the heme-sensitive phenotype of *S. aureus* Δ*hrtA* (Figure 9B). Furthermore, *hrtA-myc*:R76A, which contains a mutation outside of the conserved nucleotide binding and hydrolysis motifs, is able to complement *S. aureus* Δ*hrtA* (Figure 9B). Notably, this mutant is also able to cleave ATP *in vitro* (Figure 9C). Importantly, all of the analyzed HrtA-Myc point mutants are expressed by *S. aureus* to a similar extent as wild type HrtA-Myc (Figure 9D).

Next, we analyzed the ability of catalytically inactive HrtA-Myc point mutants to interfere with the normal functioning of HrtAB *in vivo*. We transformed wild type *S. aureus* with the plasmids described above and analyzed the ability of these strains to adapt to heme toxicity. While HrtA-Myc and HrtA-Myc:R76A have minimal impact on the ability of wild type *S. aureus* to adapt to heme toxicity, all of the HrtA-Myc mutants that are unable to catalyze the cleavage of ATP *in vitro* display dominant negative activity *in vivo* (Figure 9C). This indicates that HrtA mutants that are unable to cleave ATP interfere with the functioning of HrtAB *in vivo*.

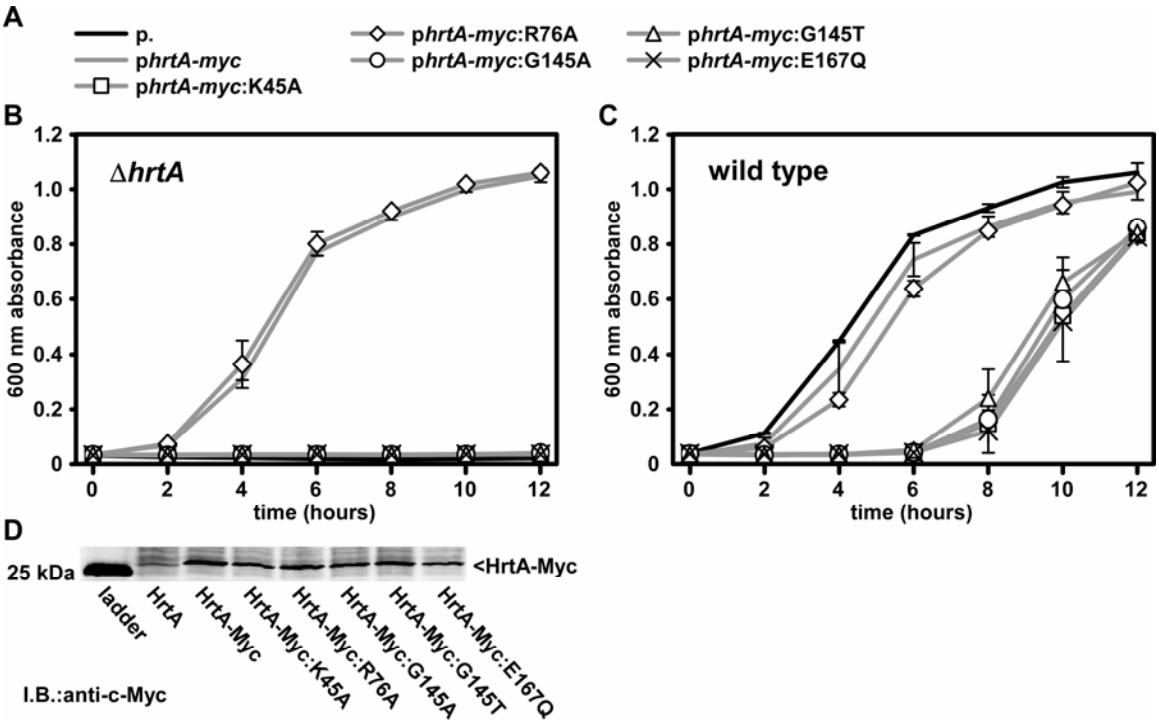

Figure 9. HrtA residues essential for resistance of *S. aureus* to heme toxicity. ***A.*** Legend of plasmids used to transform strains in *B* and *C*. Plasmids include an empty vector (black line), a plasmid encoding wild type *hrtA-myc* (grey line with no symbol) or plasmids encoding *hrtA-myc* mutants (grey lines with symbols). ***B.*** *S. aureus* Δ*hrtA* harboring the plasmids described in *A* were grown overnight in medium containing 2 μM heme and were subcultured into medium containing 10 μM heme. Bacterial growth was tracked by measuring the A_{600} of triplicate cultures. Data points represent averages of triplicate measurements; error bars represent one standard deviation from the mean. ***C.*** *S. aureus* wild type harboring the plasmids shown in *A* were grown and analyzed as in *B*. ***D.*** Immunoblot against cytoplasmic extracts of *S. aureus* Δ*hrtA* expressing C-terminal c-Myc-tagged wild type HrtA-Myc or HrtA-Myc mutants (I.B.: anti-c-Myc). Results are representative of triplicate independent experiments. Adapted from Stauff et al., 2008 (Ref. 156). Experiments were performed in collaboration with RJ.

***S. aureus* Δ*hrtA* exhibits perturbed virulence leading to increased hepatic abscess formation.** It is possible that *S. aureus*, which is capable of amassing heme during infection (134, 150, 151, 168) and overcoming heme toxicity through expression of HrtAB (Figure 4-5), may exhibit decreased fitness during infection if the ability to overcome heme toxicity is perturbed. We therefore tested the role of HrtA expression in *S. aureus* pathogenesis by infecting mice intravenously with *S. aureus* wild type and Δ*hrtA*. Animals infected with wild type *S. aureus* exhibited overt signs of disease characteristic of staphylococcal infection. Surprisingly, all animals infected with *S. aureus* Δ*hrtA* appeared more moribund than those infected with wild type, as evidenced by an absence of mobility, a pronounced hunched posture, and extensive tremors. Autopsies conducted 96 hr post-infection revealed abscess formation in the kidneys of mice infected with both of the staphylococcal strains (data not shown). In contrast, only mice infected with *S. aureus* Δ*hrtA* developed abscesses in the liver (Figure 10A). Enumeration of bacterial loads in the livers of infected animals revealed a 2 to 3 log increase in the number of mutant staphylococci as compared with wild type (Figure 10B). This perturbation of virulence was liver specific, as no difference was detected in the ability of the mutant strain to colonize the spleen or kidney compared to wild type (Figure 10B). The liver-specific virulence phenotype of *S. aureus* Δ*hrtA* is not due to intrinsically faster growth rates, because Δ*hrtA* exhibits similar growth kinetics to wild type in laboratory growth conditions (Figure 5). Histological examination of livers infected with the mutant staphylococci revealed that hepatic virulence occurs despite the recruitment of polymorphonuclear (PMN) cells (Figure 10C). More specifically, the Δ*hrtA*-induced abscesses were characterized by collections of purulent material containing PMNs, injured hepatocytes, and dense fibrous tissue (Figure 10C). Together, these findings demonstrate that *S. aureus* lacking *hrtA* exhibit altered hepatic virulence.

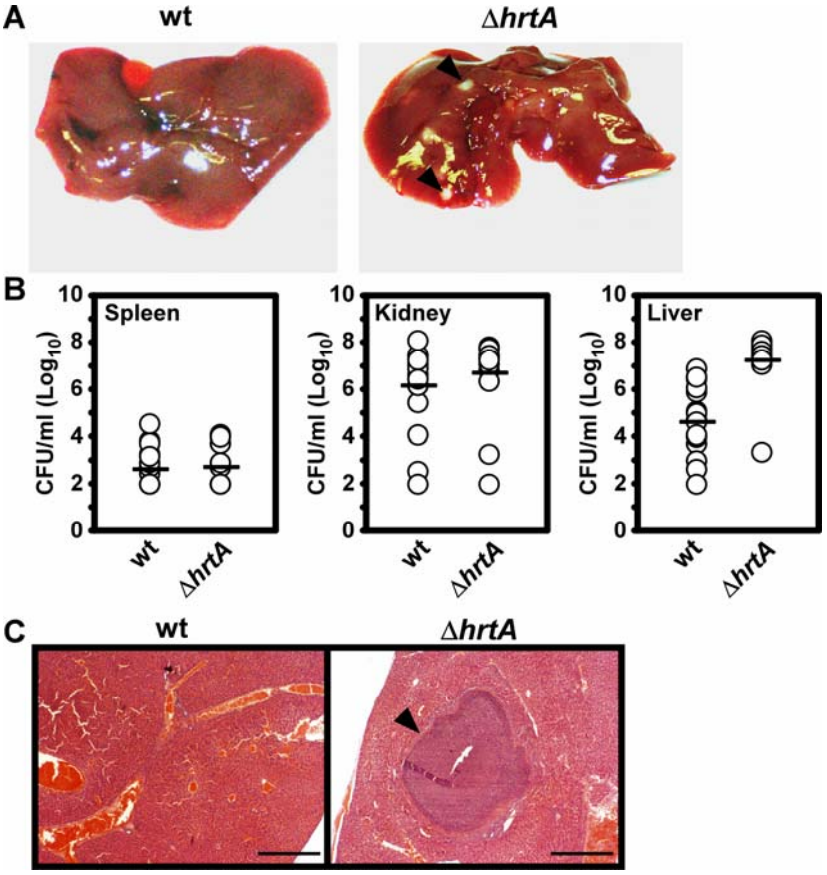

Figure 10. Perturbed virulence properties of *S. aureus* Δ*hrtA*. ***A.*** Photographs of livers dissected from BALB/c mice infected with *S. aureus* wild type (wt) and Δ*hrtA* ($1x10^6$ CFUs for all strains) 96 hr post-infection. Arrowheads mark Δ*hrtA*-induced hepatic abscesses. Photographs are representative of all livers analyzed. ***B.*** *S. aureus* multiplication in infected mouse organs as measured by tissue homogenization, dilution, and colony formation on agar media 96 hr post-infection. Each symbol represents data from one infected animal. The limit of detection in these experiments is 100 CFUs. The horizontal line denotes the mean of the log, and the asterisks denote statistically significant differences from wild type as determined by Student's *t*-test ($p < 0.05$). ***C.*** Representative hematoxylin and eosin (H&E) staining of liver sections from mice infected with wt and Δ*hrtA* at 40X magnification. Arrowheads mark Δ*hrtA*-induced hepatic abscesses. Adapted from Torres et al., (2007) (Ref. 169). Experiments were performed by VJT.

Heme induces a secreted protein profile shift in *S. aureus* Δ*hrtA*. The perturbed hepatic virulence of *S. aureus* Δ*hrtA* suggests a tip in the balance of the bacteria-phagocyte interaction in favor of *S. aureus*. *S. aureus* pathogenesis is characterized by the secretion of numerous virulence factors that defend against immune cell killing (56). Thus, we investigated whether Δ*hrtA* differs from wild type in its secreted protein profile following growth in medium containing heme. We found that exposure to heme induces changes in the abundance of multiple secreted proteins in Δ*hrtA* compared to wild type (Figure 11A). In contrast, the complemented Δ*hrtA* mutant strain displays a secreted protein profile similar to the wild type strain (Figure 11A). Mass spectrometry-based identification of the proteins overrepresented in the supernatants of Δ*hrtA* grown in heme revealed the increased expression and/or secretion of at least eight staphylococcal proteins (Figure 11B). These proteins have known roles in immunomodulation (exotoxin, exotoxin-3, -5, and -8) (181), inhibition of phagocyte recruitment (Map-w) (33), inhibition of opsonophagocytosis (fibrinogen-binding protein) (56, 98), and inhibition of neutrophil activation and chemotaxis (FLIPr) (131). Together, these data provide a potential mechanistic explanation for the perturbed virulence observed for Δ*hrtA* staphylococci. It is compelling to speculate that an increased expression of genes encoding for secreted proteins with known immunomodulatory functions is responsible for the altered virulence of staphylococcal strains unable to overcome heme toxicity.

Staphylococci lacking *hrtA* induce a dramatic transcriptional response to heme. *S. aureus* Δ*hrtA* increases the expression of a number of immunomodulatory toxins in response to heme (Figure 11). In an effort to understand the gene regulatory response of Δ*hrtA* to growth in heme, we performed genome-wide microarray analysis on *S. aureus* wild type and Δ*hrtA* grown in the presence and absence of a sub-inhibitory concentration of heme to identify transcripts with altered abundances.

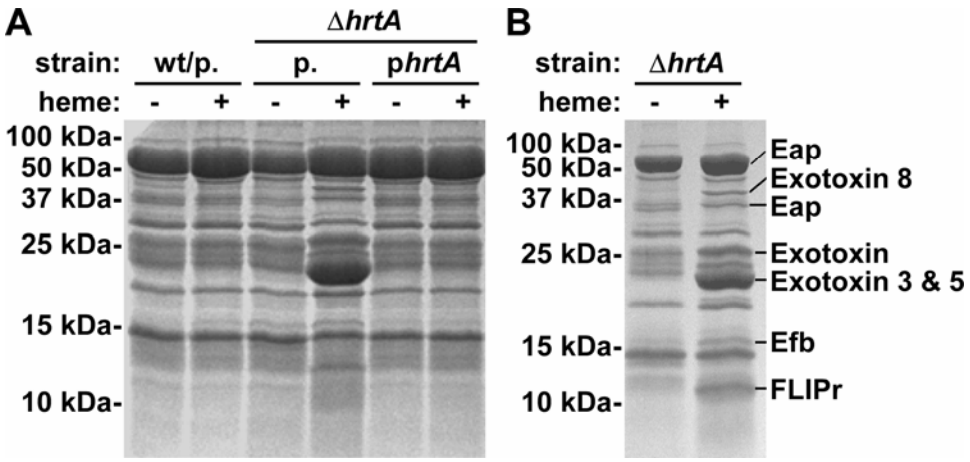

Figure 11. *S. aureus* Δ*hrtA* secretes virulence factors in response to heme. *A.* *S. aureus* wild type (wt) transformed with plasmid pOS1, Δ*hrtA* with pOS1 (p.), or Δ*hrtA* with pOS1 encoding *hrtA* (p*hrtA*) were grown for 15 hr in RPMI (-) or RPMI + 1 μM heme (+). Culture supernatants were collected, filtered, TCA precipitated, and proteins were resolved by SDS-PAGE. Gels were stained with colloidal Coomassie blue. ***B.*** Indicated proteins were excised from the gel, digested with trypsin, and tryptic fragments were subjected to mass spectrometry. The identities of the proteins are indicated. Adapted from Torres et al., (2007) (Ref. 169). Experiments were performed in collaboration with VJT.

While wild type *S. aureus* does not exhibit a significant transcriptional response to 1 μM heme, over 500 transcripts are changed in abundance greater than 2-fold in *S. aureus* Δ*hrtA* exposed to this same concentration of heme (156). Comparison of the global expression profile of heme-exposed *S. aureus* Δ*hrtA* with the global expression profiles of *S. aureus* upon cold shock, heat shock, SOS induction, stringent response induction, acid shock, alkaline shock, Mn^{2+} starvation or Zn^{2+} starvation indicates that the stringent response most closely resembles the heme response of *S. aureus* Δ*hrtA* (37.4% similarity, Table 6) (6, 38). The bacterial stringent response is induced under carbon or amino acid insufficiency through ribosome stalling, which leads to an increase in the intracellular concentration of (p)ppGpp (31). This occurs through the induction of the stringent response regulatory factor RelA (SACOL1689), the transcript of which is up-regulated upon treatment of *S. aureus* with the stringent response-inducing antimicrobial agent mupirocin and is increased 9.2-fold in *S. aureus* Δ*hrtA* exposed to heme (6, 156). A number of other stringent response-induced transcripts are increased in *S. aureus* Δ*hrtA* upon growth in heme, including those encoding virulence factors such as the transpeptidase sortase A (7.4-fold in stringent response, 9.5-fold in *S. aureus* Δ*hrtA* + heme) and fibrinogen-binding protein (7.9-fold in stringent response, 32.3-fold in *S. aureus* Δ*hrtA* + heme) (6, 156). These results indicate that in *S. aureus* Δ*hrtA*, heme induces a response that displays similarity to the *S. aureus* stringent response.

A dramatic increase in expression of a number of transcripts coding for virulence factors was observed in *S. aureus* Δ*hrtA* exposed to heme, consistent with the heme-induced secreted protein profile of this strain (Table 7). These include the transcripts for eight of the eleven staphylococcal superantigen-like exotoxins encoded within the SaPI pathogenicity island in strain Newman (NWMN_0388, NWMN_0389, NWMN_0392, NWMN_0393, NWMN_0394, NWMN_0395, NWMN_0396, NWMN_0397) as well as two predicted exotoxins located outside of this locus (NWMN_1077, NWMN_1503) (Table 7)

(10). In addition, the expression of a number of pore-forming toxins was dramatically repressed in *S. aureus* Δ*hrtA* exposed to heme. These include the transcripts encoding all three of the gamma-hemolysin subunits (SACOL2419, SACOL2421, SACOL2422) as well as the transcript for a leukotoxin (SACOL1637) (Table 7). Only one characterized class of cell wall-anchored virulence factors, the fibronectin and fibrinogen binding proteins (*fnbA*, *efb*) were differentially expressed within mutant cells (Table 7). Together, these data indicate that upon exposure to heme, *S. aureus* Δ*hrtA* undergoes a shift in toxin expression from cell lytic factors to immunomodulatory factors.

In addition to toxins, a number of transcripts encoding transcriptional regulatory factors are dramatically altered in expression in *S. aureus* Δ*hrtA* exposed to heme, providing a possible mechanistic explanation for the broad changes in gene transcription seen in heme-exposed *S. aureus* Δ*hrtA* (156). Regulatory systems with increased expression in *S. aureus* Δ*hrtA* exposed to heme include a number of characterized and uncharacterized two-component systems (including *hssS*, 4.2-fold; *lytS*, 8.1-fold; *lytR*, 20.5-fold; *vraS*, 10.4-fold; SACOL1354, 6.6-fold; SACOL1905, 9.1-fold; SACOL2645-6, 7.1-fold), known transcriptional repressors (*fur*, 9.5-fold; *czrA*, 42.9-fold; *sirR*, 5.2-fold), as well as other uncharacterized putative transcriptional regulators, some of which display dramatic alterations in expression (SACOL0403, 21.5-fold decrease; SACOL1904, 24.7-fold increase) (156). These data indicate that heme induces a profound alteration in the gene expression pattern of *S. aureus* Δ*hrtA*, possibly through novel transcriptional regulatory mechanisms. This expression change leads to an alteration in virulence gene expression (Figure 11) and may lead to the perturbed virulence of this mutant in a mouse model of systemic infection (Figure 10).

Table 6

Correlation between heme-regulated genes in ΔhrtA and stress responses

Response	Percent similarity[a]
Cold Shock	15.3%
Heat Shock	2.6%
SOS	10.6%
Stringent	37.4%
Acidic (pH 4.0)	11.3%
Alkaline (pH 10.0)	28.8%
Manganese starved	0.3%
Zinc starved	6.1%

[a] Percent similarity represents the percent of transcripts altered in abundance in Δ*hrtA* + heme which are also regulated during the given response.

Table 7

Virulence gene transcripts regulated by heme in ΔhrtA [a]

Locus[b]	Increase in heme	Gene Name[c]	Description
NWMN_0388	11.3	*set1nm*	Staphylococcal superantigen-like toxin NM1
NWMN_0389	6.9	*set2nm*	Staphylococcal superantigen-like toxin NM2
NWMN_0392	16.1	*set5nm*	Staphylococcal superantigen-like toxin NM5
NWMN_0393	8.9	*set6nm*	Staphylococcal superantigen-like toxin NM6
NWMN_0394	14.0	*set7nm*	Staphylococcal superantigen-like toxin NM7
NWMN_0395	6.7	*set8nm*	Staphylococcal superantigen-like toxin NM8
NWMN_0396	9.4	*set9nm*	Staphylococcal superantigen-like toxin NM9
NWMN_0397	6.9	*set10nm*	Staphylococcal superantigen-like toxin NM10
NWMN_1077	6.0		Staphylococcal superantigen-like toxin
NWMN_1503	3.7		enterotoxin type A, putative
SACOL0857	20.4		staphylocoagulase precursor, putative
SACOL1168	32.3	*efb*	fibrinogen-binding protein
SACOL1169	29.3	*scb/scc*	SCINb/c-related protein
SACOL1220	5.3		fibronectin/fibrinogen binding-related protein
SACOL1924	2.4		toxin exporting ABC transporter
SACOL2511	4.8	*fnbA*	fibronectin-binding protein A
SACOL2584	23.7	*isaA*	immunodominant antigen A
Locus	**Decrease in heme**	**Gene Name**	**Description**
SACOL0137	11.5	*cap5B*	capsular polysaccharide biosynthesis protein
SACOL0138	11.2	*cap5C*	capsular polysaccharide biosynthesis protein
SACOL0143	8.3	*cap5H*	capsular polysaccharide biosynthesis protein
SACOL1637	42.1	*lukD*	leukotoxin *lukD*
SACOL1865	***20.8***	*splE*	serine protease *splE*
SACOL1866	***22.2***	*splD*	serine protease *splD*
SACOL1867	***9.1***	*splC*	serine protease *splC*
SACOL1872	12.3	*epiE*	epidermin immunity protein F
SACOL1873	17.3	*epiF*	epidermin immunity protein F
SACOL2007	8.7		peptidase, M20/M25/M40 family
SACOL2419	52.8	*hlgA*	gamma-hemolysin, component A
SACOL2421	80.9	*hlgC*	gamma hemolysin, component C
SACOL2422	42.4	*hlgB*	gamma hemolysin, component B

[a] All virulence gene transcripts with at least 2-fold changes in Δ*hrtA* + heme compared to Δ*hrtA* alone which are statistically significant are shown. Grey boxes indicate that in Δ*hrtA* alone, transcript abundance approaches the lower limit of sensitivity and thus values may not be accurate. Bold, italicized values indicate that in Δ*hrtA* alone, no transcript was detected and thus values may not be accurate.

[b] All genes with SACOL designation are from *S. aureus* strain COL; because of strain specificity exhibited by toxins, all *S. aureus* superantigen-like toxins are referenced with *S. aureus* strain Newman locus designations (NWMN)

[c] Transcripts with no gene name have no designated name in the *S. aureus* COL genone annotation

Inactive HrtA point mutants complement the heme-induced secreted protein response of Δ*hrtA*. *S. aureus* Δ*hrtA* undergoes a profound transcriptional response to heme, leading to the secretion of proteins that may alter the virulence properties of this strain (Tables 6 and 7, Figures 10 and 11). However, a potential mechanism explaining how exposure of Δ*hrtA* to heme results in changes in gene expression is lacking. Originally, it was proposed that unrelieved heme toxicity experienced by Δ*hrtA* may trigger the activation of a stress-responsive regulatory system responsible for this transcriptional response. However, a number of observations are inconsistent with such an explanation. First, wild type *S. aureus* does not undergo a shift in secreted proteins even in the presence of heme concentrations that significantly inhibit its growth. However, even heme concentrations that do not impair the growth of Δ*hrtA* elicit a response by this strain (data not shown). Second, only Δ*hrtA* and not Δ*hrtAB* or other equally heme-sensitive strains (see Chapter IV) displays a heme-induced change in secreted proteins. This introduces a discontinuity between susceptibility to heme toxicity and the secreted protein profile of Δ*hrtA* and implies that Δ*hrtA* experiences a stress secondary to growth in the presence of heme.

One possible explanation for this phenomenon is that upon heme exposure, the absence of HrtA as part of the functional ABC transporter HrtAB may artificially lead to the severe stress experienced by this strain. To assess this possibility, we compared the heme-induced secreted protein profile of Δ*hrtA* to that of Δ*hrtA* expressing catalytically inactive HrtA mutants. Remarkably, even catalytically inactive HrtA mutants are able to complement the secreted protein response of Δ*hrtA* to heme (Figure 12). Δ*hrtA* expressing these mutants exhibit heme sensitivity identical to Δ*hrtA* alone, eliminating the possibility that strains expressing catalytically inactive HrtA are merely of an intermediate heme resistance (Figure 9). These data suggest that Δ*hrtA* does not undergo a change in secreted proteins due to its susceptibility to heme toxicity, but

rather due to a lack of the HrtA protein (whether functional or not) as part of HrtAB. We hypothesize that in the absence of HrtA, high levels of HrtB expression may induce a significant portion of the stress experienced by Δ*hrtA* exposed to heme. This is consistent with data showing significant *hrtAB* promoter activity in the presence of heme concentrations used to elicit a secreted protein response by Δ*hrtA* (Figure 15B). It is possible that expression of HrtB may damage the staphylococcal membrane, and that by associating with its cognate permease, even non-functional HrtA mutants may protect Δ*hrtA* from this effect.

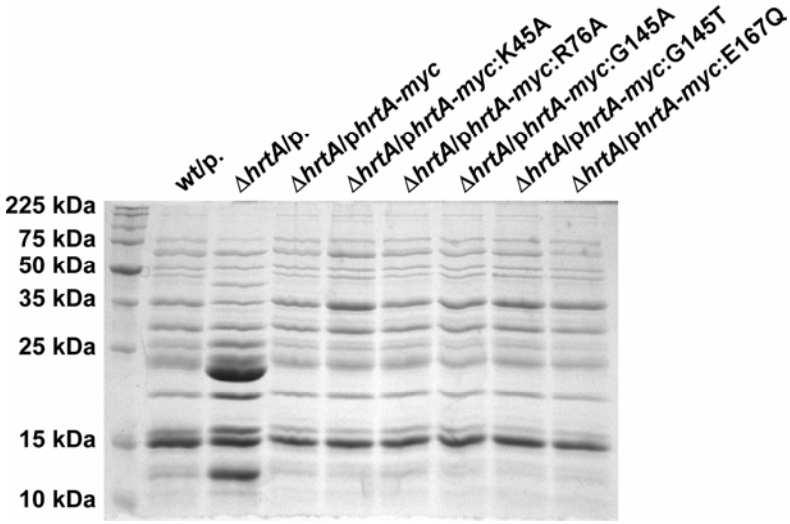

Figure 12. Catalytically inactive HrtA point mutants complement the Δ*hrtA* secreted protein response. *Staphylococcus aureus* wild type (wt) transformed with pOS1 (p.), Δ*hrtA* + pOS1, Δ*hrtA* + pOS1 encoding wild type *hrtA-myc* (p*hrtA-myc*), and Δ*hrtA* transformed with p*hrtA-myc* containing the indicated point mutations were grown overnight in RPMI + 1 μM heme. Secreted proteins were precipitated with TCA, resolved by SDS-PAGE using a 15% acrylamide gel, and visualized by Coomassie blue staining. Experiment was performed in collaboration with VJT.

Discussion

Herein, we have begun to elucidate the mechanism through which *S. aureus* avoids heme toxicity, the potentially detrimental consequence of heme acquisition by bacteria that associate with vertebrate tissues rich in heme. We show that *S. aureus* is sensitive to heme toxicity, but can adapt to heme through expression of HrtAB, a heme detoxification system. *S. aureus* lacking HrtAB easily succumb to heme toxicity and cannot adapt to growth in its presence. We demonstrate that HrtA constitutes the ATPase component of HrtAB, and displays *in vitro* ATPase activity dependent on physicochemical conditions and residues consistent with its class of ATPases. Furthermore, we show that *S. aureus* lacking the *hrtA* gene display perturbed virulence in a murine model of abscess formation, likely due to the heme-induced overexpression and secretion of immunomodulatory virulence factors.

The import of molecules and ions into the cytoplasm and the export of wastes or toxic compounds across the plasma membrane is a tightly controlled process that is essential to the viability of bacteria (78, 94, 129). Many transport pathways in bacteria depend on ABC transporters, which couple the cleavage of ATP to the transport of solutes across the membrane. *S. aureus* encodes over 50 characterized or hypothetical ABC transporters (data not shown), an indication of the importance of this particular transport scheme to staphylococci. Staphylococcal ABC transporters with described functions are involved in critical processes as diverse as fluoroquinolone resistance (NorA, (170, 185)), antimicrobial peptide and/or glycopeptide resistance (GraRS/ApsRS and VraFG (74, 101, 114)), metal ion acquisition (FhuC (155), SirABC (41), MntABC (81)), molybdate transport (ModABC (122)), and oligopeptide import (Opp-3, (77)). Heme-iron acquisition, a process important to the outcome of infection, also depends on ABC transporters (IsdDEF and HtsABC (112, 151)). In addition, the proper metabolism of heme at high concentrations is critically dependent on the ABC transporter HrtAB.

Importantly, the identity of the transport substrate for HrtAB is unknown. We have postulated that HrtAB is capable of exporting heme that accumulates to toxic levels within the cytoplasm of *S. aureus*, thereby alleviating heme toxicity (169). However, inductively coupled plasma mass spectrometry (ICPMS)-based tracking experiments using isotopically labeled heme have failed to reveal a role for HrtAB in heme efflux from staphylococcal cells (data not shown). Furthermore, it is not clear that heme export would alleviate heme toxicity, especially if the Isd and Hts systems are continually and efficiently importing heme into the cytoplasm and if the cytoplasm is not the compartment in which heme exerts its toxic effects. Biochemical fractionation experiments suggest that most exogenous non-degraded heme accumulates in the *S. aureus* membrane fraction and not the cytoplasm (150). Based on these observations and speculations, we favor the idea that heme is accumulating in the staphylococcal membrane and perturbing *S. aureus* metabolism or respiration in a way that leads to the formation of reactive oxygen species, inducing cell death. Furthermore, heme is known to damage lipid bilayers through lipid peroxidation and disruption of membrane fluidity (53, 95, 134, 161, 162). We hypothesize that, rather than exporting heme directly, HrtAB may protect against heme-mediated cell damage through the export of as-yet-unidentified toxic compounds that accumulate in *S. aureus* when this organism encounters heme.

Here, we have provided insight into the biochemical details of HrtA function and into the gene regulatory response of *S. aureus* Δ*hrtA* to growth in the presence of heme. We demonstrate that HrtA is capable of cleaving ATP *in vitro*, an activity that is dependent on temperature, pH, substrate concentration, and metal cofactor. We further show that HrtA ATPase activity is sensitive to perturbations in predicted nucleotide binding residues, and that these residues are critical for the ability of *S. aureus* to adapt to the toxicity of heme. These latter observations demonstrate that the catalytic activity

of HrtA and thus the functionality of HrtAB are essential for the survival and growth of *S. aureus* in the presence of heme. The fact that HrtA mutants that are unable to cleave ATP exhibit dominant negative activity against wild type HrtAB *in vivo* suggests that these mutants are capable of associating with endogenous HrtA, HrtB, or both in order to block the normal functioning of HrtAB. ABC transporter permeases typically function as dimers, with one associated ATPase per monomer (78, 144). The dominant negative activity of HrtA point mutants that we observe is consistent with the known associations that occur between ABC transporter ATPases and their cognate permeases. It is also consistent with the finding that in many ABC transporters, a single functioning ATPase per transporter multimer is insufficient for proper function, but that both ATPases need to be functional (83, 105, 146).

Expression analysis revealed that *S. aureus* Δ*hrtA* induces changes in the abundance of over 500 transcripts when exposed to heme, many of which encode for important virulence factors, gene regulatory systems, and as-yet-uncharacterized systems. Interestingly, many (37.4%) *S. aureus* Δ*hrtA* heme-induced transcripts are components of the staphylococcal stringent response (Table 6). Consistent with this observation, RelA, the major activator of the stringent response, was up-regulated > 9-fold within heme challenged mutant cells. This observation may suggest that heme accumulation redirects transcript synthesis in a manner that promotes up-regulation of alternative transport systems which are major components of the stringent response; this may represent an attempt to overcome heme toxicity.

Based on the fact that no virulence defect is observed for *S. aureus* Δ*hrtA*, it is likely that in our murine model of infection staphylococci do not encounter enough heme to induce cell death in this heme-sensitive strain. However, the observations of perturbed virulence and heme-induced overexpression of a number of toxins in *S. aureus* Δ*hrtA* indicate that *S. aureus* may encounter low levels of heme for use as an

iron source. This is consistent with the fact that low heme concentrations induce changes in the secreted protein profile of Δ*hrtA* (0.5 μM), while significantly higher heme levels are needed to inhibit growth of Δ*hrtA* (>5 μM; data not shown). It is possible that during infection, enough heme is acquired to satisfy the nutrient iron requirement of *S. aureus* and to induce virulence perturbation in Δ*hrtA*. This possibility is consistent with virulence defects observed for strains inactivated for Isd genes (133, 150, 168). Currently, it is unclear why virulence perturbation is only observed in the murine liver. It is possible that more heme is acquired in the liver than in other tissues; it is also possible that the local microenvironment in the liver may predispose staphylococci to the toxicity of heme, leading to HrtAB expression. This latter possibility is supported in part by experiments suggesting that HrtAB levels may respond to the severity of heme toxicity, rather than to levels of heme itself (see Chapter VI).

The toxin transcript expression profile of *S. aureus* Δ*hrtA* exposed to heme may reveal new regulatory mechanisms or signals that *S. aureus* recognizes in order to coordinate a specific toxin expression profile upon exposure to distinct host environments. It is important to note that not only does the total quantity of toxins secreted by *S. aureus* Δ*hrtA* exposed to heme appear to be altered, but the profile of toxin secretion is dramatically changed to decrease the expression of host cell lytic toxins and increase the expression of immunomodulatory toxins such as the staphylococcal superantigen-like toxins. It may be that certain types of stress, such as that experienced by *S. aureus* Δ*hrtA* grown in heme, may mimic a physiologically relevant cue which *S. aureus* senses in order to adjust its toxin expression and secretion profile accordingly. It is tempting to speculate that this stressor is one that represents a signal for invading staphylococci to switch from a cytolytic toxin secretion profile to an immunoevasive response. Importantly, it is unclear at this point what fraction of the 500 transcripts regulated by Δ*hrtA* in heme results from the sensitivity of this strain to heme

toxicity, and what fraction is altered as a result of the lack of HrtA as part of the functional holotransporter, HrtAB (see *Inactive HrtA point mutants complement the heme-induced secreted protein response of ΔhrtA*). Protein secretion experiments suggest that the latter fraction may be quite large. It is possible that we have serendipitously stumbled upon a strain that reveals key toxin regulatory mechanisms linked to membrane integrity, as this is the likely compartment of the *S. aureus* cell perturbed by expression of dysregulated HrtAB.

Taken together, these studies have identified a mechanism whereby *S. aureus* avoids the toxicity of heme imported into cells for use as a nutrient iron source. Upon heme exposure, staphylococci dramatically increase the expression of the ABC transporter HrtAB, which alleviates heme toxicity, likely through the export of a toxic small molecule induced by heme in the *S. aureus* cytoplasm. It has not escaped our attention that as a member of the ABC transporter superfamily, HrtAB bears similarity to detoxification systems that provide antibiotic resistance to many bacteria. We have not been able to demonstrate a role for HrtAB in resistance to any member of a large set of clinically relevant antibiotics. However, it is possible that ABC transporters such as HrtAB may alleviate more general types of cellular stress, conferring antibiotic resistance in spite of the fact that such transporters were clearly not selected throughout the course of evolution to specifically alleviate the toxicity of novel antibiotics (such as is almost certainly the case for fluoroquinolone resistance conferred by NorA (170, 185)). It is possible that HrtAB may also have a broader role in staphylococcal physiology. This possibility will be more clearly assessable as the transport substrate for HrtAB is identified and as the mechanism of HrtAB regulation is elucidated.

CHAPTER IV

REGULATION OF HrtAB EXPRESSION BY THE HssRS TWO-COMPONENT SYSTEM

Introduction

Staphylococcus aureus induces expression of the heme-regulated transporter HrtAB when exposed to heme and staphylococci require HrtAB for adaptation to and survival in otherwise toxic concentrations of heme. However, the mechanism of HrtAB regulation remains uncharacterized. To this end, we sought to elucidate the mechanism by which heme is sensed, leading to an increase in HrtAB expression and the alleviation of heme toxicity.

Here, we show that *hrtAB* is genomically co-localized with a previously uncharacterized two-component system (TCS) on the staphylococcal chromosome. This TCS is required for HrtA induction and for promoter-driven expression of the *hrtAB* genes in response to heme. We designated this TCS the *h*eme *s*ensor *s*ystem (HssRS), and show that HssS signaling to HssR impinges on a critical direct repeat within the *hrtAB* promoter, driving expression of HrtAB. These studies begin to elucidate the mechanism by which HrtAB is regulated at a transcriptional level, and characterize the signaling events critical to the function of a novel staphylococcal TCS that responds to a host-specific molecule.

Methods

Bacterial strains and plasmids – *S. aureus* Δ*hssR* was created by following a similar protocol to that described for generation of Δ*hrtA* (see Chapter III Methods). An *hssS* knockout was obtained from the Phoenix (N) library; clone PhiNE 01562 (SAV2362) (11) was transduced into Newman.

2D-DIGE – Triplicate samples of cytoplasmic extract from *S. aureus* wild type or an isogenic Δ*hssR* mutant grown for 15 hours at 37 °C with shaking at 180 rpm in the presence or absence of 5 μM heme were subjected to 2D-DIGE. Samples were prepared, labeled, resolved and individual protein features with altered expression patterns were identified as described (Chapter II Methods).

Purification of HssR *and* HssS – The entire *hssR* open reading frame and the signaling domain of *hssS* (corresponding to amino acids 185-457) were cloned into the *E. coli* expression plasmid pET15b, making pET15b.*hssR* and pET15b.*hssS* for the expression of hexahistidine N-terminal fusions of both proteins. Pfu mutagenesis (176) was used to create expression constructs for the mutants HssR:D52A and HssS:H249A. pET15b.*hssR*:D52A and pET15b.*hssS*:H249A were verified by sequencing (Vanderbilt University DNA sequencing facility). Protein expression and purification was performed as described previously (Chapter 3 Methods, *Purification of* HrtA *and* HrtA *mutants*).

In vitro phosphorelay - 70 μl of HssS or HssS:H249A labeling reaction was prepared (50 mM Tris, pH 8.0, 5 mM $MgCl_2$, 200 mM KCl, 0.2 mM DTT, 10 % glycerol, 20 μM ATP, 5 μM HssS or HssS:H249A). Twenty μCi of [γ-^{32}P]ATP (Amersham biosciences) was added to both labeling reactions and samples were incubated at 37 °C. At 5, 15, and 45 minutes after the addition of radiolabeled ATP, 10 μl samples were removed and mixed with 2X SDS loading buffer. At 45 minutes, HssR or HssR:D52A were added to the appropriate reactions to a final concentration of 17.5 μM. Ten μl samples were taken 5, 15, and 45 minutes after the addition of HssR or HssR:D52A. Samples were loaded

onto 15% polyacrylamide gels and after SDS-PAGE, gels were dried and analyzed using a PhosphorImager.

XylE reporter constructs/hrtAB Promoter Truncations and Mutations – Construction of p*hrtAB.xylE* was generated by PCR-SOE (82). A reporter construct in which the *xylE* gene is controlled by the *S. aureus* lipoprotein diacylglycerol transferase (*lgt*) promoter (29) was made by removing an NdeI site from *xylE* by Pfu mutagenesis (176) and cloning *xylE* lacking an NdeI site into pOS1p*lgt* (29) between the NdeI and BamHI sites of this vector, making p*lgt.xylE*. Using p*hrtAB.xylE* as a template, five truncations were made in the *hrtAB* promoter by PCR amplification using 5 different 5' primers which anneal to sites within the *hrtAB* promoter and a 3' primer matching the 3' end of *xylE*. These promoter-*xylE* fragments were inserted into pOS1 (143), making p*hrtAB.xylE*.T1-5. Mutations were confirmed by sequencing from the 5' end of the *hrtAB* promoter to the 3' end of *xylE*. Four residues within the direct repeat sequence upstream of the *hrtAB* start site were mutated by PCR-SOE. p*hrtAB.xylE* with 4 direct repeat base mutations (p*hrtAB.xylE*.DR) was confirmed by sequencing as above.

Complementation constructs – A plasmid containing a copy of *hssR* under the control of its native promoter was created by PCR amplifying *hssR* with its promoter using *S. aureus* Newman genomic DNA as a template and inserting amplified DNA into pOS1, making p*hssR*. A plasmid containing a copy of *hssS* under the control of the *lgt* promoter was created by PCR amplifying *hssS* and inserting amplified DNA into pOS1p*lgt*, creating p*hssS*. A C-terminal c-*myc* tagged *hssR* was created by PCR amplifying *hssR* from *S. aureus* genomic DNA using a 5' primer within the *hssR* promoter and a 3' primer matching the 3' end of *hssR* and including the coding sequence for the c-Myc epitope (EQKLISEEDL). Amplified DNA was inserted into pOS1, creating p*hssR-myc*. A C-terminal c-*myc* tagged *hssS* was created in the same manner as for *hssR*. Amplified DNA was inserted into pOS1p*lgt*, generating p*hssS-myc*.

The *hssR-myc* D52N mutation and the *hssS-myc* H249A mutation were introduced as described above for the generation of *E. coli* expression constructs, generating p*hssR-myc*:D52N and p*hssS-myc*:H249A. Mutations were confirmed and secondary mutations were ruled out by sequencing.

HssS-Myc and HssR-Myc immunoblotting - Expression of tagged HssS and HssR was tested by preparing bacterial extracts and immunoblotting as follows. For HssR-Myc, 15 ml cultures of bacteria grown for 15 hours were centrifuged, washed with wash buffer (50 mM Tris, pH 7.5, 150 mM NaCl), and lysed in 800 µl of lysis buffer (wash buffer containing 2 complete protease inhibitor tablet per ml (Roche Diagnostics)) by mechanical disruption using a FastPrep 24 (MP Biomedicals). For HssS-Myc, bacteria were grown and washed as above. Bacteria were then re-suspended in TSM (100 mM Tris, pH 7.0, 500 mM sucrose, 10 mM $MgCl_2$, 20 µg/ml lysostaphin), incubated at 37 °C for 30 minutes, and protoplasts were harvested by centrifugation. Protoplasts were re-suspended in 800 µl of lysis buffer as above and were sonicated. Triton X-100 was added to 1%, insoluble material was removed by centrifugation, and supernatant was removed for analysis. Thirty µg of lysate from HssR-Myc or HssS-Myc expressing *S. aureus* was subjected to SDS-PAGE, transferred to nitrocellulose, and blotted with sc-789 polyclonal rabbit anti-c-Myc primary (Santa Cruz Biotechnology) and AlexaFluor-680-conjugated anti-rabbit secondary (Invitrogen) antibodies. Membranes were dried and scanned using an Odyssey Infrared Imaging System (LI-COR Biosciences).

S. aureus Growth Kinetics – Growth curve experiments were performed as described previously (see Chapter III Methods, *Growth curve assays and heme adaptation analysis*)

XylE activity assay – Appropriate strains were grown overnight at 37 °C with shaking at 180 rpm and were then subcultured into 1.5 ml Eppendorf tubes containing TSB with heme dilutions and were grown for 5 hours. Bacteria were pelleted by centrifugation,

and spent medium was aspirated. The pellet was washed once with 500 ml of 20 mM potassium phosphate (pH 7.6) and re-suspended in 150 µl of 100 mM potassium phosphate buffer (pH 8.0), 10% (v/v) acetone, and 25 mg/ml lysostaphin. After a 20 minute incubation at 37°C and 5 minute incubation on ice, samples were centrifuged at 20,000 g for 30 minutes at 4°C. 20 µl of supernatant was added to a 96-well plate, and 200 µl of 100 mM potassium phosphate (pH 8.0), 0.2 mM pyrocatechol was added to each well. Formation of 2-hydroxymuconic semialdehyde was tracked by measuring the absorbance at 375 nm every minute for 30 minutes on a Varian MP 50 microplate reader. Protein concentration in samples was determined by BCA (Pierce). One unit of specific activity of XylE in a sample is defined as the formation of 1 nmol of 2-hydroxymuconic semialdehyde per minute per milligram of cellular protein at 30°C (35).

Magnetic bead pull-down – For capture of HssR-Myc from *S. aureus* extracts, *S. aureus* harboring p*hssR-myc* was subcultured 1:100 from an overnight culture into 100 ml of TSB with or without 7 µM heme. Bacteria were grown for 7 hours at 37 °C with shaking at 180 rpm and were then pelleted, washed with 20 ml of 50 mM Tris, pH 7.5, 150 mM NaCl, and re-suspended in 20 ml of TSM for 30 minutes. Bacterial protoplasts were then pelleted, re-suspended in 10 ml of lysis buffer (50 mM Tris, pH 7.5, 150 mM NaCl, 0.1 mM EDTA, 2 mM $MgCl_2$), and lysed by French press. Mechanically sheared salmon sperm DNA was added to lysates to a final concentration of 10 µg/ml. Bead-DNA complexes were prepared by adding 5 µg of biotinylated 300 base pair *hrtB* coding sequence DNA or *hrtAB* promoter DNA prepared by PCR using a 5'-biotinylated primer to 500 µg of Dynabeads M-280 streptavidin (Dynal Biotech) in 400 µl of bead binding and wash buffer (50 mM Tris, pH 7.5, 1 M NaCl, 0.5 mM EDTA) and rotating on a rotisserie at room temperature for 15 minutes. DNA-bead complexes were washed three times in 1 ml of bead binding and wash buffer, re-suspended in 50 µl of lysis buffer, and added to 5 ml of *S. aureus* cytoplasmic extract. Mixtures were rotated for 30

minutes at room temperature and DNA-bead complexes were washed four times with 1 ml of lysis buffer and were eluted with 50 µl of 50 mM Tris, pH 7.5, 500 mM NaCl. For oligonucleotide elution experiments, DNA-protein-bead complexes were prepared using extracts from heme-treated *S. aureus* as above and were eluted in increasing concentrations (0.001, 0.01, 0.1, 1, 12.5 µM) of double-stranded oligonucleotides dissolved in 50 mM Tris, pH 7.5, and prepared by allowing complementary 40-mers corresponding to the wild type (AAAAACAATTGTTCATATTGAGTTCATATTTCAACCTTAT) or mutant (AAAAACAATTGT**A**CATAT**A**GAG**A**TC**T**TATTTCAACCTTAT) *hrtAB* direct repeat to cool to room temperature from 90 °C. Samples from triplicate experiments were analyzed by SDS-PAGE and immunoblotting as described above. For quantification, band intensities were determined using Odyssey Infrared Imaging System software (LI-COR Biosciences). For each elution series, band intensities were adjusted for background intensity, summed, and each band intensity was expressed as a percentage of the sum. For pull-down of *in vitro* phosphorylated purified HssR, 200 µl phosphorylation reactions were prepared by incubating 1 µM HssR or HssR:D52A in 50 mM Tris, pH 7.5, 50 mM KCl, 2 mM $MgCl_2$ with or without 20 µM potassium acetyl phosphate for 2 hours at 37 °C. Samples were centrifuged at 13000 rpm for 2 minutes to remove precipitated protein and 10 µl of soluble protein was removed for SDS-PAGE analysis. 25 µl of bead-DNA complexes prepared as described above were added to 75 µl of soluble protein in 1 ml of 50 mM Tris, pH 7.5, 150 mM NaCl, 0.1 mM EDTA, 2 mM $MgCl_2$, 10 µg/ml sheared salmon sperm DNA. Samples were rotated on a rotisserie at room temperature for 15 minutes, after which beads were washed four times and eluted with 50 µl of 50 mM Tris, pH 7.5, 500 mM NaCl. Samples were analyzed by SDS-PAGE followed by immunoblotting using an anti-hexahistidine tag antibody as described for the detection of c-Myc-tagged proteins.

Results

***hrtAB* is co-localized on the *S. aureus* chromosome with a putative heme sensing system required for heme resistance.** Conceivably, heme-induced HrtAB expression could be regulated by any class of regulator at any location on the *S. aureus* chromosome. However, in bacteria genes with associated functions are often found co-localized spatially on the chromosome. We therefore analyzed the genomic context of *hrtAB* for potential heme sensing systems.

Remarkably, the two genes upstream of *hrtAB* (SAV2361/62) encode a putative two-component system (TCS, Figure 13A). TCS represent a major regulatory scheme shared by most bacterial species (15, 17, 109). Typically, TCS consist of a membrane-localized or cytoplasmic histidine kinase and a cytoplasmic response regulator. Histidine kinases typically detect an input stimulus, triggering histidine autophosphorylation. Phosphorylated histidine kinases are then recognized by a cognate cytoplasmic response regulator, which triggers trans-phosphorylation, leading to response regulator activation. Activated response regulators carry our effector functions, including gene regulation. In *S. aureus*, SAV2362 is predicted to encode a membrane-localized histidine kinase, while SAV2361 is predicted to encode a cytoplasmic response regulator with a DNA-binding domain involved in gene regulation. To reflect the genomic localization of SAV2361/2 with *hrtAB*, we named this TCS the *h*eme *s*ensor *s*ystem (*hssRS*; *hssR*, response regulator; *hssS*, histidine kinase, Figure 13A).

Next, we tested whether *hssRS* is required for heme resistance in *S. aureus*. We found that *S. aureus* lacking *hssR* or *hssS* display a heme-sensitive phenotype similar to *S. aureus* Δ*hrtA*, and that HssRS is required for the adaptation of *S. aureus* to heme toxicity (Figure 13B, 13C). These data connect HssRS with HrtAB and suggest that HssRS may detect heme to induce expression of HrtAB, alleviating heme toxicity.

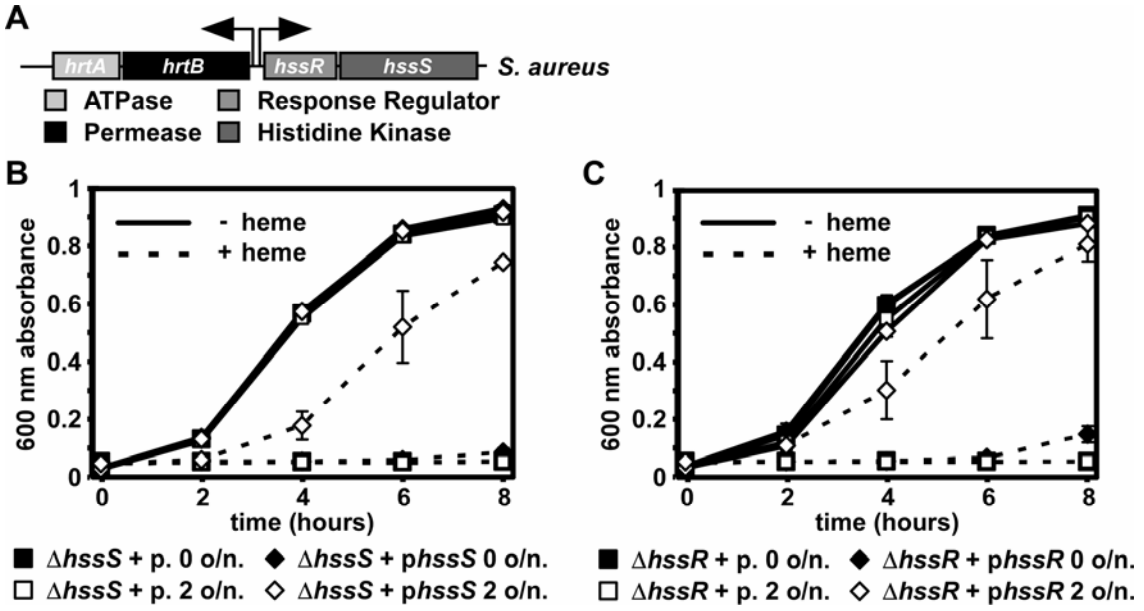

Figure 13. HssS and HssR are required for adaptation of *S. aureus* to heme toxicity. ***A.*** Schematic of the *S. aureus hssRS/hrtAB* locus. *hrtAB* is predicted to encode a putative co-transcribed ABC transporter (consisting of an ATPase, *hrtA*, and a permease, *hrtB*); arrow indicates the direction of transcription. *hssRS* is predicted to encode a putative co-transcribed two-component system (consisting of a response regulator, *hssR*, and a histidine kinase, *hssS*). ***B.*** *S. aureus* Δ*hssS* harboring an empty vector (Δ*hssS* + p.) or a plasmid harboring a full-length copy of *hssS* (Δ*hssS* + p*hssS*) were grown overnight in medium without heme (solid squares) or medium containing 2 μM heme (empty squares). Overnight cultures were then subcultured into medium without heme (solid lines) or medium containing 10 μM heme (dashed lines). In all assays, 600 nm absorbance readings were taken on triplicate cultures at the indicated times after inoculation and averages +/- one standard deviation are shown (in most cases, error bars are too small to be seen). ***C.*** Δ*hssR* harboring an empty vector (Δ*hssR* + p.) or a plasmid harboring a full-length copy of *hssR* (Δ*hssR* + p*hssR*) were grown overnight and subcultured as in *A*. Adapted from Torres et al., 2007 (Ref. 169) and Stauff et al., 2008 (Ref. 158).

***hssRS* is required for heme-induced expression of HrtA.** To test whether the TCS response regulator HssR is required for the heme-induced increase in abundance of HrtA and to identify additional HssR-regulated proteins, we performed 2D-DIGE. Cytoplasmic extracts were prepared in triplicate from *S. aureus* wild type or Δ*hssR* grown in the presence or absence of 5 μM heme, the highest heme concentration in which Δ*hssR* is able to grow with near-wild type kinetics. Proteins were labeled with amino-reactive fluorescent dyes, resolved on two-dimensional gels, and protein features with differential expression patterns were excised and identified by mass spectrometry.

Upon exposure of wild type to 5 μM heme, HrtA increased in abundance by a factor of 2.44 (p = 0.024) (Figure 14 and Table 8). This heme-dependent increase in HrtA expression is less than we have previously observed (Table 5) (61) because of the lower concentration of heme used in the present experiment. Importantly, strains inactivated for *hssR* did not up-regulate HrtA expression upon exposure to heme (Figure 14 and Table 8). Furthermore, no cytoplasmic protein features that require HssR for a heme-dependent increase in expression other than HrtA were identified by 2D-DIGE analysis (Table 8). Although HrtB is likely to be expressed in a heme-dependent, HssR-dependent manner as judged by the localization of *hrtB* in a bicistronic operon with *hrtA*, HrtB is predicted to be a membrane protein and is not present in the cytoplasmic fractions used in our 2D-DIGE experiment. A number of stress-related and metabolic proteins displayed changes in abundance only in Δ*hssR* exposed to heme, consistent with a role for HssR in protection of *S. aureus* from heme toxicity through regulation of HrtAB expression. Based on these results, we conclude that *hssR* is necessary for the heme-induced increase in HrtA and that, within the window of the *S. aureus* cytosolic proteome resolvable by 2D-DIGE, HrtA is the major target of activation by HssR upon exposure of *S. aureus* to heme.

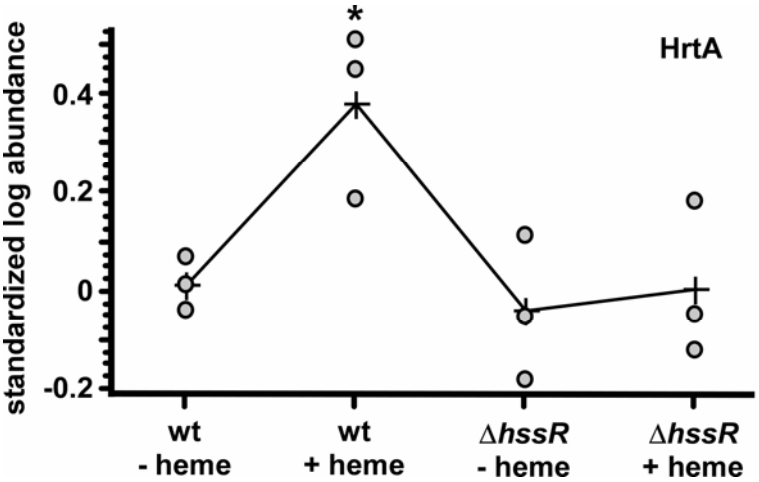

Figure 14. HssR is required for the heme-dependent increase in expression of HrtA. Cytoplasmic extracts were prepared from wild type *S. aureus* (wt) or Δ*hssR* grown without heme (- heme) or in the presence of 5 μM heme (+ heme). Extracts from triplicate cultures were labeled with fluorescent dyes and were resolved by two-dimensional difference gel electrophoresis (2D-DIGE). The standardized log abundances of one protein feature corresponding to HrtA are shown for each tested condition. The asterisk above the HrtA abundances from wild type grown in heme denotes that the observed change is statistically significant when compared with the other three conditions ($p < 0.05$). Quantification of changes in HrtA abundance as well as additional proteins with differential expression are listed in Table 8. Adapted from Stauff et al., 2007 (Ref. 158). Experiments were performed in collaboration with DBF and CW.

Table 8
Proteins affected by heme and *hssR*

gene information			*regulation pattern*[a]					
gene number[b]	gene name	function	wt + heme vs. wt[c]	Δ*hssR* vs. wt[d]	Δ*hssR* + heme vs. wt[e]	Δ*hssR* vs. wt + heme[f]	Δ*hssR* + heme vs. wt + heme [g]	Δ*hssR* + heme vs. Δ*hssR* [h]
SAV0387	N/A	conserved hypothetical protein	-1.2 (0.31)	1.12 (0.67)	-2.08 (0.0034)	1.35 (0.3)	-1.73 (0.071)	-2.33 (0.017)
SAV0539	*rplJ*	50S ribosomal protein L10	1.09 (0.89)	-1.06 (0.77)	1.17 (0.3)	-1.16 (0.74)	1.07 (0.63)	1.24 (0.038)
SAV0752	N/A	ribosomal subunit interface protein	-1.15 (0.68)	1.21 (0.45)	-1.49 (0.29)	1.39 (0.32)	-1.3 (0.69)	-1.8 (0.037)
SAV0776	*eno*	phosphoglycerate dehydrogenase	1.16 (0.065)	1.02 (0.88)	1.61 (0.014)	-1.14 (0.26)	1.39 (0.053)	1.58 (0.031)
SAV1694	*citC*	isocitrate dehydrogenase	-1.11 (0.75)	1.36 (0.58)	-3.15 (0.033)	1.5 (0.46)	-2.85 (0.076)	-4.28 (0.031)
SAV2029	*groEL*	chaperone	1.14 (0.45)	1.54 (0.015)	-1.28 (0.064)	1.36 (0.092)	-1.45 (0.058)	-1.98 (0.0029)
SAV2030	*groES*	chaperone	-1.23 (0.18)	-1.09 (0.62)	1.29 (0.1)	1.13 (0.44)	1.59 (0.0033)	1.41 (0.056)
SAV2113	*glyA*	serine hydroxymethyl-transferase	1.13 (0.27)	1 (0.97)	1.44 (0.017)	-1.12 (0.24)	1.28 (0.043)	1.44 (0.013)
SAV2125	*fbaA*	fructose bisphosphate aldolase	-1.63 (0.047)	1.09 (0.88)	1.03 (0.86)	1.79 (0.12)	1.68 (0.35)	-1.06 (0.8)
SAV2144	*N/A*	NAD-dependent epimerase/dehydratase	-1.29 (0.97)	-1.09 (0.88)	-2.32 (0.31)	1.18 (0.76)	-1.81 (0.04)	-2.13 (0.083)
SAV2359	*hrtA*	heme-regulated ABC transporter ATPase	2.44 (0.024)	-1.1 (0.58)	1.02 (0.92)	-2.68 (0.032)	-2.4 (0.049)	1.12 (0.74)
SAV2382	*N/A*	general stress protein 26	-1.28 (0.36)	-1.1 (0.46)	-1.99 (0.0096)	1.16 (0.51)	-1.55 (0.36)	-1.8 (0.011)
SAV2524	*ddh*	D-specific lactate dehydrogenase	3.4 (0.31)	1.18 (0.25)	1.98 (0.04)	-2.87 (0.27)	-1.71 (0.79)	1.68 (0.0038)
SAV2581	*N/A*	hypothetical hydrolase	-1.09 (0.97)	-1.08 (0.99)	-2.29 (0.087)	1.01 (0.97)	-2.11 (0.028)	-2.13 (0.026)

[a]Regulation pattern is given as the fold change in abundance of the first condition listed compared to the second condition listed (first condition vs. second condition). p value from Student's t-test is shown in parentheses. Statistically significant changes are boxed in grey.
[b]SAV number corresponds to position in the annotated *S. aureus* Mu50 genome.
[c]Fold change in wild type grown in TSB + heme (wt + heme) compared to wild type grown in TSB (wt).
[d]Fold change in Δ*hssR* grown in TSB (Δ*hssR*) compared to wild type grown in TSB (wt).
[e]Fold change in Δ*hssR* grown in TSB + heme (Δ*hssR* + heme) compared to wild type grown in TSB (wt).
[f]Fold change in Δ*hssR* grown in TSB (Δ*hssR*) compared to wild type grown in TSB + heme (wt + heme).
[g]Fold change in Δ*hssR* grown in TSB + heme (Δ*hssR* + heme) compared to wild type grown in TSB + heme (wt + heme).
[h]Fold change in Δ*hssR* grown in TSB + heme (Δ*hssR* + heme) compared to Δ*hssR* grown in TSB (wt)

HssR and HssS are required for heme-dependent activation of the *S. aureus hrtAB* promoter. HssR is predicted to be a TCS response regulator that contains an N-terminal phosphoacceptor domain and a C-terminal DNA binding domain. Response regulators with this type of domain architecture often bind the promoters of the genes they regulate, recruiting RNA polymerase and inducing gene transcription. We therefore reasoned that HssR may regulate HrtAB expression by activating the *hrtAB* promoter.

To analyze *hrtAB* promoter activity, we fused the *hrtAB* promoter to the coding sequence for XylE, a common reporter enzyme used in Gram-positive organisms (35). We found that when *S. aureus* is transformed with a plasmid containing this *hrtAB* promoter-*xylE* fusion, heme induces expression of XylE (Figure 15A). This activity is specific to the *hrtAB* promoter, as a promoterless *xylE* plasmid does not respond to heme (Figure 15A). Furthermore, mutation of *hssR* or *hssS* eliminates *hrtAB* promoter heme responsiveness. Importantly, strains bearing a plasmid that constitutively expresses XylE are not reduced in activity upon heme treatment, allowing us to conclude that a lack of XylE activity in the absence of heme is not due to heme toxicity in the heme-sensitive strain Δ*hssR* (Figure 15B). Furthermore, *hrtAB* promoter reporter activity is dose-dependent with respect to heme (Figure 15B). These data are consistent with those presented in Figure 14 and suggest that the *hrtAB* promoter requires a functional HssRS TCS to respond to heme.

Next, we tested whether HssRS-dependent *hrtAB* promoter activation is triggered by exposure to numerous relevant iron sources. We found that neither iron sulfate nor transferrin (which is not a heme-containing protein) activate the *hrtAB* promoter (Figure 15C). In contrast, hemoglobin and blood (which contain heme) both induce robust *hrtAB* promoter activity. This connects HssRS-mediated *hrtAB* promoter activation specifically to heme and heme-containing proteins that represent a biologically relevant source of nutrient iron for staphylococci.

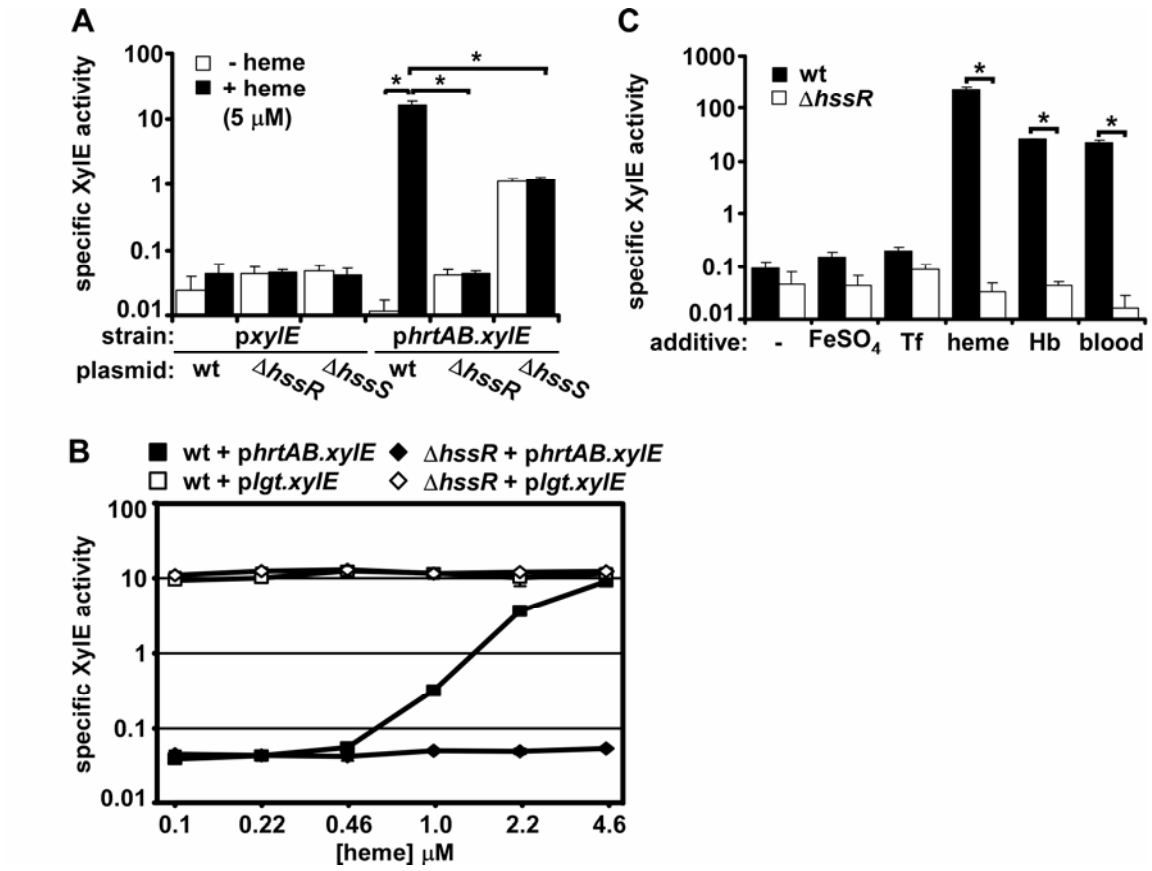

Figure 15. HssRS is required for activation of the *S. aureus hrtAB* promoter in response to heme and host-derived heme sources. ***A.*** Wild type, Δ*hssR*, and Δ*hssS* *S. aureus* transformed with either a promoterless *xylE*-containing plasmid (p*xylE*) or an *hrtAB* promoter-*xylE* fusion-containing plasmid (p*hrtAB.xylE*) were grown in medium lacking heme or containing 5 μM heme. Following growth to stationary phase, XylE activity was measured. ***B.*** *hssR* is required for dose-responsive activation of the *hrtAB* promoter. *S. aureus* wild type and Δ*hssR* harboring either p*hrtAB.xylE* or a plasmid with *xylE* under the control of the constitutive *lgt* promoter (a positive control) were grown in triplicate in the presence of the indicated concentration of heme and XylE activity was measured. ***C.*** *S. aureus* wild type or Δ*hssR* harboring p*hrtAB.xylE* were grown in TSB (-) or TSB supplemented with $FeSO_4$, transferrin (Tf), heme, hemoglobin (Hb), or mouse blood and XylE activity was determined. Adapted from Torres et al., 2007 (Ref. 169) and Stauff et al., 2007 (Ref. 158).

A direct repeat within the *hrtAB* promoter is necessary for heme-dependent promoter activation. Based on the predicted function of HssR as a DNA-binding response regulator, and based on the role of HssR in induction of *hrtAB* promoter activity in response to heme, it is likely that HssR binds to promoter sequences upstream of *hrtAB* upon exposure of staphylococci to heme in order to regulate transcription. To identify candidate DNA sequences upstream of *hrtAB* required for HssR-dependent expression, we aligned the *hrtAB* promoter (shown in schematic form in Figure 16A) from eight different species of Gram-positive bacteria that contain potential orthologues of the Hss/Hrt (Figure 16B). This analysis reveals a perfectly conserved direct repeat (DR) sequence within the predicted *hrtAB* promoter of *S. aureus* and other *Firmicutes* predicted to contain homologues of *hssRS* and *hrtAB*. A number of bases are invariant across genera and a greater degree of variation exists in the bases between and outside of the repeats, suggesting that this DR is critical for HssRS/HrtAB function. Because TCS response regulators are known to bind to DR sequences (22), we hypothesized that this DR is the *cis*-acting element with which HssR interacts.

To test whether the DR upstream of *hrtAB* is necessary for promoter activation, a series of truncation mutants within the *hrtAB* promoter were constructed within the context of the *hrtAB* promoter-*xyl*E reporter construct and tested for heme-induced reporter activity. While truncation of the *hrtAB* promoter up to the DR sequence has no effect on promoter activity (Figure 16C), removal of half or all of the DR eliminates heme-induced reporter activity (Figure 16C). Furthermore, induction of the *hrtAB* promoter by heme is eliminated by the mutation of four bases that are conserved within the DR of all organisms analyzed. Promoters containing any of the listed alterations to the DR display reporter activity at comparable levels to those of *hrtAB* promoters lacking a predicted TATA box or ribosome binding site. We conclude that the DR present within the *hrtAB* promoter is essential for the induction of promoter activity by heme.

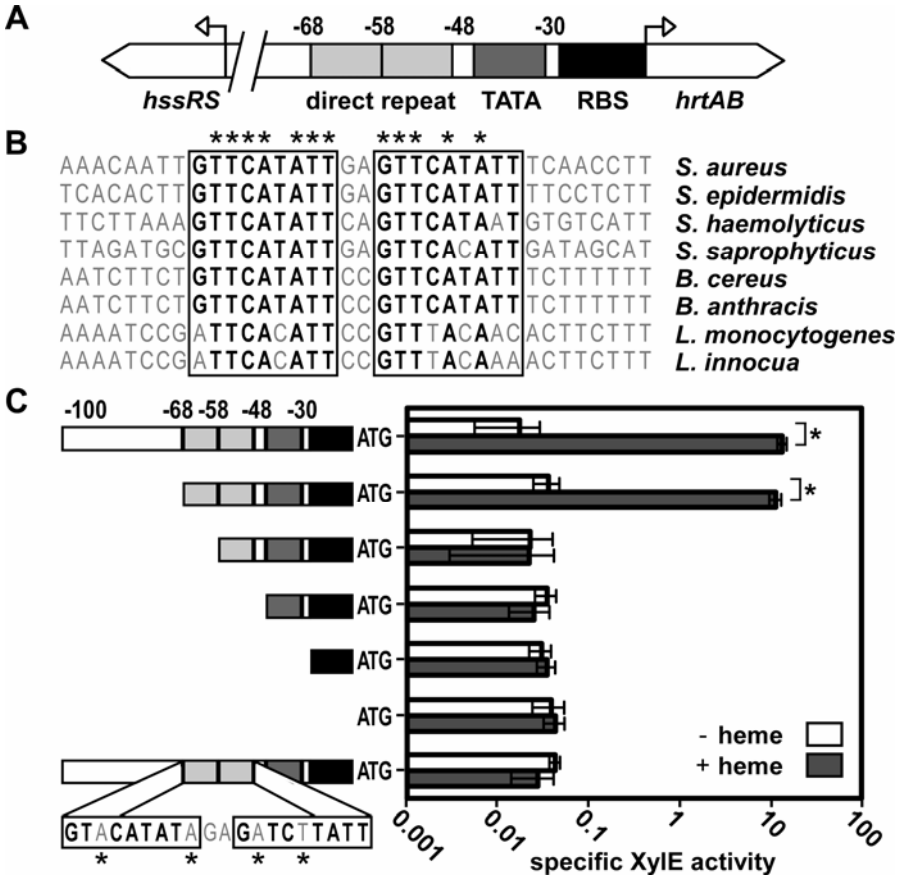

Figure 16. A direct repeat within the *hrtAB* promoter is required for heme-dependent promoter activity. ***A.*** Schematic of the *hrtAB* promoter showing the direct repeat (light grey), predicted TATA box (dark grey), ribosome binding site (RBS, black), and the *hrtAB* and *hssRS* coding sequences. Numbers indicate base position with respect to the *hrtB* start codon. ***B.*** Alignment of the direct repeat from several Gram-positive bacteria. Residues in bold occur at the given position in more than 50% of the examined sequences and match the *S. aureus* direct repeat. Asterisks above residues indicate absolute conservation across the sequences examined. ***C.*** *hrtAB* promoter truncation and mutation analyses using the p*hrtAB.xylE* reporter construct from *A*. Sequences within the *hrtAB* promoter were deleted as indicated. In addition, four conserved residues within the *hrtAB* promoter were mutated in the context of the full-length reporter construct (asterisks denote mutated bases). *S. aureus* harboring the indicated constructs were grown in triplicate in medium lacking heme (white bars) or containing 5 μM heme (grey bars) and reporter activity was measured. Asterisks denote that the observed changes are statistically significant ($p < 0.05$ using Student's *t*-test). Adapted from Stauff et al., 2007 (Ref. 158).

HssS-HssR undergo phosphotransfer *in vitro.* HssS and HssR display significant sequence and domain similarity to other bacterial TCS histidine kinases and response regulators, respectively. Upon receiving appropriate signals, bacterial histidine kinases undergo autophosphorylation at a specific histidine residue, allowing a cognate response regulator through which they signal to subsequently catalyze phosphotransfer to an aspartate residue (109). To predict the HssR and HssS residues that participate in phosphotransfer, the intracellular domain of HssS was aligned with the dimerization/phosphorylation domain from five characterized bacterial TCS histidine kinases (Figure 17A) (PhoQ (117); EnvZ (118); CheA (75); YycG (54); KdpD (121)). Likewise, HssR was aligned with the phosphoacceptor domain from five known bacterial TCS response regulators (Figure 17B) (PhoP (70); OmpR (164); CheY (160); YycF (54); KdpE (173)). Consistent with their assignment as members of TCS, a conserved histidine residue was identified in the predicted dimerization/phosphorylation domain of HssS (H249) and a conserved aspartate residue was identified in the predicted phosphoacceptor domain of HssR (D52) (Figures 17A & 17B).

To determine whether HssS undergoes autophosphorylation and whether HssR catalyzes phosphotransfer, and to determine whether H249 of HssS and D52 of HssR are the signaling residues of HssRS, *in vitro* phosphotransfer experiments were performed using purified HssS and HssR as well as alanine substitution mutants at both putative signaling residues. The signaling domain from both wild type and mutant HssS (HssS and HssS:H249A) and full-length wild type and mutant HssR (HssR and HssR:D52A) were expressed as hexahistidine-tagged fusion proteins in *E. coli* and purified to homogeneity. Because *in vitro* autophosphorylation of sensor kinase signaling domains is a common property of TCS histidine kinases that occurs in the absence of any ligand or other signaling input, we added γ^{32}P-ATP to HssS and tested autophosphorylation by SDS-PAGE followed by autoradiography. We found that

exposure of HssS to γ^{32}P-ATP results in rapid autophosphorylation that is not observed with HssS:H249A (Figures 17C & 17D). Addition of HssR to phosphorylated HssS results in the dephosphorylation of HssS and phosphorylation of HssR, while HssS dephosphorylation and HssR phosphorylation are not observed when HssR:D52A is added (Figures 17C, 17D & 17E). These results are consistent with a model in which HssS undergoes autophosphorylation at histidine 249 and subsequently transfers its phosphate group to aspartate 52 of HssR.

HssS-HssR phosphotransfer residues are required for resistance of *S. aureus* to heme toxicity. To test whether phosphotransfer between HssS and HssR is required by *S. aureus* for resistance to a high concentration of heme, we tested HssS and HssR phosphotransfer mutants for functionality *in vivo*. Full-length c-Myc-tagged versions of wild type HssS and HssR as well as their respective phosphotransfer site mutants were cloned into an *S. aureus* expression vector, transformed into *S. aureus* Δ*hssS* and Δ*hssR*, and assessed for complementation. While *S. aureus* wild type resists 10 μM heme, in Δ*hssS* growth is arrested (Figure 18A). Expression of HssS-Myc *in trans* in Δ*hssS* restores heme adaptation. However, HssS-Myc:H249A is not able to complement the heme-sensitive phenotype of Δ*hssS* (Figure 18A) in spite of expression levels similar to those of wild type HssS-Myc (Figure 18B). In similar experiments, we found that an epitope-tagged HssR-Myc is able to complement the heme-sensitive phenotype of *ΔhssR* (Figure 18C). HssR-Myc:D52N, a phosphotransfer site mutant chosen instead of HssR-Myc:D52A due to poor expression of HssR-Myc:D52A in *S. aureus*, is not able to complement in spite of significant expression (Figure 18C, 18D). Taken together with the data presented in Figures 13 through 15, these data suggest that functional signaling between HssS and HssR is necessary for the adaptation of *S. aureus* to heme toxicity, presumably through the regulated expression of HrtAB.

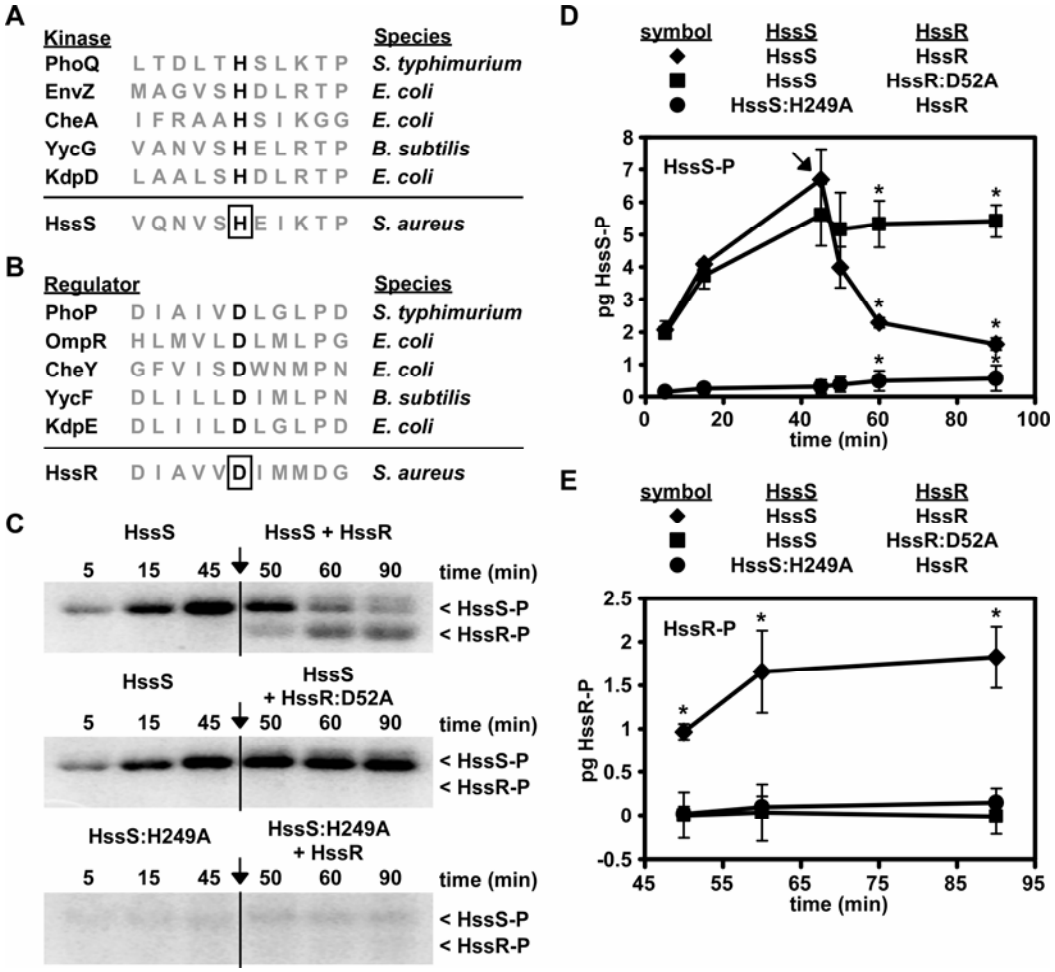

Figure 17. *S. aureus* HssS-HssR phosphotransfer is dependent on conserved signaling residues. ***A.*** Alignment of phosphorylated histidine residues from bacterial histidine kinases. Histidine residues are in bold. The predicted phosphotransfer histidine of HssS (H249) is boxed. ***B.*** Alignment of phosphorylated aspartic acid residues from cognate response regulators to histidine kinases from *A*. Phosphoacceptor aspartate residues are shown in bold. The predicted phosphorylated aspartate of HssR (D52) is boxed. ***C.*** *In vitro* phosphotransfer between HssS and HssR. HssS or mutant HssS:H249A were added to γ^{32}P-ATP and samples were collected at intervals after the start of labeling. Following 45 minutes of labeling, HssR or mutant HssR:D52A were added to HssS (vertical arrow) and samples were collected. Proteins were separated by SDS-PAGE and gels were exposed by autoradiography. ***D.*** Quantification of HssS phosphorylation from triplicate experiments described in *D*. Addition of HssR is indicated by a diagonal arrow. Asterisks denote statistically significant differences in HssS-P amount when compared to any other condition at that time point by Student's *t*-test ($p < 0.05$). x axis represents time after the start of labeling. ***E.*** Quantification of HssR ^{32}P-phosphorylation (HssR-P) as described for HssS in *E*. x axis represents time after the start of labeling (or 5, 15, or 45 minutes after the addition of HssR). Error bars correspond to one standard deviation from the mean. Adapted from Stauff et al., 2007 (Ref. 158).

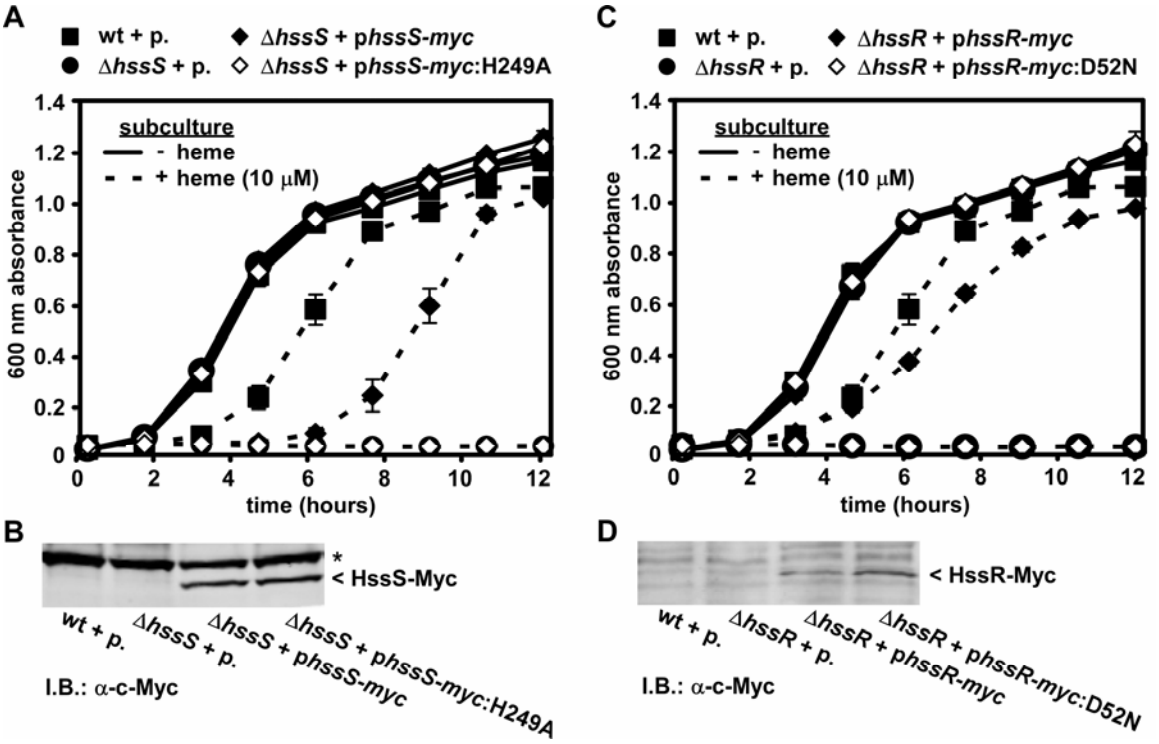

Figure 18. Residues essential for HssRS-HssR phosphotransfer are required for resistance of *S. aureus* to heme toxicity. ***A.*** Sensitivity of *S. aureus* Δ*hssS* expressing HssS:H249A to heme toxicity. *S. aureus* wild type harboring an empty plasmid (wt + p., solid squares), Δ*hssS* harboring an empty plasmid (Δ*hssS* + p., solid circles), Δ*hssS* harboring p*hssS-myc* (Δ*hssS* + p*hssS-myc*, solid diamonds) and Δ*hssS* harboring p*hssS-myc*:H249A (Δ*hssS* + p*hssS-myc*:H249A, empty diamonds) were cultured in medium lacking heme (solid lines) or containing 10 μM heme (dashed lines). A_{600} readings were taken on triplicate cultures at the indicated times after inoculation and averages +/- one standard deviation are plotted. ***B.*** Anti-c-Myc immunoblot (I.B.: α-c-Myc) of protoplasts from *S. aureus* strains described in *A*. Immunoblot is representative of results obtained from three independent experiments. Asterisk denotes a consistently observed cross-reactive band. ***C.*** Sensitivity of *S. aureus* Δ*hssR* expressing HssR:D52N to heme toxicity. *S. aureus* wild type harboring an empty plasmid (wt + p., solid squares), Δ*hssR* harboring an empty plasmid (Δ*hssR* + p., solid circles), Δ*hssR* harboring p*hssR-myc* (Δ*hssR* + p*hssR-myc*, solid diamonds) and Δ*hssR* harboring p*hssR-myc*:D52N (Δ*hssR* + p*hssR-myc*:D52N, empty diamonds) were grown and analyzed as described in *A*. ***D.*** Anti-c-Myc immunoblot (I.B.: α-c-Myc) of cytoplasmic fractions of *S. aureus* strains described in *C.* Immunoblot is representative of results obtained from three independent experiments. Adapted from Stauff et al., 2007 (Ref. 158).

HssR binds to the *hrtAB* promoter when phosphorylated and when *S. aureus* encounters heme. Phosphorylation of bacterial TCS response regulators induces conformational changes that lead to the binding of these proteins to their target DNA sequences (26). To test whether HssR can bind to the *hrtAB* promoter when phosphorylated, purified HssR and its phosphotransfer site mutant HssR:D52A were incubated with the phosphorylating reagent acetyl phosphate. After incubation, proteins remain soluble (Figure 19A, top) but only phosphorylated HssR and not HssR:D52A is captured by streptavidin-conjugated beads coated with biotinylated *hrtAB* promoter DNA (Figure 19A, bottom). Binding of phosphorylated HssR to DNA is specific to the *hrtAB* promoter, as HssR is not captured by beads coated with biotinylated *hrtB* coding sequence DNA. This suggests that HssR specifically binds to the *hrtAB* promoter when it is phosphorylated at aspartate residue 52.

To test whether HssR binds to the *hrtAB* promoter upon exposure of *S. aureus* to heme, cytoplasmic extracts were prepared from heme-treated and untreated Δ*hssR* carrying a plasmid encoding an epitope-tagged *hssR-myc*. Extracts were added to the same bead-DNA complexes described above and capture of HssR-Myc was tested by eluting bound proteins, performing SDS-PAGE, and immunoblotting against the epitope tag of HssR-Myc. We found that HssR-Myc is only captured by *hrtAB* promoter DNA, consistent with the binding specificity observed with *in vitro* phosphorylated protein (Figure 19B). Furthermore, HssR-Myc only associates with the *hrtAB* promoter when *S. aureus* encounters heme (Figure 19B). This indicates that in *S. aureus*, phosphorylation of HssR by HssS is the mechanism by which binding of HssR to the *hrtAB* promoter is controlled.

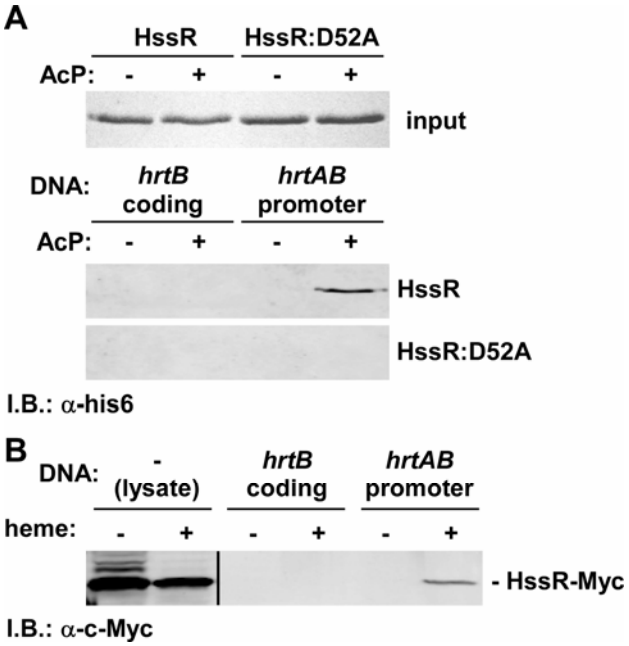

Figure 19. HssR binds to the *hrtAB* promoter when phosphorylated and when *S. aureus* encounters heme. ***A.*** Purified HssR and HssR:D52A were incubated in the absence (-) or presence (+) of acetyl phosphate (AcP) and soluble protein was analyzed by SDS-PAGE and coomassie blue staining (*top*). Acetyl phosphate-treated or untreated HssR or HssR:D52A was added to streptavidin-conjugated magnetic beads bound to biotinylated DNA corresponding to the *hrtB* coding sequence or the *hrtAB* promoter (*bottom*). Beads were removed with a magnet, washed four times, and bound protein was eluted with high salt buffer. Samples were analyzed by SDS-PAGE followed by immunoblotting with an anti-hexahistidine tag antibody (I.B.: α-his6). Both panels (HssR and HssR:D52A) are from a single membrane; result is representative of triplicate independent experiments. ***B.*** Cytoplasmic extract was prepared from wild type *S. aureus* harboring p*hssR-myc* and grown to early stationary phase in the absence of heme (-) or in the presence of 7 μM heme (+). Bead-DNA complexes prepared as described in *A* were added to lysate from heme-treated or untreated *S. aureus*, removed with a magnet, washed four times, and proteins were eluted with high salt buffer. Samples were analyzed by SDS-PAGE followed by anti-c-Myc immunoblotting (I.B.: α-c-Myc). Lysate represents 1% of input into binding reactions; vertical bar designates cropped empty wells. Result is representative of triplicate independent experiments. Adapted from Stauff et al., 2007 (Ref. 158).

HssR binds to the direct repeat within the *hrtAB* promoter. To test whether HssR-Myc specifically associates with the direct repeat sequence within the *hrtAB* promoter, HssR-Myc bound to *hrtAB* promoter DNA-complexed beads was eluted in a competitive elution experiment. Double-stranded 40-mer oligonucleotides were prepared that correspond to the *hrtAB* promoter direct repeat or a direct repeat mutated in the four conserved residues essential for heme-induced promoter activity (Figures 16C). Bound proteins were sequentially eluted with increasing concentrations of double-stranded oligonucleotides and were detected by SDS-PAGE followed by immunoblotting against the epitope tag of HssR-Myc (Figure 20A). While double-stranded oligonucleotides containing a wild type direct repeat elute HssR-Myc from the *hrtAB* promoter at concentrations as low as 0.1 μM, oligonucleotides with a mutant direct repeat do not elute HssR-Myc at concentrations up to 12.5 μM, a result that is reproducible across multiple experiments (Figure 20B). Taken together, these results suggest that HssR binds to the direct repeat sequence within the *hrtAB* promoter in order to induce expression of HrtAB when *S. aureus* senses heme.

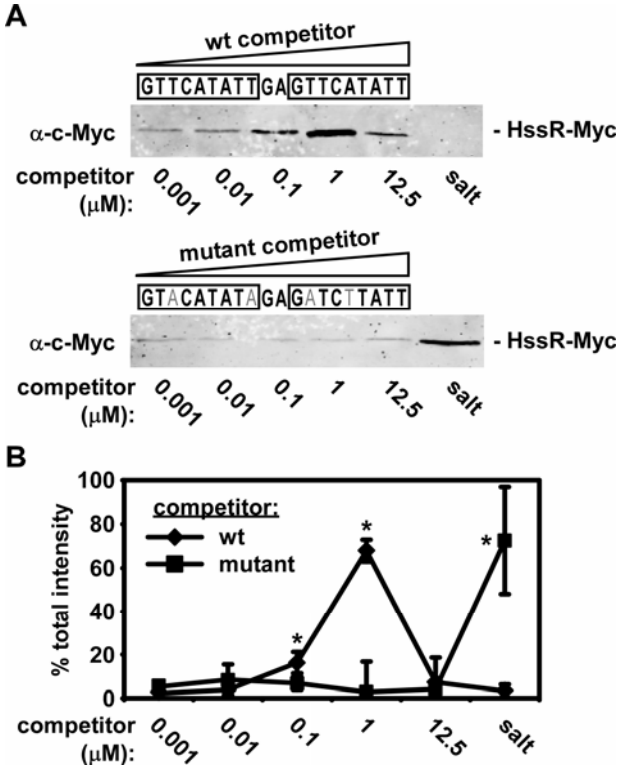

Figure 20. HssR binds to the direct repeat within the *hrtAB* promoter. ***A.*** Double-stranded 40-mer oligonucleotides were synthesized that match the sequences adjacent to and including the wild type *hrtAB* promoter direct repeat and a direct repeat in which four conserved residues are mutated (grey residues). Lysate from heme-treated *S. aureus* harboring *phssR-myc* was applied to streptavidin-conjugated magnetic beads bound to biotinylated *hrtAB* promoter DNA. Increasing concentrations (0.001, 0.01, 0.1, 1, 12.5 μM) of wild type and mutant direct repeat double-stranded oligonucleotides were used to sequentially elute bound proteins. Remaining protein was eluted with high salt buffer. Samples were analyzed by SDS-PAGE followed by anti-c-Myc immunoblotting (α-c-Myc). ***B.*** Quantification of results from triplicate experiments described in *A*. Individual band intensities were determined and are expressed as the percentage of total band intensity for a given elution series. Asterisks denote that the difference in the average percent intensity of bands corresponding to an indicated elution is statistically significant when compared to any other average percent intensity within the elution series ($p < 0.05$ using Student's *t*-test). Error bars represent one standard deviation from the mean. Adapted from Stauff et al., 2007 (Ref. 158).

Discussion

Gene regulation is one of the most widely studied areas of *S. aureus* physiology. To date, six different staphylococcal TCS histidine kinases and their cognate response regulators have been characterized: AgrAC, SaeRS, SrrAB/SrhRS, ArlRS, LytRS, YycGF, and GraRS/ApsRS (28, 36, 48, 57, 64, 74, 84, 101, 114, 132, 166, 184). Although these systems have been identified and confirmed to play important roles in gene regulation, the signals that are recognized and the molecular mechanisms responsible for signal transduction have only been well-characterized in a few cases. Herein, we have provided insight into the mechanism by which *hrtAB* expression is induced upon exposure of *S. aureus* to heme. We show that the TCS HssRS regulates expression of the *hrtAB* promoter in response to heme and is required for heme resistance in *S. aureus.* We present evidence that *hrtA* is the major cytoplasmic target of activation by HssRS. Furthermore, we elucidate the signaling events by which HssRS controls expression of HrtAB in response to heme. Our observations are consistent with the model presented in Figure 21. We propose that (1) heme liberated from host hemoglobin is imported into the staphylococcal cytoplasm through the Isd and Hts systems, (2) resulting in HssS activation that leads to (3) autophosphorylation and (4) phosphotransfer to HssR. (5) Phosphorylated HssR binds to the *hrtAB* promoter direct repeat, (6) increasing the transcription of the *hrtAB* genes by recruitment of RNA polymerase. (7) Newly synthesized HrtAB alleviates heme toxicity (8) through the export of an unknown molecule that accumulates in the *S. aureus* cytoplasm upon heme exposure (for discussion of the potential HrtAB transport substrate, see Chapters III and VI). These studies connect HssRS with the adaptive response of staphylococci to heme and reveal the functional details of a newly identified *S. aureus* TCS.

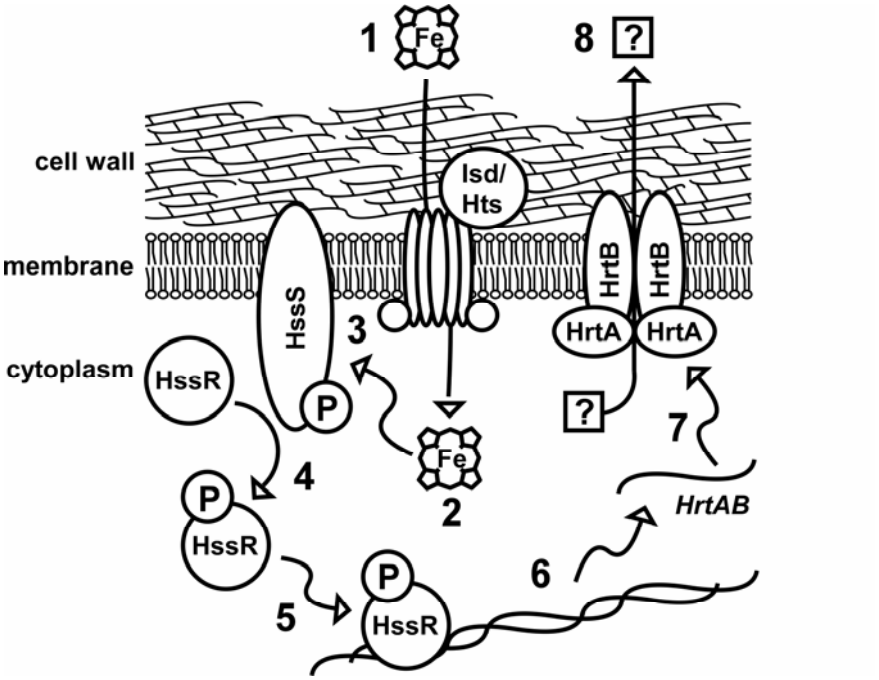

Figure 21. Signaling events that connect heme sensing by the HssRS two-component system to up-regulation of HrtAB and heme detoxification. (1) Heme is imported into the staphylococcal cytoplasm through the Isd and Hts systems. (2) Heme activates HssS, possibly by sensing the heme-induced accumulation of a toxic metabolite. Activation of HssS results in (3) HssS autophosphorylation and (4) phosphotransfer to HssR. (5) Phosphorylated HssR binds to a direct repeat within the *hrtAB* promoter, (6) increasing the transcription of the *hrtAB* genes by recruitment of RNA polymerase. (7) Newly synthesized HrtAB alleviates heme toxicity (8) through the export of an unknown molecule that accumulates in the *S. aureus* cytoplasm upon heme exposure. Adapted from Stauff et al., 2008 (Ref. 157).

The mechanism by which HssS senses heme is unknown. Although HssS may sense heme by direct binding, HssS also could sense one of the toxic effects that heme has on the cell. Genomics-based approaches have not revealed a potential heme-binding domain in HssS, and the predicted sensing domain of this kinase has little sequence similarity to any protein with a known function (169). Furthermore, no amino acids that typically engage in axial coordination of the iron atom of heme are conserved in the putative sensing domain of all of the potential HssS orthologues (unpublished observations). Identification of the ligand for HssS will lay the groundwork for a mechanistic understanding of how this histidine kinase is activated upon heme exposure (see Chapter VI). This would represent a significant advance for understanding HssS function and the mechanism employed by *S. aureus* to regulate the tight balance between heme acquisition and heme toxicity.

HssS is one of the few histidine kinases that respond to a molecular marker of vertebrate tissue. Importantly, other TCS that recognize heme are found in the Gram-positive pathogen *Corynebacterium diphtheriae*, a bacterium that is not closely related to *S. aureus* (20, 21, 140, 141). In *C. diphtheriae*, the TCS ChrAS and HrrAS are capable of responding to heme or hemoproteins (140). However, in addition to the absence of any significant sequence identity between the staphylococcal and corynebacterial systems, two major aspects of ChrAS and HrrAS distinguish them from the *S. aureus* HssRS system. First, ChrAS and HrrAS both regulate expression of the *C. diphtheriae* heme oxygenase HmuO, while HssRS does not appear to regulate expression of the *S. aureus* heme oxygenases (21, 140, 158). HmuO is capable of catabolizing heme and is therefore a critical factor required for heme metabolism in *C. diphtheriae* (142). In *S. aureus*, IsdG and IsdI are iron-regulated heme oxygenases that also break down heme (134, 149, 182). However, our 2D-DIGE experiments have failed to reveal a role for HssRS in the regulation of IsdG/I expression, indicating that HssRS does not regulate

these heme-degrading enzymes in *S. aureus* (Table 8). Second, despite the fact that HssRS from *S. aureus* and ChrAS/HrrAS from *C. diphtheriae* both respond to heme, the histidine kinase HssS and the kinases ChrS/HrrS differ dramatically in terms of the predicted structure of their signal-sensing domains. While HssS is predicted to have an N-terminal periplasmic sensing domain flanked by two transmembrane helices, ChrS/HrrS are predicted to have sensing domains composed of five transmembrane helices flanked by short loops (21, 169). This difference in predicted structure suggests that HssS may sense heme through a mechanism that is different from that of ChrS/HrrS or that these TCS might sense different effects that heme has on the Gram-positive bacterial cell. Interestingly, *C. diphtheriae* strains lacking the *chrAS* genes exhibit elevated heme sensitivity that is not dependent on reduced HmuO expression (20). This suggests the presence of a ChrAS-regulated heme-detoxification system in *Corynebacterium diphtheriae* (20). Accordingly, interrogation of the *C. diphtheriae* genome using *S. aureus hrtAB* as query reveals the presence of genes encoding an HrtAB-like ABC transporter (DIP2323/24, unpublished data). Remarkably, these genes are a single open reading frame away from *chrAS* on the *C. diphtheriae* chromosome. This indicates that *C. diphtheriae* DIP2323/24 may be heme- and ChrAS-regulated orthologues of the *S. aureus* HrtAB system that protect this organism from heme toxicity.

The ability of bacterial pathogens to sense and respond to heme is not limited to Gram-positive organisms. The Gram-negative mammalian pathogen *Bordetella pertussis* also encodes a heme sensing system (25, 89-91, 171, 172). In *B. pertussis*, the heme receptor BhuR binds to heme, transducing signals into the periplasm that activate the cytoplasmic membrane protein RhuR (89, 90, 172). RhuR alters the activity of the cytoplasmic protein RhuI, which regulates the expression of the *B. pertussis* heme uptake system BhuRSTUV (89, 90, 172). Through this mechanism, *B. pertussis* is able to sense exogenous heme and increase the expression of systems required for heme

uptake from the host. Thus the *B. pertussis* RhuIR/BhuR system differs from the HssRS system of *S. aureus* in that the former is devoted to the sensing of host heme for the purposes of heme acquisition, whereas the latter is required for sensing host heme to avoid heme toxicity (25, 89-91, 120, 158, 169, 171, 172). Furthermore, HssRS is a two-component system, while RhuI is an extracytoplasmic function sigma factor and RhuR is a regulator of RhuI activity. Thus, the mechanism by which heme is sensed by these systems as well as the details of signaling appear to be distinct. It appears that the pathogens *S. aureus* and *B. pertussis* are both able to sense host heme and transduce signals that alter gene expression, but that these events occur through distinct mechanisms and for different reasons.

We demonstrate here that binding of phosphorylated HssR to *hrtAB* promoter DNA is sensitive to alterations in the direct repeat sequence to which it binds. A consensus sequence for HssR (GTTCATATT$(N)_2$GTTCATATT) can be predicted by comparing the *hrtAB* direct repeat across all available bacterial genomes. Using genomic analyses, we have been unable to identify an *S. aureus* gene or operon other than *hrtAB* that contains this perfect direct repeat within its promoter (data not shown). However, an HssR consensus site containing 3-4 mismatches can be detected in the predicted promoter region of 14 *S. aureus* genes. Three of these with potential roles in the pathogenesis of *S. aureus* include SAV1553 (the superoxide dismutase *sodA*), SAV1159 (a predicted fibrinogen-binding protein precursor), and SAV2644 (a predicted autolysin) (data not shown). Although 2D-DIGE analyses did not reveal protein features other than HrtA that are up-regulated in a heme-dependent, HssR-dependent manner, it remains a possibility that additional *S. aureus* genes are regulated by HssR upon exposure of staphylococci to high concentrations of heme.

This study is one of the first examples of the *in vitro* reconstitution of a *S. aureus* TCS; furthermore, it represents the characterization of signaling and DNA binding events

important for the functioning of one of the few bacterial TCS that is responsible for sensing an abundant host molecule. Understanding the mechanisms by which bacterial pathogens recognize host molecules will provide insight into the ways in which pathogenic bacteria sense and respond to the host environment.

CHAPTER V

CONSERVATION OF HEME SENSING AMONG GRAM-POSITIVE BACTERIA

Introduction

The evolutionarily related Gram-positive pathogens *Staphylococcus aureus* and *Bacillus anthracis* are both capable of causing devastating disease upon breaching host epithelial barriers (46, 59, 119). *S. aureus*, a commensal of the skin and nares, is able to infect virtually any site within the human body, leading to diseases including skin and soft tissue infections, endocarditis, and pneumonia (59). In contrast, *B. anthracis* is a spore-forming livestock pathogen that causes a rare zoonotic disease in humans known as anthrax (46, 119). Anthrax arises when spores germinate within host tissues and can progress to systemic bacteremia followed by sudden death (46, 119). Although the life cycles and pathogenic strategies of *S. aureus* and *B. anthracis* differ markedly, both pathogens must circumvent mechanisms of innate immunity including host-mediated sequestration of iron.

To overcome cellular stress resulting from iron paucity, both *S. aureus* and *B. anthracis* express similar (Isd) systems devoted to the acquisition and degradation of host heme for nutrient iron needs (106, 107, 112, 151). The fact that *S. aureus* and *B. anthracis* express functionally similar Isd systems implies that nutrient iron acquisition is a challenge that is faced and met in a similar way by both pathogens despite differences in their life cycles and mechanisms of pathogenesis. Although it is known that both bacteria acquire heme from the host during infection, it is currently unclear whether heme sensing and detoxification is a general feature of Gram-positive pathogens that associate with host tissues rich in heme. It is likely that a pathogen such as *B. anthracis*, which is capable of replicating to a high density within the bloodstream of its host (46),

inducing hemolysis (147), and acquiring heme (106, 107), may require systems devoted to the avoidance of heme toxicity.

Here, we demonstrate that *B. anthracis* encodes functional HssRS and HrtAB systems required for protection from heme toxicity. We show that differential heme resistance within the *Bacilli* correlates with the presence of *hssRS/hrtAB* genes. Furthermore, *B. anthracis* HssRS exhibits an elevated autophosphorylation and phosphotransfer rate that correlates with the increased *in vivo* activity of this TCS. More specifically, we report that domains of the histidine kinase HssS are likely responsible for the elevated function of *B. anthracis* HssS. *B. anthracis* is highly sensitive to heme toxicity in the absence of HrtAB function, and may therefore require an increased ability to mount a heme detoxification response through heme sensing by HssS and signal transduction through HssR. We also present evidence implicating the previously uncharacterized signal recognition domain of HssS in heme sensing. Last, we show that the *hrtAB* promoter is activated in a cutaneous model of anthrax, suggesting a role for heme sensing during *B. anthracis* infection. These results demonstrate that heme sensing by HssRS and subsequent heme detoxification by HrtAB are conserved in *B. anthracis* and that heme stress may be encountered by a wide range of pathogenic or saprotrophic Gram-positive bacteria.

Methods

Bacterial strains and growth conditions –B. cereus, B. thuringiensis, B. israelensis, B. licheniformis, and B. subtilis were acquired from the Bacillus Genetic Stock Center (College of Biological Sciences, The Ohio State University, www.bgsc.org). *B. anthracis* Sterne was used for all experiments (159). *S. aureus* was grown in TSB or BHI; *Bacilli* were grown in BHI or LB. All plasmid construction was performed using *Escherichia coli* DH5α. Plasmid DNA to be introduced into *B. anthracis* was propagated in the *E. coli* strain K1077 (88). Plasmid selection was performed in *S. aureus* and *B. anthracis* by supplementing media with 10 μg/ml chloramphenicol (complementation and reporter plasmids) or 20 μg/ml kanamycin (knockout constructs).

Genetic manipulation of S. aureus – Genetic manipulation of *S. aureus* and construction of *S. aureus* Δ*hssRS* was performed as described previously (12, 158).

Genetic manipulation of B. anthracis – Electroporations were performed as previously described (88), with modifications. *E. coli* K1077 harboring plasmids to be introduced into *B. anthracis* were grown overnight in 15 ml of LB in 50 ml conical tubes. DNA was miniprepped from K1077 and dialyzed against water to remove traces of salt prior to electroporation. Electrocompetent *B. anthracis* cells were prepared by growing bacteria in BHI + 0.5 M D-sorbitol to OD600 = 0.2 and washing cells three times in SMG (0.5 M D-sorbitol, 0.5 M D-mannitol, 10% glycerol) without proteinase K treatment. Four μl of DNA was added to 50 μl competent cells and mixtures were incubated on ice 10 minutes. Electroporations were carried out in 1 mm gap cuvettes with a Bio-Rad Gene Pulser using an exponential decay protocol set to 2500 V, 1 ms time constant. After electroporation, cells were recovered in BHI + 0.5 M D-sorbitol for 2 hours at 30 °C with shaking and plated onto BHI + antibiotic. For generation of *B. anthracis hrtA, hssRS,* and *hssS* knockout constructs for insertion/deletion mutagenesis, the erythromycin

resistance gene *ermC* was inserted between 1 kilobase regions flanking *hrtA*, *hssRS*, or *hssS* in the thermosensitive mutagenesis plasmid pLM4 (86). Mutagenesis was performed as described previously (86). The incorporation of mutations, loss of pLM4, and maintenance of pXO1 were confirmed by PCR.

Epitope tagging of hssS – A C-terminal *c-myc* epitope tag was incorporated into *S. aureus* and *B. anthracis hssS* alone and *hssS* within the *hssRS* operon using a PCR-based approach as described previously (158). Briefly, PCR reactions were assembled containing a 5' primer annealing to the 5' end of *hssR* (for amplification of *hssR-hssS-myc*) or *hssS* (for *hssS-myc*), dilutions of a 3' primer annealing to the 3' end of *hssS-myc* and encoding the c-Myc epitope tag (EQKLISEEDL), and excess of a 3' primer annealing to the *c-myc* coding region and incorporating a restriction endonuclease site. Tagged *hssS* is designated *hssS-myc* and tagged *hssRS* is designated *hssR-hssS-myc*.

Construction of complementation plasmids – All complementation and reporter plasmids were constructed in a pOS1 (143) or pOS1p*lgt* (29) background. A *B. anthracis hrtA* complementation construct was generated by PCR-SOE (82) using a method described previously (169). This resulted in a seamless fusion between the *B. anthracis hrtAB* promoter and the *B. anthracis hrtA* open reading frame. PCR-SOE DNA was digested with EcoRI and BamHI and inserted into pOS1p*lgt*. For generation of a complementation plasmid containing *B. anthracis hssRS* under the control of its native promoter, *hssRS* was amplified by PCR and inserted into pOS1 between the PstI and BamHI sites. For generation of complementation plasmids containing *S. aureus*/*B. anthracis hssR-hssS-myc* under the control of the *S. aureus hssRS* promoter, the *S. aureus hssRS* promoter was first inserted between the EcoRI and NdeI sites of pOS1p*lgt* to make pOS1p*hssRS*. Promoterless *S. aureus* and *B. anthracis hssR-hssS-myc* were then amplified by PCR and inserted between the NdeI and BamHI sites of pOS1p*hssRS*. For generation of complementation plasmids containing *S. aureus*/*B.*

anthracis hrtAB under the control of their native promoters, *hrtAB* was amplified by PCR and inserted into pOS1p*lgt* between the XhoI and EcoRI sites. To construct plasmids encoding *hssS-myc* under the control of the *S. aureus hssRS* promoter, *hssS-myc* was PCR amplified and inserted into pOS1p*hssRS* between the NdeI and BamHI sites. Chimeric forms of *hssS-myc* were constructed by cloning *S. aureus* and *B. anthracis hssS-myc* in tandem in pCR2.1 (Invitrogen) and joining HssS domains together by inverse PCR followed by blunt-end ligation (see *Construction of XylE reporter plasmids* below). Chimeric forms of *hssS-myc* were then inserted into pOS1p*hssRS*.

B. anthracis HssS alignment and mutagenesis – An alignment of conserved residues in HssS was created by assembling HssS amino acid sequences from all available sequenced *Firmicute* genomes (with the exception of *Exiguobacterium sibiricum*, which clusters outside of the *Staphylococcus, Listeria,* and *Bacillus* clusters) and aligning by Clustal V method using the Lasergene 6 software package.

HssS-Myc immunoblotting – For *S. aureus* HssS-Myc immunoblots, cell lysates were prepared from bacteria grown in 5 ml TSB in 15 ml conical tubes for 15 hours at 37 °C with shaking. For *B. anthracis* HssS-Myc immunoblots, cell lysates were prepared from bacteria grown in 5 ml BHI in 15 ml conical tubes for 12 hours at 30 °C with shaking. Bacteria were pelleted, washed in 5 ml TBS (50 mM Tris, pH 7.5, 150 mM NaCl), digested in 0.5 ml TSM (100 mM Tris, pH 7.0, 500 mM sucrose, 10 mM $MgCl_2$) with 12.5 µg/ml lysostaphin (*S. aureus*) or 2 mg/ml lysozyme (*B. anthracis*), and protoplasts were sonicated in 0.5 ml TBS. Equal amounts of lysate and 2X SDS loading buffer were mixed, boiled and loaded onto 10% acrylamide gels, subjected to SDS-PAGE, and transferred to nitrocellulose membranes. Membranes were probed with 9E10 anti-c-Myc monocolonal primary and AlexaFluor-680-conjugated anti-mouse secondary (Invitrogen) antibodies. Membranes were dried and scanned using an Odyssey Infrared Imaging System (LI-COR Biosciences).

Construction of XylE reporter plasmids –Mutagenesis of the *S. aureus hrtAB* promoter-*xylE* fusion was carried out by inverse PCR-based mutagenesis. Briefly, a non-overlapping non-mutagenic primer and a primer introducing the desired mutation were designed which amplify in opposite directions on the plasmid template. Inverse PCR was carried out using *S. aureus hrtAB* promoter-*xylE* fusion as template and 5' phosphorylated oligos. Amplified DNA was blunt end ligated, transformed into *E. coli*, miniprepped, and mutagenized constructs were validated by DNA sequencing.

Construction of Lux reporter plasmids – To generate a construct in which the *Lux* genes of pXen-1 (Xenogen) (58) are under the control of the *S. aureus hrtAB* promoter, primers containing a 5' EcoRI site and a 3' BamHI site were used to amplify the *hrtAB* promoter from *S. aureus* genomic DNA. PCR-amplified DNA was inserted into pXen-1 to create the plasmid p*hrt*.*Lux*.

Construction of plasmids for expression of recombinant proteins – For construction of expression constructs for *S. aureus* HssR:D52N and *B. anthracis* HssR, HssS, HssS:H248A and HssR:D54N, *B. anthracis hssR* or *hssS* were amplified by PCR and inserted between the NdeI and BamHI sites of pET15b (Invitrogen). Constructs were validated by sequencing and were then mutagenized by inverse PCR. Protein expression was carried out as previously described (see Chapter III Methods). To validate the integrity of recombinant HssS, *S. aureus* and *B. anthracis* HssS were analyzed by mass spectrometry (Vanderbilt University Proteomics Core Facility). Intact masses were determined for both proteins and N- and C-termini were validated by MS/MS following digestion with trypsin protease.

XylE reporter assays –Bacteria harboring reporter plasmids were grown overnight in BHI (*S. aureus* and *B. anthracis* when analyzing heme induction of *hrtAB* promoter) or LB (*B. anthracis* when analyzing heme-independent *hrtAB* promoter activity) and subcultured 1:50 into 2 ml BHI in 15 ml conical tubes. Bacteria were grown for 5 hours at 37 °C and

cytoplasmic fractions were prepared and analyzed as previously reported (Chapter IV Methods) except that for *B. anthracis*, lysozyme (2 mg/ml) was used instead of lysostaphin. Absolute XylE activities were determined for *B. anthracis* reporters due to lysozyme interference during protein quantification.

Bacterial growth curve analyses – Triplicate cultures of bacteria were grown 12 hours at 30 °C with shaking in 5 ml of BHI (*B. anthracis*) or TSB (*S. aureus*) in 15 ml tubes. Each culture was subcultured 1:50 into 150 µl fresh medium in a 96-well round-bottom plate. Plates were wrapped to avoid evaporation and were grown at 37 °C with shaking at 180 rpm. 600 nm absorbance readings were taken on a Cary 50 MPR microplate reader coupled to a Cary 50 Bio UV-visible spectrophotometer (Varian, Inc.). For all experiments, absorbance readings of the triplicate subcultures were averaged and one standard deviation from the mean was plotted as error bars.

Heme preparation and concentrations - Heme (Fluka) stocks were made by dissolving heme in 0.1 M NaOH to a concentration of 10 mM. Heme concentrations were chosen based on the following considerations. For all experiments attempting to assess *hrtAB* promoter activity without any detectable interference of heme toxicity with strain growth (such as in heme-sensitive mutants), promoter induction, or XylE synthesis, 2 µM heme was utilized. Five µM heme fully induces the *hrtAB* promoter in *S. aureus* with no detectable heme toxicity and was therefore utilized to pre-adapt *B. anthracis* to heme toxicity. Ten µM heme was selected for growth curve analysis of *B. anthracis hss/hrt* mutants as a heme concentration known to completely inhibit growth of *S. aureus hss/hrt* mutants within 12 hours of subculture, and as a heme concentration known to slightly inhibit growth of wild type *S. aureus* in TSB. Twenty µM heme is known to inhibit growth of *S. aureus* in BHI and was therefore used to inhibit growth of *Bacilli*; 20 µM heme also completely inhibits growth of *S. aureus* and *B. anthracis* Δ*hssS* up to 24 hours and was therefore used in experiments assessing the heme resistance of complemented

derivatives of Δ*hssS*. Thirty μM heme was used to inhibit the growth of *S. aureus* and *B. anthracis* Δ*hssRS* due to the significant heme resistance of strains harboring *hssRS* complementation plasmids. Fifty μM heme was chosen in experiments analyzing the native or pre-adapted heme resistance of wild type strains in BHI due to the inherent heme resistance of these strains.

HssS-HssR autophosphorylation and phosphotransfer assays –Autophosphorylation of *S. aureus* and *B. anthracis* HssS signaling domain was carried out similar to previously described assays (see Chapter IV Methods). Briefly, 25 μl reaction mixtures were prepared containing 288 μg/ml HssS, 50 mM Tris, pH 8.0, 5 mM $MgCl_2$, 200 mM KCl, 0.2 mM DTT, 10 % glycerol, 20 μM unlabeled ATP, 5 μCi [γ^{32}P]ATP. Five μl samples were mixed with 2X SDS-PAGE loading buffer at various time points after the addition of radiolabeled ATP, samples were resolved by SDS-PAGE, and gels were dried and analyzed using a PhosphorImager. To analyze phosphotransfer from HssS to HssR, *B. anthracis* and *S. aureus* HssS were labeled for 15 and 50 minutes, respectively, in reaction mixtures described above. HssR or HssR mutant was added to this reaction to a final concentration of 890 μg/ml. Samples were taken and analyzed as described above.

Bacterial heme killing assays – 5 ml cultures of *S. aureus* and *B. anthracis* wild type and Δ*hrtA* were grown in 15 ml conical tubes for 12 hours at 30 °C with shaking at 180 rpm. Bacteria were subcultured 1:100 into BHI or BHI + 10 μM heme and incubated at 37 °C for 4 hours. At the time of subculture and following incubation, bacterial colony forming units (CFU) were enumerated by performing serial dilutions in PBS and plating cells on BHI agar.

B. anthracis infections and in vivo imaging system (IVIS)-based imaging – Spores for infection of mice were prepared as described previously (108) with modifications. Briefly, *B. anthracis* harboring pXen-1 or p*hrt.Lux* were grown for 12 hours in 5 ml 2X SG

medium (100) in 15 ml conical tubes at 30 °C with shaking. Cells were subcultured 1:100 into 250 ml flasks containing 30 ml 2X SG and were shaken at 37 °C for 4 days. Spore-containing cultures were then pelleted and washed three times with water, heated to 70 °C for 30 minutes, and then washed again with water. Purified spores were serially diluted and plated onto BHI to obtain a viable spore count. Spore preparations were stained using malachite green to microscopically confirm the presence of spores and the absence of vegetative bacilli. For injection of 200 or 2000 wild type or Δ*hrtA B. anthracis* spores for virulence studies, spore preparations were diluted to a concentration of 2 or 20 spores/µl in sterile PBS. 100 µl of spore dilutions were injected subcutaneously into the inguinal region of 6-week-old A/J mice (two groups of 10 on different weeks). Following spore inoculation, mice were monitored for signs of disease and were sacrificed when found to be moribund. Mice were grouped according to the 12-hour interval in which they were sacrificed. For IVIS studies, spores harboring *Lux* plasmids were diluted to a concentration of 200 spores/µl in sterile PBS. 100 µl of spore dilutions (20000 spores/mouse) were injected subcutaneously into the inguinal region of 6-week-old A/J mice (two groups of 5 mice). Following spore inoculation, mice were visualized at 12-hour intervals using a Xenogen IVIS 200. Mice were monitored for signs of disease and were sacrificed when found to be moribund.

Results

Multiple Gram-positive bacteria encode putative orthologues of *S. aureus* HrtAB and HssRS. Consistent with the supposition that *B. anthracis* may need to avoid the lethal side effects of heme acquisition, Van Heyningen demonstrated in 1948 that *B. anthracis* is capable of proliferating on plates containing a high amount of heme (76). Interestingly, *B. subtilis* (a bacterium not commonly associated with vertebrate tissues containing heme) is sensitive to heme toxicity (76). We found a potential explanation for this observation while interrogating *Firmicute* genomes for putative *hssRS/hrtAB* systems. These searches revealed that *B. anthracis* encodes putative orthologues of *S. aureus hssRS/hrtAB* (Figure 22), whereas *hss/hrt* genes are absent from the genome of *B. subtilis*. Furthermore, a number of other *Firmicutes* with pathogenic or saprotrophic lifestyles are also predicted to encode *hss/hrt* (Figure 22). This implies that *B. anthracis* and other pathogenic or saprotrophic *Firmicutes* may overcome heme toxicity through a similar mechanism to that utilized by *S. aureus*.

Phylogenetically related *Bacilli* display differential heme resistance. To test whether encoding *hss/hrt* correlates with resistance to heme toxicity, we assessed the heme resistance of four *Bacilli* that contain these genes (*B. anthracis, B. cereus, B. thuringiensis,* and *B. israelensis*) and two with no identifiable *hss/hrt* orthologues (*B. licheniformis* and *B. subtilis*) (Figure 23). We found that each of the four *Bacilli* encoding putative Hss/Hrt systems are able to proliferate in 20 μM heme, while both *Bacilli* lacking Hss/Hrt systems are unable to proliferate in this concentration of heme (Figure 23). These data link the presence of *hss/hrt* genes with resistance to heme toxicity.

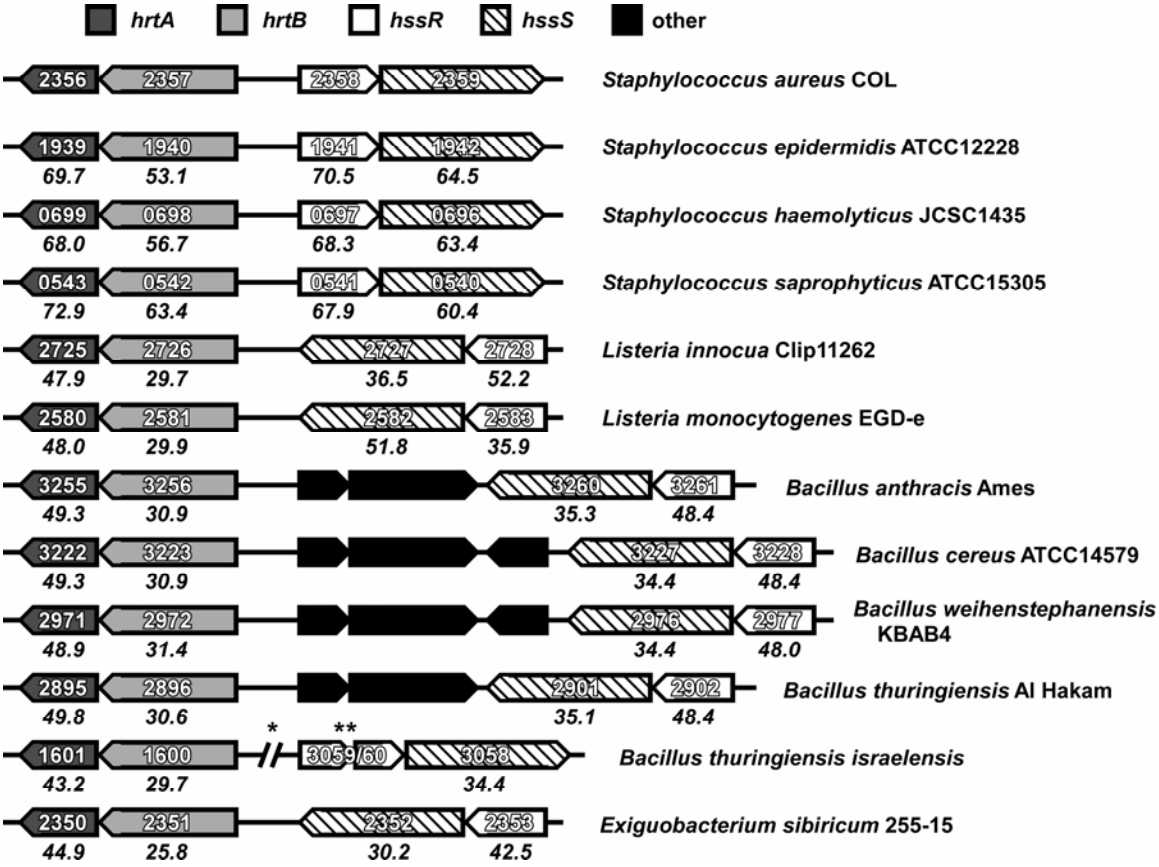

Figure 22. Conservation of HssRS and HrtAB across Gram-positive bacteria. Sequenced bacterial genomes were interrogated for potential orthologues of *S. aureus hssRS* and *hrtAB* by BLAST analyses. The indicated bacterial strains were found to encode potential Hss/Hrt systems. Boxes indicate open reading frames and point in the direction of transcription. Dark grey boxes: HrtA; light grey boxes: HrtB, empty boxes: HssR, boxes with diagonal lines: HssS; black boxes: non-Hss/Hrt open reading frames (other genes). Numbers within boxes indicate the annotated gene number. Numbers below boxes are percent similarities with respect to the corresponding *S. aureus* COL Hss/Hrt gene. Percent similarities were calculated at the amino acid level using a Lipman-Pearson Protein Alignment (gap penalty = 4, gap length penalty = 12). Single asterisk denotes large separation between genes; double asterisk denotes that this potential HssR orthologue is split into two open reading frames in the genome of this species. Adapted from Stauff et al., 2008 (Ref. 157).

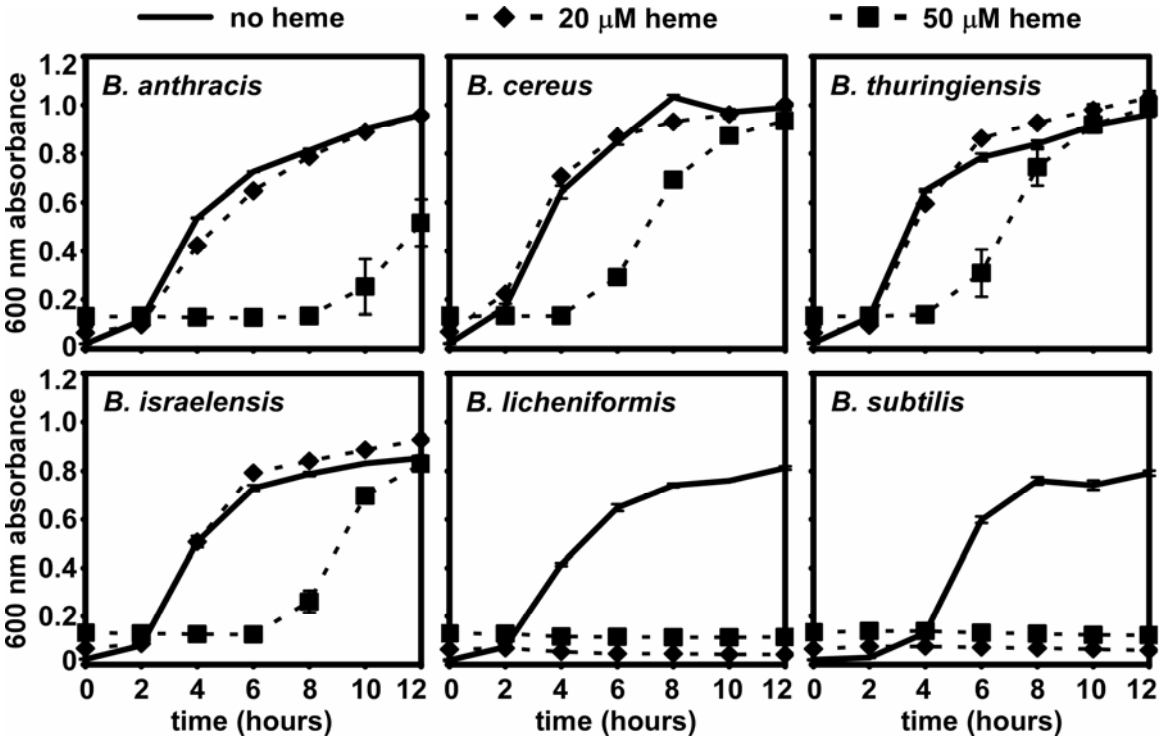

Figure 23. *Bacillus* species exhibit differential heme resistance. Growth curve analysis was performed on triplicate cultures of *Bacillus anthracis*, *B. cereus, B. thuringiensis, B. israelensis, B. licheniformis,* and *B. subtilis* grown in triplicate in BHI without heme (solid lines), BHI + 20 μM heme (a heme concentration observed to inhibit growth of *S. aureus* in previous experiments; dotted lines with diamonds) or BHI + 50 μM heme (a heme concentration similar to that used by Van Heyningen et al. to inhibit *Bacilli*; dotted lines with boxes). Culture densities were determined and averaged at 2-hour intervals following subculture. Error bars correspond to one standard deviation from the mean density of the three cultures.

***B. anthracis* encodes *hss/hrt* genes required for heme resistance.** We chose to investigate Hss/Hrt function in *B. anthracis* based on the fact that this organism is a mammalian pathogen and one that displays an intimate association with host blood during infection. *B. anthracis* HrtAB and HssRS share significant amino acid identity with the corresponding proteins in *S. aureus* (Figure 22) (157, 169). The *hrtAB* and *hssRS* operons of *B. anthracis* are located less than 3 kb apart on the chromosome and are separated by two open reading frames, one of which encodes an uncharacterized transcription factor (BAS3024, Figure 24A). An HssR consensus binding site can be found within the promoter of *B. anthracis hrtAB* (GTTCATATT(N_2)GTTCATATT) (43, 158), suggesting that HssRS may regulate HrtAB expression in *B. anthracis* (Figure 24A). Furthermore, we found that *B. anthracis* is capable of adapting to heme toxicity (Figure 24B), a phenotype that is likely due to expression of HrtAB in heme-treated cells prior to exposure to toxic levels of heme (169). These observations are consistent with the proposition that *B. anthracis* adapts to heme through HssRS-dependent expression of HrtAB.

Accordingly, we assessed the ability of *B. anthracis* mutants lacking *hrtA* and *hssRS* to resist heme toxicity. While wild type *B. anthracis* is able to proliferate in 10 μM heme, *B. anthracis* Δ*hrtA* and Δ*hssRS* are unable to proliferate in this heme concentration, phenotypes that can be complemented by providing a full-length copy of the corresponding gene *in trans* (Figure 24C-F). Importantly, *B. anthracis* Δ*hrtA* and Δ*hssRS* display no growth defect in the absence of heme (Figure 24C, 24D). This demonstrates that *B. anthracis* requires functional Hss/Hrt systems for heme resistance.

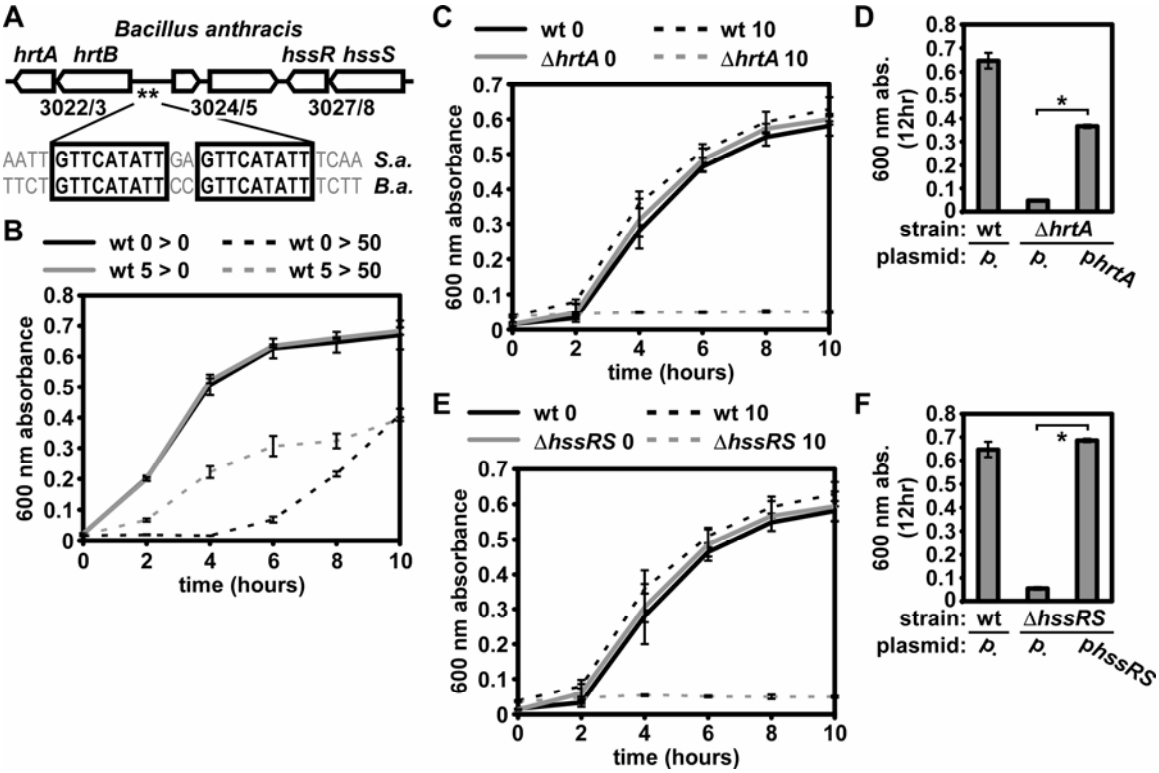

Figure 24. *Bacillus anthracis* requires HrtAB and HssRS for heme resistance. *A*. Schematic of the *B. anthracis hss*/*hrt* locus. Open arrows represent open reading frames (ORF). Designations above ORFs denote predicted gene function. Numbers below ORFs correspond to gene numbers in the *B. anthracis* Sterne genome. Double asterisks signify a putative HssR binding site upstream of *hrtAB*; alignment shows the known *S. aureus* (*S.a.*) and predicted *B. anthracis* (*B.a.*) HssR binding sites. ***B.*** *B. anthracis* adapts to heme toxicity. *B. anthracis* grown in BHI (black lines) or BHI + 5 μM heme (grey lines) was subcultured in triplicate into BHI (solid lines) or BHI + 50 μM heme (dashed lines). Bacterial proliferation was tracked by growth curve. ***C.*** Contribution of *hrtAB* to heme resistance of *B. anthracis*. *B. anthracis* wild type (wt, black lines) and Δ*hrtA* (grey lines) were grown in BHI (solid lines) or BHI + 10 μM heme (dashed lines). Growth was followed as in *B*. ***D.*** Complementation of *B. anthracis* Δ*hrtA*. *B. anthracis* wild type harboring an empty plasmid (p.) or Δ*hrtA* harboring either an empty plasmid or a plasmid containing *B. anthracis hrtA* (p*hrtA*) were analyzed as described in *C*. Culture densities at 12 hours are shown. ***E.*** Contribution of *B. anthracis* HssRS to heme resistance. *B. anthracis* wild type and Δ*hssRS* were analyzed as described in *C*. ***F.*** Complementation of *B. anthracis* Δ*hssRS*. *B. anthracis* wild type harboring an empty plasmid or Δ*hssRS* harboring an empty plasmid or a plasmid containing *B. anthracis hssRS* (p*hssRS*) were analyzed as described in *C*. Culture densities at 12 hours are shown. All results are representative of at least three independent experiments. Error bars correspond to one standard deviation from the mean of triplicate samples within the same experiment; asterisks denote statistically significant differences by Student's *t* test ($p<0.05$).

The *B. anthracis hrtAB* promoter displays enhanced constitutive and heme-induced activity. Although *S. aureus* and *B. anthracis* both require HrtAB for heme resistance, it is unclear whether these systems display overlapping function. We therefore performed interspecies complementation experiments and found that *B. anthracis* or *S. aureus hrtAB* restore heme resistance to *S. aureus* Δ*hrtAB*, suggesting orthology at the level of transporter function between HrtAB from these organisms (Figure 25A). In addition, we found that in *S. aureus* both the *S. aureus* and *B. anthracis hrtAB* promoters respond to heme in a similar manner (Figure 25B). These results confirm that *S. aureus* HssR is capable of activating the *S. aureus* and *B. anthracis hrtAB* promoters, consistent with the presence of an HssR consensus site within these promoters (Figure 24A).

However, in *B. anthracis* the *hrtAB* promoter exhibits elevated levels of activation in response to heme (Figure 25C). Furthermore, the *B. anthracis hrtAB* promoter displays increased activity in the absence of heme when compared with the *S. aureus hrtAB* promoter (Figure 25C). In keeping with this, we tested whether the elevated constitutive activity of the *B. anthracis hrtAB* promoter depends on HssRS signaling and binding of HssR to the *hrtAB* promoter DR. Mutation of the DR or disruption of *hssRS* eliminates the heme responsiveness and reduces the constitutive activity of the *B. anthracis hrtAB* promoter (Figure 25D). This demonstrates that *B. anthracis* HssRS responds to heme and activates the *hrtAB* promoter in a DR-dependent manner. Furthermore, these data suggest that in *B. anthracis*, HssRS constitutively induces HrtAB expression even in the absence of heme, an activity not exhibited by *S. aureus* HssRS (158, 169).

The fact that *hrtAB* promoters from both species respond to heme in a similar manner in *S. aureus* (Figure 25B) but not in *B. anthracis* (Figure 25C) despite similar DR sequences indicates that bases outside of the *hrtAB* promoter DR may be important for

promoter activity in *B. anthracis*. Accordingly, we found that single-base DR mutations have similar effects on the ability of *S. aureus* and *B. anthracis* HssR to activate the *hrtAB* promoter. Specifically, we found that mutation of four conserved DR residues, or removal or addition of spacer residues between the repeats eliminates the ability of *S. aureus* and *B. anthracis* HssR to activate the *S. aureus hrtAB* promoter in response to heme (Figure 25E, constructs 3, 8 - 10). Furthermore, mutation of T3 of the first repeat or T2 of the second repeat decreases heme responsiveness in both species to the same extent (Figure 25E, constructs 5 and 7). While *B. anthracis* HssR is more sensitive to mutation of A5 of repeat 2 and *S. aureus* is more sensitive to mutation of T9 of repeat 1 (Figure 25E, constructs 4 and 6), both mutations decrease *hrtAB* promoter activity in response to heme. This provides the first indication that HssR is exquisitely sensitive to alterations in the distance between each repeat and mutation of single DR residues. Overall, this suggests that HssR-*hrtAB* promoter interactions display similarity in *S. aureus* and *B. anthracis*, pointing to sequences outside of the DR for heme-independent, HssRS-dependent *hrtAB* promoter activity observed specifically in *B. anthracis*.

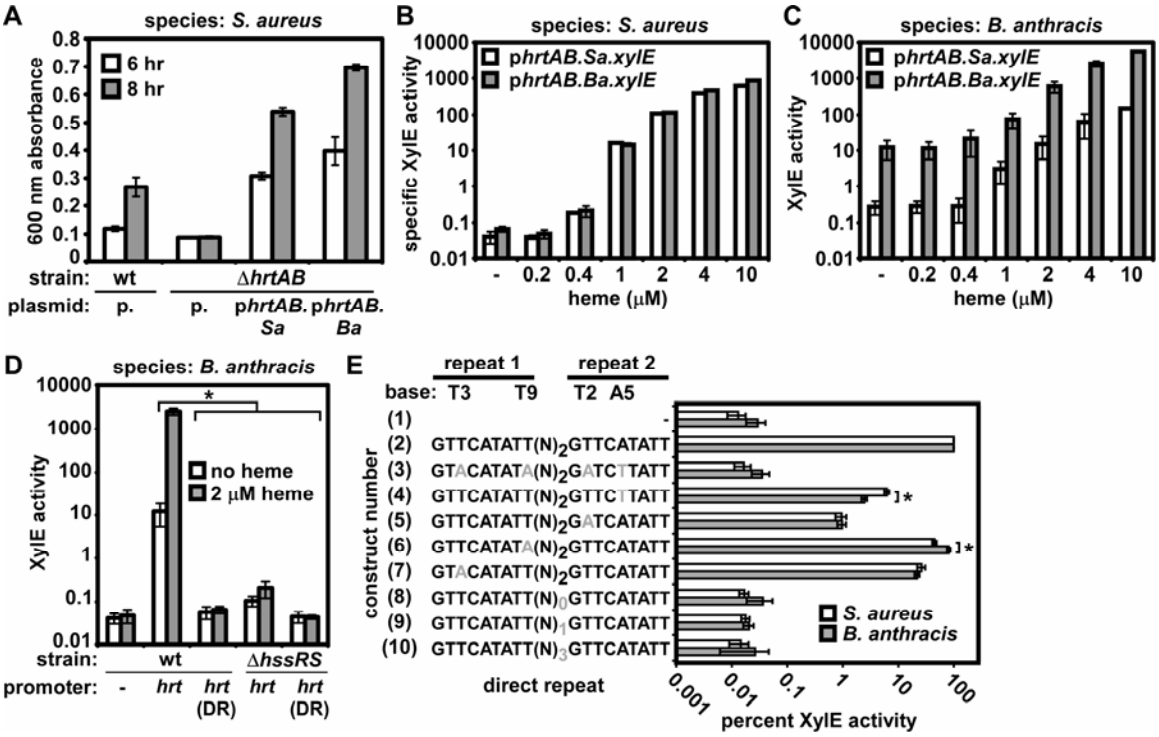

Figure 25. Orthology of *S. aureus* and *B. anthracis* HrtAB. ***A.*** Complementation of *S. aureus* Δ*hrtAB* with *S. aureus*/*B. anthracis hrtAB*. *S. aureus* wild type (wt) transformed with pOS1 (p.), Δ*hrtAB* + pOS1, Δ*hrtAB* + pOS1 encoding *S. aureus hrtAB* (p*hrtAB.Sa*)), and Δ*hrtAB* + pOS1 encoding *B. anthracis hrtAB* (p*hrtAB.Ba*) were grown in TSB + 10 μM heme. Proliferation was tracked by growth curve analysis. Culture densities at 6 hour and 8 hour time points are shown. ***B.*** Reporter assay monitoring *S. aureus*/*B. anthracis hrtAB* promoter activity in *S. aureus*. *S. aureus* harboring either an *S. aureus* (p*hrtAB.Sa.xylE*, solid lines) or *B. anthracis* (p*hrtAB.Ba.xylE*, dashed lines) *hrtAB* promoter XylE reporter were grown in the indicated concentration of heme and reporter activity was measured. ***C.*** Reporter assay monitoring *S. aureus* and *B. anthracis hrtAB* promoter activity in *B. anthracis*. ***D.*** Dependence on HssRS and the *hrtAB* promoter direct repeat (DR) for constitutive and heme-induced *hrtAB* promoter activity in *B. anthracis*. *B. anthracis* wild type (wt) or Δ*hssRS* harboring either promoterless *xylE* (-), p*hrtAB.Ba.xylE* (*hrt*), or p*hrtAB.Ba.xylE* with four DR base mutations (*hrt*(DR)) were grown in +/- 2 μM heme and XylE activity was measured. Asterisk denotes that activity for wild type in the absence of heme is statistically different from wt + *hrt*(DR), Δ*hssRS* + *hrt*, and Δ*hssRS* + *hrt*(DR) in the presence or absence of heme ($p < 0.05$). ***E.*** Reporter assay measuring sensitivity of *S. aureus* and *B. anthracis* HssRS to perturbations in the *hrtAB* promoter DR. *S. aureus* or *B. anthracis* harboring promoterless *xylE* (construct 1), p*hrtAB.Sa.xylE* (2), or p*hrtAB.Sa.xylE* with DR mutations (3-10) were grown in +/- 2 μM heme. Reporter activity was measured and is expressed as the percent of heme-induced activity observed for the wild type promoter. Error bars correspond to one standard deviation from the mean; asterisks denote statistically significant differences by Student's *t* test ($p<0.05$).

***S. aureus* and *B. anthracis* HssRS provide differential heme resistance.** We next tested whether *S. aureus* and *B. anthracis* HssRS display differential activity *in vivo* by assessing the ability of HssRS from *S. aureus* and *B. anthracis* to complement *S. aureus* Δ*hssRS*. To account for potential differences in protein abundance, we tagged *hssS* in the context of an *hssRS*-encoding plasmid, creating *hssR-hssS-myc* plasmids for the expression of HssR and HssS-Myc from either species. We found that both *S. aureus* and *B. anthracis* HssS-Myc are expressed in these strains and that HssR-HssS-Myc from either species is able to complement *S. aureus* Δ*hssRS* (Figure 26A). Furthermore, we noticed that *B. anthracis* HssR-HssS-Myc provides significantly greater complementation than HssR-HssS-Myc from *S. aureus* (Figure 26A), a difference that is conserved in *B. anthracis* (Figure 26B). These results indicate that the molecular function of *B. anthracis* HssRS may differ from that of *S. aureus* HssRS in a way that provides for an increased ability to sense and respond to heme.

***S. aureus* and *B. anthracis* HssS exhibit differential function *in vivo*.** The ability of *B. anthracis* HssR-HssS-Myc to impart elevated heme resistance may be due to differences in HssR, HssS, or both. We reasoned that HssS differences are likely to contribute to differential TCS activity, as *B. anthracis/S. aureus* HssS share significantly less sequence identity than HssR (Figure 22). Accordingly, we found that *B. anthracis* HssS-Myc provides greater heme resistance to *S. aureus* Δ*hssS* than HssS-Myc from *S. aureus* (Figure 27A). We next attempted to repeat these observations in *B. anthracis*. Notably, HssS-Myc from *B. anthracis* complements *B. anthracis* Δ*hssS*, while HssS-Myc from *S. aureus* fails to complement this strain in spite of similar expression of both proteins (Figure 27B). These results suggest that, although *S. aureus* and *B. anthracis* HssRS are functionally orthologous TCS, *B. anthracis* HssRS provides elevated heme resistance to bacteria due to differences in HssS function.

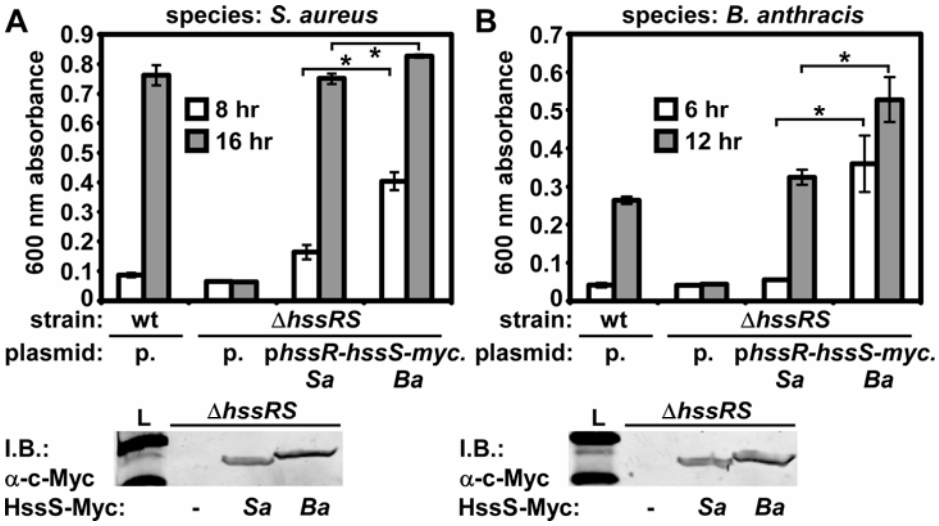

Figure 26. *S. aureus* and *B. anthracis* HssRS display differential activity *in vivo*. *A.* Complementation of *S. aureus* Δ*hssRS* by *S. aureus* and *B. anthracis* HssRS. Top: triplicate cultures of *S. aureus* wild type (wt) harboring pOS1 (p.), Δ*hssRS* with pOS1, Δ*hssRS* with pOS1 encoding *S. aureus* HssR-HssS-Myc (p*hssR-hssS-myc.Sa*), and Δ*hssRS* with pOS1 encoding *B. anthracis* HssR-HssS-Myc (p*hssR-hssS-myc.Ba*) were grown in TSB + 30 μM heme. Proliferation was tracked by growth curve analysis. Average culture density at 8 hour (white bars) and 16 hour (grey bars) time points are shown. Bottom: anti-c-Myc immunoblot showing expression of *S. aureus* and *B. anthracis* HssS-Myc in *S. aureus* Δ*hssRS*. Lane 1: molecular weight ladder (L). Lanes 2-4: *S. aureus* Δ*hssRS* transformed with empty plasmid (-), p*hssR-hssS-myc.Sa* (*Sa*), or p*hssR-hssS-myc.Ba* (*Ba*). ***B.*** Top: Complementation of *B. anthracis* Δ*hssRS* by *S. aureus* and *B. anthracis* HssRS (same plasmids described in *A*). Experiment was carried out as described in *A*, except that earlier time points (6 hour (white) and 12 hour (grey)) are shown due to sporulation and autolysis observed at late time points in *B. anthracis* cultures. Bottom: anti-c-Myc immunoblot showing expression of *S. aureus* and *B. anthracis* HssS-Myc in *B. anthracis* Δ*hssRS*. Lanes are the same as those described in *A*. All results are representative of at least three independent experiments. Error bars correspond to one standard deviation from the mean of triplicate samples within the same experiment. Asterisks denote statistically significant differences in complementation by Student's *t*-test ($p < 0.05$)

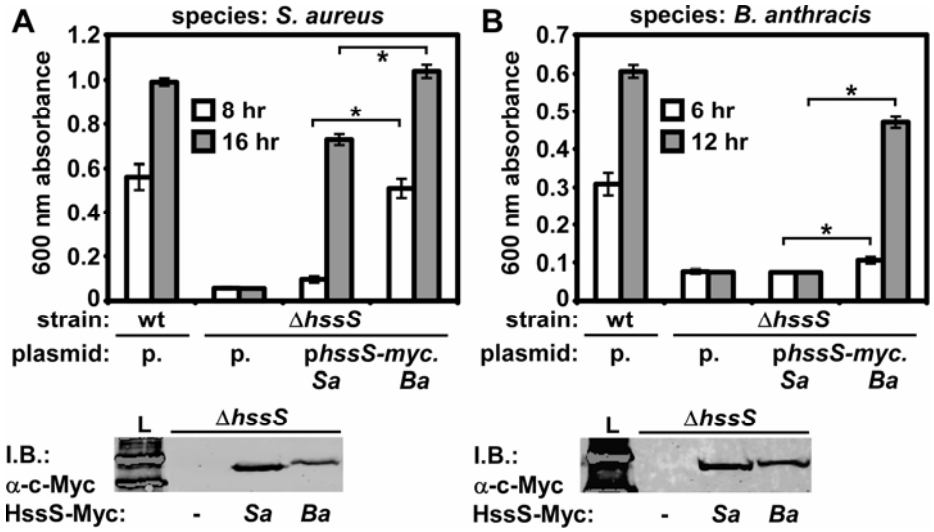

Figure 27. *B. anthracis* HssS displays elevated heme sensing activity *in vivo*. *A.* Top: Complementation of *S. aureus* Δ*hssS* by *S. aureus* and *B. anthracis* HssS. Top: *S. aureus* wild type harboring plasmid pOS1, Δ*hssS* with pOS1, Δ*hssS* with pOS1 encoding *S. aureus* HssS-Myc (p*hssS-myc*.*Sa*), and Δ*hssS* with pOS1 encoding *B. anthracis* HssS-Myc (p*hssS-myc*.*Ba*) were grown in TSB + 20 μM heme. Proliferation was tracked by growth curve analysis. Average culture density at 8 hour (white bars) and 16 hour (grey bars) time points are shown. Bottom: anti-c-Myc immunoblot showing expression of *S. aureus* and *B. anthracis* HssS-Myc in *S. aureus* Δ*hssS*. Lane 1: molecular weight ladder (L). Lanes 2-4: *S. aureus* Δ*hssS* transformed with empty plasmid (-), p*hssS-myc.Sa* (*Sa*), or p*hssS-myc.Ba* (*Ba*). ***B.*** Top: Complementation of *B. anthracis* Δ*hssS* by *S. aureus* and *B. anthracis* HssS. Experiment was performed as described in *A*. Bottom: anti-c-Myc immunoblot showing expression of *S. aureus* and *B. anthracis* HssS-Myc in *B. anthracis* Δ*hssS*. Lanes are the same as those described in *A*. All results are representative of at least three independent experiments. Error bars correspond to one standard deviation from the mean of triplicate samples within the same experiment. Asterisks denote statistically significant differences in complementation by Student's *t*-test ($p < 0.05$)

HssS chimeras reveal a complex domain interplay leading to elevated *B. anthracis* HssS activity. The ability of *B. anthracis* HssS to provide greater heme resistance than *S. aureus* HssS may be due to differences in the function of any of the domains comprising HssS. A membrane-localized histidine kinase, HssS is predicted to contain four domains: an N-terminal signal recognition domain flanked by two transmembrane helices (109), and a tripartite signaling domain consisting of a HAMP linker domain (8), a phosphate-accepting and response regulator recognition HisKA domain (68), and a C-terminal ATPase domain (68).

To define HssS domains required for the increased *in vivo* activity of *B. anthracis* HssS, we constructed chimeric forms of HssS-Myc with either the sensing, HAMP, HisKA, or ATPase domain of *S. aureus* HssS in place of the respective *B. anthracis* HssS domain (Figure 28). The function of each chimera was then tested in *S. aureus*. Surprisingly, all chimeras that are expressed in *S. aureus* and contain a single *S. aureus* domain allow this organism to proliferate to similar levels as *S. aureus* expressing full length *B. anthracis* HssS-Myc (Figure 28). In contrast, all chimeras containing two or more *S. aureus* HssS domains (with the exception of a chimera containing the entire *S. aureus* signaling domain, which is non-functional) function similar to *S. aureus* HssS *in vivo*, requiring over 8 hours to proliferate in 20 μM heme (Figure 28). These data indicate that *B. anthracis* HssS is able to withstand single domain swapping with *S. aureus* HssS and retain its elevated function. It is likely that a complex interplay between HssS domains is responsible for the differential activity between *S. aureus* and *B. anthracis* HssS, an interplay that is perturbed by the insertion of more than one *S. aureus* HssS domain into *B. anthracis* HssS.

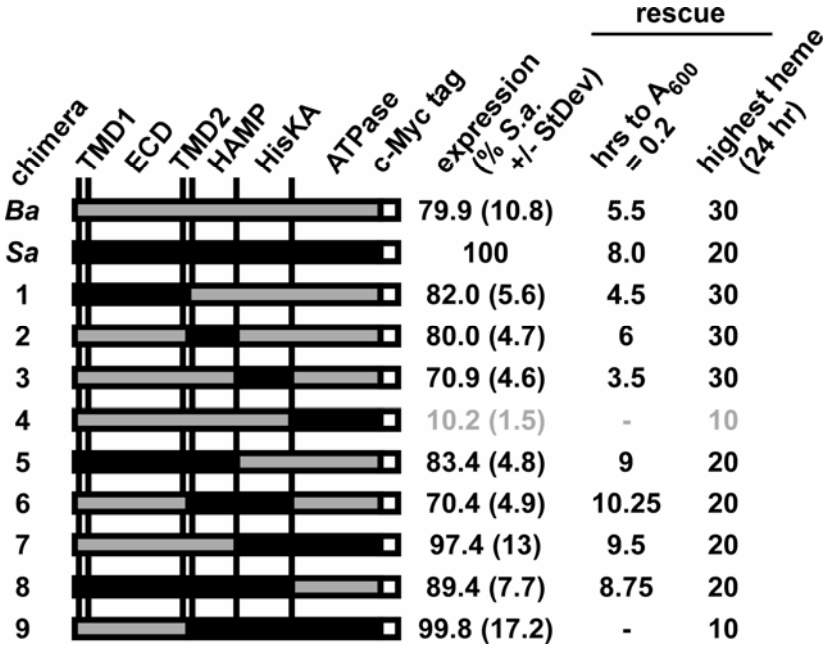

Figure 28. Rescue of *S. aureus* Δ*hssS* by *S. aureus*/*B. anthracis* HssS chimeras. Left: schematic of HssS chimeras. Black: *S. aureus* HssS; grey: *B. anthracis* HssS; white: C-terminal c-Myc epitope tag. TMD1/2, predicted transmembrane domains; ECD, predicted extracytoplasmic sensing domain; HAMP, intracytoplasmic linker domain; HisKA, phosphate acceptor domain; ATPase, ATP hydrolysis domain. Right side: chimera functional data. Column 1: Expression of HssS chimeras. Triplicate cultures of *S. aureus* Δ*hssS* expressing each shown HssS variant were prepared and HssS expression was analyzed by immunoblot followed by LiCor-based quantification. Chimera levels relative to abundance of *S. aureus* HssS were determined and averaged. Standard deviations are shown. Data corresponding to chimeras with less than 50% expression are highlighted in grey. Columns 2 and 3: rescue of Δ*hssS* by HssS chimeras. Column 2: strains were inoculated into medium containing 20 μM heme and proliferation was tracked by growth curve analysis. The length of time required to initiate growth (OD600 = 0.2) was determined. Column 3: strains were inoculated into medium containing 10, 20, or 30 μM heme. The highest heme concentration each strain was able to grown in by 24 hours is indicated. Results are representative of at least three experiments.

***B. anthracis* HssS requires conserved residues in the predicted extracytoplasmic sensing domain for heme recognition.** In HssS, signal recognition is predicted to occur within the putative extracytoplasmic domain, which is flanked by transmembrane helices (see Figure 29A for schematic). However, no studies have addressed the importance of this input domain in HssS function. In this regard, we subjected the predicted HssS sensing domain to mutational analysis to test whether it is required for heme recognition. First, we identified residues required for HssS-dependent heme sensing by aligning HssS sequences from *Firmicutes* predicted to encode *hss/hrt*. This analysis revealed a number of conserved residues within the predicted sensing domain (Figure 29B). We selected 15 perfectly or highly conserved residues and a single non-conserved residue in *B. anthracis* HssS for alanine substitution mutational analysis, focusing on two patches of conserved residues (T124-N129 and F149-F165, Figure 29B). We also mutated the predicted phosphorylated histidine residue (H248) of HssS. We then expressed these point mutants in *B. anthracis* Δ*hssS* and analyzed their expression and function.

By immunoblotting against the C-terminal c-Myc epitope tag added to HssS, we found that all point mutants with the exception of HssS:F149A are expressed to levels similar to wild type HssS (Figure 29C). As expected, HssS:H248A is unable to rescue the heme sensitivity of *B. anthracis* Δ*hssS*, presumably due to an inability to signal to HssR (Figure 29D). Furthermore, HssS:Q145A, a mutant in a non-conserved HssS residue, complements Δ*hssS* at levels similar to wild type HssS (Figure 29D). However, many of the point mutants are unable to complement *B. anthracis* Δ*hssS* (Figure 29D). Specifically, *B. anthracis* HssS mutants at residues K42, T124, F127, R151, E160, or R162 are unable to complement Δ*hssS* to varying degrees. These data confirm that the predicted HssS sensing domain is involved in signal recognition, the initial event in heme recognition and detoxification by HssRS/HrtAB.

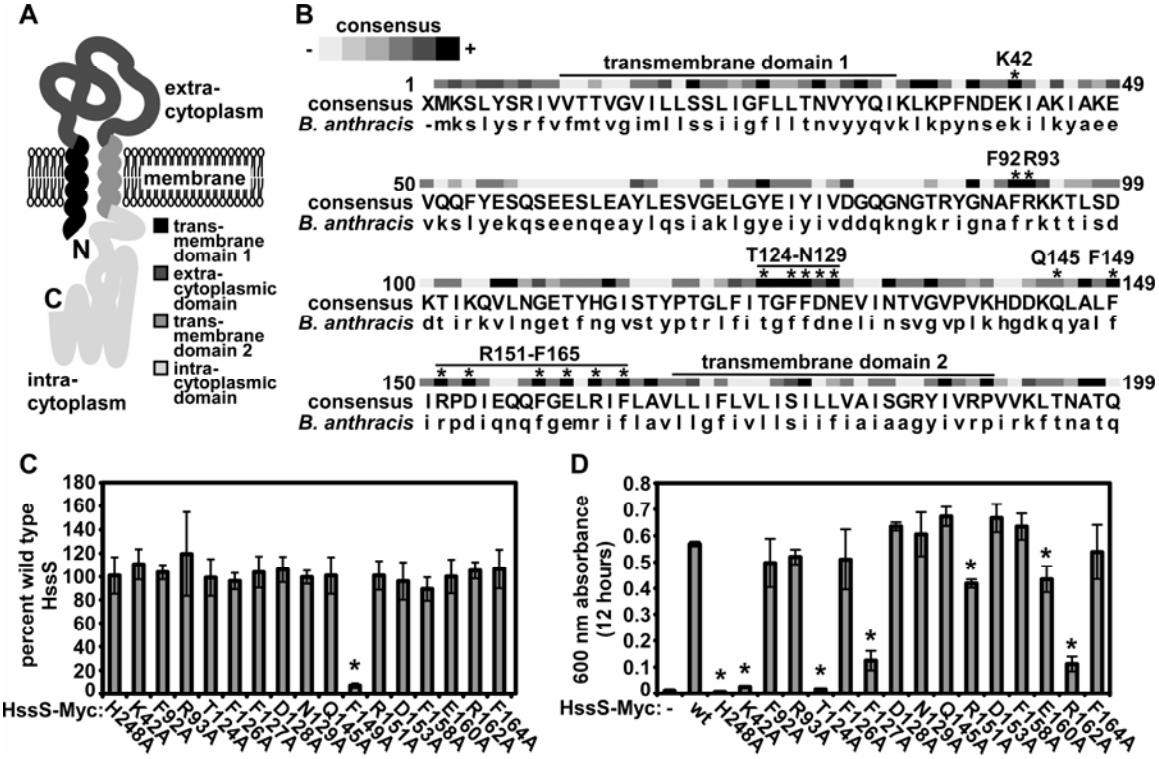

Figure 29. HssS sensing domain residues required for heme recognition. ***A.*** Schematic of HssS. ***B.*** Alignment of conserved HssS sensing domain residues. An HssS consensus sequence was generated from an alignment performed using data from all species with complete genome sequences that are predicted to contain *hss/hrt* (capital letters). Greyscale code indicates level of conservation (light grey, little conservation; black, absolute conservation). Asterisks above residues designate amino acids subjected to alanine substitution mutagenesis. The signaling domain autophosphorylated histidine residue (H248) was also selected for mutagenesis. ***C.*** Expression of *B. anthracis* HssS point mutants. Triplicate cultures of *B. anthracis* Δ*hssS* expressing each HssS point mutant were prepared and HssS expression was analyzed by immunoblot followed by LiCor-based quantification. Mutant levels relative to abundance of wild type *B. anthracis* HssS were determined and averaged. Error bars correspond to standard deviations; asterisk denotes point mutant with expression significantly lower than wild type. This point mutant was not selected for subsequent analyses. ***D.*** Rescue of *B. anthracis* Δ*hssS* by HssS point mutants. Strains were inoculated into BHI containing 20 μM heme and grown for 12 hours. The mean optical density of triplicate cultures was determined. Error bars correspond to standard deviations; asterisks denote strains with culture density significantly lower than wild type.

***B. anthracis* HssS-HssR undergoes rapid autophosphorylation and phosphotransfer.** Because autophosphorylation is the major catalytic activity of histidine kinases (109), we hypothesized that differences in autophosphorylation between *S. aureus* and *B. anthracis* HssS may correlate with the increased ability of *B. anthracis* HssS to provide heme resistance (Figure 27A, Figure 28). *In vitro*, *B. anthracis* HssS undergoes autophosphorylation that is dependent on conserved histidine 248 (Figure 30B), correlating with its lack of functionality *in vivo* (Figure 29D). Significantly, we found that the autophosphorylation rate of *B. anthracis* HssS is 208 (+/- 50) times greater than that of *S. aureus* HssS (Figure 30A, 30B). This correlates with the ability of *B. anthracis* HssS to provide enhanced heme resistance to *S. aureus* Δ*hssS* (Figure 27A, Figure 28).

We next tested HssS-HssR phosphotransfer and found that both *S. aureus* and *B. anthracis* HssRS are capable of engaging in intraspecies phosphotransfer dependent on a conserved aspartic acid residue of HssR (Figure 30C). We next analyzed interspecies phosphotransfer using *S. aureus* HssS and found that *B. anthracis* HssR fails to catalyze phosphotransfer from *S. aureus* HssS (Figure 30D, 30F), providing a potential explanation for the inability of *S. aureus* HssS to complement *B. anthracis* Δ*hssS* (Figure 27B). This indicates that evolutionary divergence has occurred between *S. aureus* and *B. anthracis* HssRS. We also tested interspecies phosphotransfer with *B. anthracis* HssS and found that HssR from both species are capable of catalyzing phosphotransfer from *B. anthracis* HssS (Figure 30C, 30E, 30G). Notably, when phosphorylated *B. anthracis* HssS is incubated with *S. aureus* HssR, phosphorylated *B. anthracis* HssS levels do not decrease because of the fact that *B. anthracis* HssS continues to undergo autophosphorylation even after HssR is added.

In these experiments, we observed differences in the rate of *B. anthracis* and *S. aureus* HssS-HssR phosphotransfer. Specifically, we found that *B. anthracis* HssS-

HssR phosphotransfer occurs rapidly (peaking in under 10 seconds, Figure 30G) while *S. aureus* HssS-HssR phosphotransfer occurs at a relatively slow rate (peaking at about 10 minutes, Figure 30F). Phosphotransfer rate appears to be a property of HssR rather than HssS, as slow phosphotransfer on the part of *S. aureus* HssR also occurs in a phosphotransfer reaction containing *B. anthracis* HssS (Figure 30G). These results indicate evolutionary divergence between *S. aureus* and *B. anthracis* HssR that favors rapid phosphorylation of *B. anthracis* HssR. Importantly, the increased rate of *B. anthracis* HssS phosphorylation and HssS-HssR phosphotransfer may in part explain the ability of this TCS to provide elevated heme resistance to *S. aureus* (Figure 26A).

***B. anthracis* Δ*hrtA* is more sensitive to heme toxicity than *S. aureus* Δ*hrtA*.** We reasoned that the enhanced function of *B. anthracis* HssRS may confer elevated heme resistance to *B. anthracis* when compared with *S. aureus.* However, we found that both species display similar heme resistance by growth curve analysis (Figure 31A). We next reasoned that in the absence of Hss/Hrt function, *B. anthracis* may display enhanced sensitivity to heme toxicity and may therefore require elevated HssRS activity to compensate. We therefore tested the relative heme sensitivity of *S. aureus* Δ*hrtA* and *B. anthracis* Δ*hrtA* and found that after 4 hours in 10 μM heme, *S. aureus* Δ*hrtA* exhibits a slight growth inhibition, while *B. anthracis* Δ*hrtA* exhibits a dramatic decrease in surviving bacteria (Figure 31B). Together with previous data, these results suggest that *B. anthracis* may have evolved a highly active HssRS system to cope with the fact that this organism is extremely susceptible to heme toxicity.

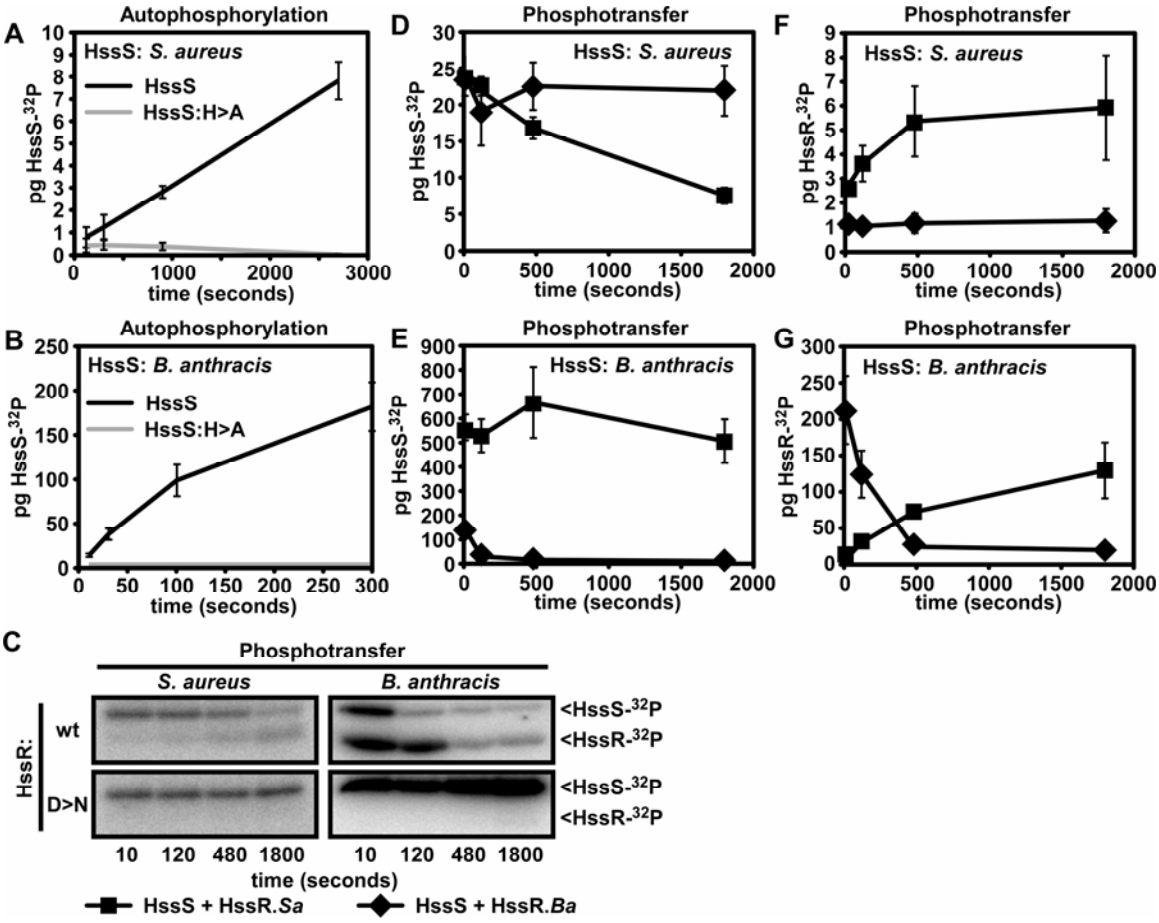

Figure 30. Phosphotransfer between *S. aureus* and *B. anthracis* HssS and HssR. *Symbols for proteins used in A and B*. Black lines: wild type HssS (*S. aureus* HssS in *A*, *B. anthracis* HssS in *B*); grey lines: mutant HssS with alanine substituted for phosphohistidine residue (HssS:H>A). ***A.*** Autophosphorylation of *S. aureus* HssS. HssS and HssS:H>A were incubated with ^{32}P-ATP for the indicated time and samples were analyzed by SDS-PAGE followed by quantification via PhosphorImager analysis. ***B.*** Autophosphorylation of *B. anthracis* HssS and HssS:H>A. ***C.*** Intraspecies HssS-HssR phosphotransfer. Phosphorylated *S. aureus* (left panels) or *B. anthracis* (right panels) HssS (HssS-^{32}P) was added to wild type HssR (wt, top panels) or HssR mutated at phosphoaspartate residue (D>N, bottom panels). Samples were analyzed as described in *A*. ***D through G: interspecies phosphotransfer. Symbols for reactions analyzed in D through G*:** Black lines with squares: reactions containing HssS (*S. aureus* in *D* and *F*, *B. anthracis* in *E* and *G*) and wild type *S. aureus* HssR (HssR.*Sa*); black lines with diamonds: reactions containing HssS and wild type *B. anthracis* HssR (HssR.*Ba*). Reactions were repeated in quadruplicate, and phosphorylated proteins were quantified and averaged. ***D.*** Amount of HssS-^{32}P after initiation of reactions containing *S. aureus* HssS. ***E.*** Amount of HssS-^{32}P in reactions containing *B. anthracis* HssS. ***F.*** HssR-^{32}P levels in phosphotransfer reactions containing *S. aureus* HssS. ***G.*** HssS-^{32}P levels in phosphotransfer reactions containing *B. anthracis* HssS.

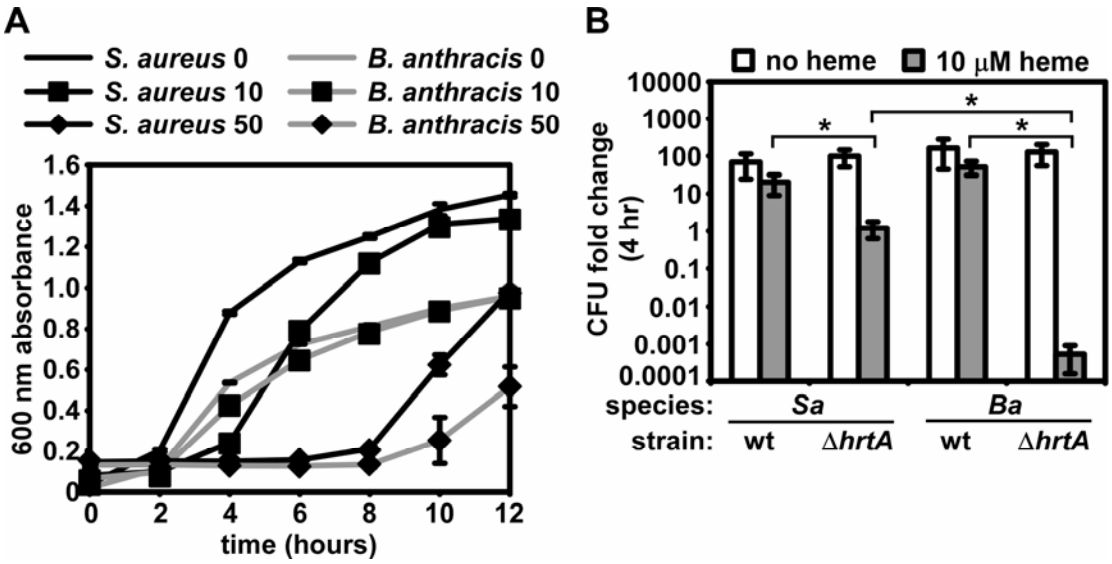

Figure 31. Differential heme sensitivity of *S. aureus* and *B. anthracis* Δ*hrtA*. *A.* Proliferation of wild type *S. aureus* and *B. anthracis* in heme. Growth curve analysis was performed on *S. aureus* (black lines) and *B. anthracis* (grey lines) grown in BHI without heme (no symbols), BHI + 10 μM heme (a heme concentration that inhibits *hss/hrt* mutants; boxes), or BHI + 50 μM heme (a heme concentration that inhibits wt *S. aureus* and *B. anthracis*; diamonds). ***B.*** Resistance of wild type and Δ*hrtA S. aureus* and *B. anthracis* to heme. *S. aureus* (*Sa*) and *B. anthracis* (*Ba*) wild type (wt) and Δ*hrtA* were grown overnight and subcultured into BHI or BHI + 10 μM heme. At the time of subculture and after the four-hour incubation, serial dilutions were performed and plated and colony forming units (CFU) were enumerated. Data is presented as the fold change in CFU following incubation in the presence or absence of heme (log scale). Asterisks denote statistically significant differences by Student's *t*-test ($p < 0.05$). All results are representative of triplicate independent experiments. Error bars correspond to one standard deviation from the mean of triplicate samples within the same experiment; asterisks denote statistically significant differences by Student's *t* test ($p<0.05$).

***B. anthracis* experiences heme stress during growth within vertebrates.** Given the capacity of *B. anthracis* to acquire heme (62, 106, 107, 148) and to avoid heme toxicity through HssRS-regulated expression of HrtAB (Figure 24 and Figure 25), we wondered whether *B. anthracis* lacking the ability to respond to heme toxicity would display attenuation of virulence. To test this, we infected mice with spores of *B. anthracis* wild type or Δ*hrtA* and tracked the survival of mice over time (32, 66, 96, 175). We found a slight but not statistically significant increase in survival of mice infected with *B. anthracis* Δ*hrtA* compared to wild type using this infection model (Figure 32).

Although the Hss/Hrt system does not appear to be required for full virulence in our murine model of infection, we wondered whether HssRS nonetheless senses heme to activate HrtAB expression during systemic anthrax infection. To this end, we constructed a luminescence-based *hrtAB* promoter reporter by fusing the *S. aureus hrtAB* promoter to the *luxABCDE* operon in the plasmid pXen-1 (58). We utilized the *S. aureus hrtAB* promoter instead of the *B. anthracis hrtAB* promoter because the latter displays significant activity in the absence of heme (Figure 25C). When *B. anthracis* is transformed with this construct, bacilli undergo luminescence in response to heme (Figure 33A).

We next infected mice subcutaneously with spores prepared from *B. anthracis* harboring either pXen-1 or p*hrt.Lux* and tracked bioluminescence of germinating *B. anthracis* cells over time. We found that *B. anthracis* harboring pXen-1 do not undergo detectable bioluminescence during infection (Figure 33B, top), but that *B. anthracis* harboring p*hrt.Lux* induces detectable levels of bioluminescence 24-36 hours post infection (Figure 33B, bottom). Although the amount of heme encountered by *B. anthracis* does not appear to be high enough to result in a significant virulence defect in strains inactivated for *hrtAB* (Figure 32), these data suggest that during infection, *B. anthracis* HssRS senses heme to control expression of HrtAB.

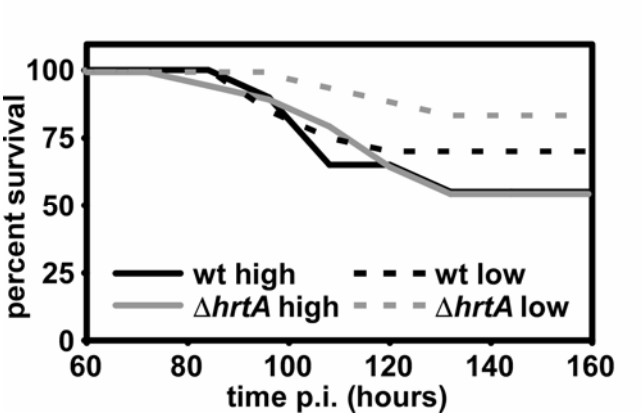

Figure 32. Effect of *hrtA* mutation on *B. anthracis* pathogenesis. A high dose (2000) or low dose (200) of spores from *B. anthracis* wild type or Δ*hrtA* was used to infect groups of 10 A/J mice using a sub-dermal inoculum. Survival was tracked following inoculation with spores. Shown is the compiled result from two independent experiments (20 mice per group). No statistically significant differences were observed at any time point between wild type and Δ*hrtA* using Fisher's exact test.

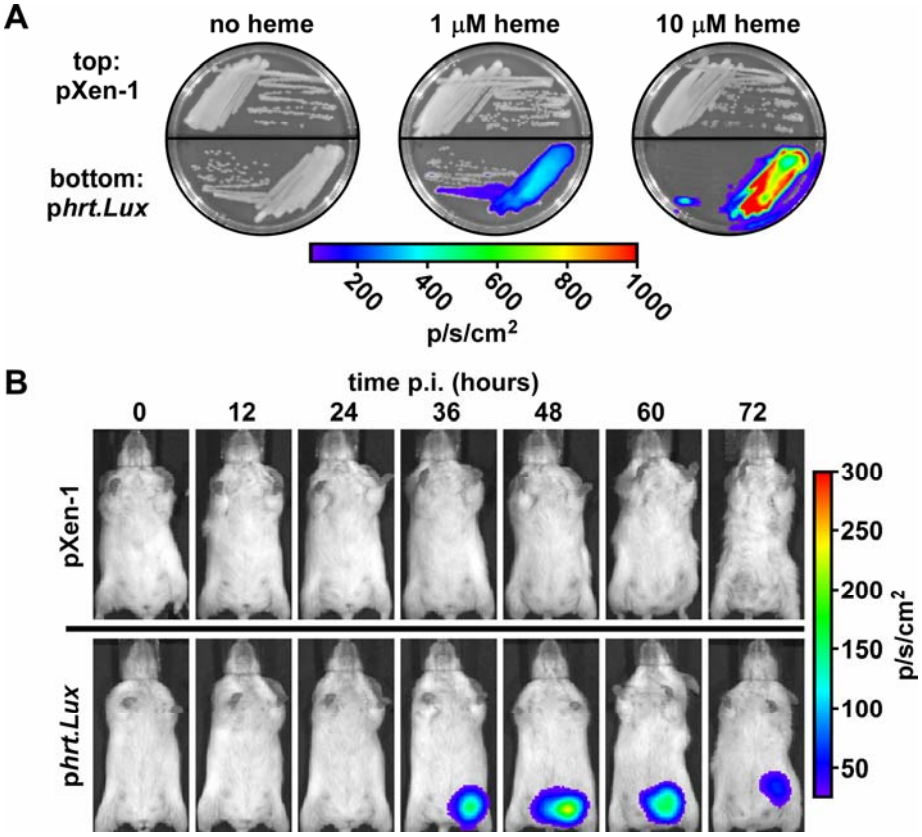

Figure 33. HrtAB expression during anthrax infection. ***A.*** Heme-dependent luminescence of *B. anthracis* harboring p*hrt*.Lux. *B. anthracis* harboring promoterless pXen-1 or pXen-1 with the *Lux* genes under the control of the *hrtAB* promoter (p*hrt.Lux*) were grown on BHI agar containing no heme, BHI + 1 μM heme, or BHI + 10 μM heme. Plates were visualized by IVIS. ***B.*** Activation of the *hrtAB* promoter during anthrax infection. Spores of *B. anthracis* harboring pXen-1 or p*hrt.Lux* were used to infect groups of five A/J mice via a sub-dermal injection in the left inguinal region. Luminescence of *B. anthracis* was tracked every 12 hours post infection (p.i.) by IVIS. Shown is one mouse representative of each group.

Discussion

Bacillus anthracis is a pathogen that is capable of invading host tissues to cause disease. During infection, *B. anthracis* is capable of acquiring host heme to satisfy nutrient iron needs (62, 106, 107, 134). It appears that for *B. anthracis*, amassing of exogenous heme as a nutrient must be balanced with the need to overcome the toxicity of the heme molecule.

We have demonstrated a high level of orthology between the *S. aureus* and *B. anthracis* Hss/Hrt systems. *S. aureus* and *B. anthracis* mutants lacking members of these operons display a similar heme-sensitive phenotype (Figures 5, 13, 24). Also, *B. anthracis hssRS* and *hrtAB* are able to complement *S. aureus* mutants lacking these genes, indicating orthologous function of both systems (Figure 25, 26, 27). Furthermore, our data demonstrate functional overlap between the *S. aureus* and *B. anthracis* heme sensor systems at the levels of signal sensing, signal transduction, autophosphorylation by HssS, phosphotransfer to HssR, interaction between HssR and the *hrtAB* promoter, and activation of the *hrtAB* promoter by HssR (Figure 26, 27, 30). These similarities point to the overall evolutionary conservation of Hss/Hrt function between *S. aureus* and *B. anthracis*, a further indication that these systems are important for the fitness of both bacteria at some point throughout their life cycles.

Nonetheless, we have observed significant functional differences between HssRS/HrtAB from *S. aureus* and *B. anthracis*. First, the *B. anthracis hrtAB* promoter displays significant activity in the absence of heme (Figure 25). This activity is dependent on HssRS and the DR to which HssR binds, suggesting that *B. anthracis* HssRS engages in constitutive signaling that induces low-level activation of the *hrtAB* promoter. The fact that this occurs only in *B. anthracis* and that most DR mutations are tolerated to a similar extent by both species points to sequences outside of the DR that

may be important for HrtAB expression. It is possible that other unidentified factors expressed only by *B. anthracis* (such as the putative transcriptional regulator located between *hssRS* and *hrtAB*, Figure 1A) may interact with the *hrtAB* promoter outside of the DR, functioning with HssR to increase expression of HrtAB. Alternatively, another *B. anthracis*-specific two-component systems may utilize the *hrtAB* promoter DR, overlapping with HssRS to induce expression of HrtAB. This latter possibility is becoming increasingly likely given the bioinformatics-based discovery of an HssRS-like TCS widespread amongst the *cereus*-group *Bacilli* (43). Annotated in the *B. anthracis* Sterne genome as BAS1816/17, this TCS is also predicted to bind the HssR consensus site (GTTCATATT(N_2)GTTCATATT) and auto-regulate its own expression and that of a co-transcribed ABC transporter (BAS1814/15) through an HssR consensus sequence-like motif upstream of BAS1814 (43). It is intriguing to speculate that BAS1816/17 may overlap with HssRS to activate HrtAB expression, a possibility supported by small but significant HssRS-independent, DR-dependent *hrtAB* promoter activity observed in *B. anthracis* (Figure 25D). Future studies will be aimed at assessing the role (if any) of BAS1816/17 in *hrtAB* promoter regulation, as well as the potential of BAS1814-17 promoter regulation by HssRS.

Another key functional difference between the *S. aureus* and *B. anthracis* heme sensor systems occurs at the levels of HssS autophosphorylation and phosphotransfer to HssR (Figure 30). The signaling domain of *B. anthracis* HssS displays a significantly elevated rate of autophosphorylation *in vitro* compared to the corresponding *S. aureus* HssS domain, and *B. anthracis* HssS-HssR phosphotransfer occurs more rapidly than *S. aureus* HssS-HssR phosphotransfer. These activities are likely to allow the rapid induction of HrtAB expression in *B. anthracis*, alleviating heme toxicity. Accordingly, *S. aureus* expressing *B. anthracis* HssRS is significantly more resistant to heme toxicity than wild type *S. aureus*. These results suggest that a certain degree of functional

divergence has occurred throughout the course of evolution between *S. aureus* and *B. anthracis* HssRS.

In the absence of the ability to respond to growth in the presence of heme, *B. anthracis* is hypersensitive to heme toxicity (Figure 31). It is possible that *B. anthracis* may amass heme more rapidly than *S. aureus* or that *B. anthracis* may be more sensitive to heme-induced perturbation than *S. aureus*. It should be noted that the Isd heme iron acquisition system is not expressed in the conditions used in these experiments (data not shown), indicating that heme toxicity can occur independent of Isd-mediated heme uptake. Regardless of the reason for increased heme susceptibility in the absence of a functional heme detoxification response, the heme resistance of wild type *B. anthracis* is similar to that of wild type *S. aureus*. This is an indication that in *B. anthracis*, HssRS and/or HrtAB function more efficiently than the corresponding systems in *S. aureus*. Throughout the course of evolution, *B. anthracis* may have accumulated amino acid substitutions in HssRS that lead to constitutive activity of this TCS, increased autophosphorylation of HssS, and rapid HssS-HssR phosphotransfer. It is possible that these activities compensate for the heme sensitivity of *B. anthracis* and that such compensatory mutations may have been necessitated by the association between *B. anthracis* and host tissues rich in heme.

As the first component in the HssRS/HrtAB-mediated process of heme detoxification, the histidine kinase HssS controls heme resistance by detecting exogenous heme and transducing signals through the membrane. However, the mechanism of heme sensing by this histidine kinase remains elusive. Here, we present data showing that mutation of any of a number of conserved residues in the predicted HssS sensing domain eliminates the ability of *B. anthracis* to respond to heme. These residues cluster within two conserved patches, a possible indication that these regions of the protein interface with the HssS ligand. Although these studies do not identify the

signal directly recognized by HssS, they do highlight the importance of the previously uncharacterized sensing domain in heme detection. The fact that this sensing domain is flanked by transmembrane helices and is predicted to reside in the extracytoplasmic space indicates that HssS detects a signal located either between the membrane and the cell wall, or within the membrane itself. We hypothesize that the HssS ligand may be heme or a molecule that is either modified or induced by heme exposure, and that this molecule is recognized by conserved HssS sensing domain residues shown here to be required for HssS activity.

B. anthracis activates the *hrtAB* promoter during infection of vertebrates (Figure 33). However, HrtAB does not appear to be required for full virulence of *B. anthracis* in a mouse model of infection (Figure 32). It is possible that during the type of infection replicated with our animal model, enough heme is acquired by *B. anthracis* to activate HssRS, but not enough is imported into bacterial cells to necessitate HrtAB function. This is consistent with the observations that the *hrtAB* promoter is significantly activated in response to 1 μM heme, (Figure 25) but that Δ*hrtA* is not significantly inhibited by this heme concentration (data not shown). It is also possible that the A/J mouse model of anthrax infection using a non-encapsulated *B. anthracis* strain does not provide the sensitivity needed to dissect subtle virulence defects (47, 177). In general, mouse models of *B. anthracis* infection appear to be limited in sensitivity, as is evidenced by the apparent lack of a pathogenic defect for strains containing deletions of virulence factors including anthrax toxin in mouse models of infection (73). Further studies utilizing a fully virulent strain of *B. anthracis* lacking *hssRS/hrtAB* in a more susceptible host will be needed to conclusively test the role of these genes in anthrax pathogenesis. It is also possible that during a different type of anthrax infection in which bacilli are immersed in high levels of host heme sources (e.g. *B. anthracis* bacteremia associated with inhalational anthrax), HrtAB function may be necessary for full bacterial virulence.

Future studies will be directed at addressing the question of whether HrtAB/HssRS are involved in anthrax pathogenesis using a variety of strains and infection models.

A number of pathogenic and saprotrophic relatives of *S. aureus* and *B. anthracis* including *B. cereus* and *Listeria monocytogenes* are predicted to express HssRS/HrtAB (157, 169). It is therefore likely that heme sensing and detoxification are processes engaged in by a number of related Gram-positive organisms. This is supported by the observation made by Van Heyningen of differential heme resistance among phylogenetically related *Bacilli* (76). Van Heyningen's method may have differentiated organisms that express functional Hss/Hrt systems from those that do not based solely upon the heme resistance of the organism. Importantly, the fact that HssRS/HrtAB orthologues are only found in those *Bacilli* that exhibit pathogenic or saprotrophic lifestyles indicates that these systems are not required for the fitness of bacteria that do not encounter exogenous heme throughout their life cycles.

It has been suggested that heme sensing and detoxification evolved in dense microbial communities rich in heme-synthesizing bacteria (116, 127). This may explain the recent discovery of a heme-regulated HrtAB orthologue required for heme resistance in the lactic acid bacterium *Lactococcus lactis* (127). Although *L. lactis* is not a pathogen, it may encounter environmental heme synthesized by nearby bacteria (163), necessitating HrtAB function (127). Notably, *L. lactis* does not possess *hssRS* genes and may regulate expression of *hrtAB* through a mechanism other than TCS-based signal sensing (127). This indicates evolutionary conservation of HrtAB function but divergence of HrtAB regulation between the *Lactobacillales* (which include the *Streptococci* as well as *L. lactis*) and the *Bacillales* (including *S. aureus* and *B. anthracis*).

Throughout the course of evolution, the pathogenic or saprotrophic *Firmicutes* may have acquired heme detoxification systems from bacteria such as *L. lactis*, thereby

being provided with a means to facilitate survival within host tissues rich in heme. Within the *Firmicutes*, selective pressure to maintain a heme sensor system and a heme detoxification system may only be exerted on bacteria that commonly associate with exogenous heme. The evolutionary origin of the bacterial heme detoxification response will become clearer as the mechanism of heme sensing and detoxification are elucidated and as more organisms are identified that are capable of sensing and responding to heme toxicity.

CHAPTER VI

A SMALL MOLECULE SCREEN FOR ACTIVATORS OF THE HssRS TWO-COMPONENT SYSTEM

Introduction

Upon exposure of Gram-positive bacteria to heme, the TCS HssRS is activated, leading to expression of HrtAB and the alleviation of heme toxicity. Although progress has been made toward developing an understanding of the signaling events connecting HssRS activation to HrtAB expression in both *S. aureus* and *B. anthracis*, little is known about the mechanism by which the histidine kinase HssS senses heme. Understanding the signal that is directly sensed by HssS will be a critical step in discerning the mechanism of heme sensing and detoxification by Hss/Hrt. Furthermore, such a mechanism will represent a significant advance in understanding of histidine kinase activation in general, as the molecules that directly activate histidine kinases are only known in a limited number of cases.

Here, we unlink the metalloporphyrin structure from HssRS activation by demonstrating that closely related non-heme metalloporphyrins display differential capacity to activate HssS depending on whether these compounds are toxic to *S. aureus*. We also present preliminary results of a small molecule library screen designed to identify molecules other than heme that activate HssRS, with the intention of collecting a set of similar structures that may point toward the identity of the HssS ligand. One non-metalloporphyrin compound identified in this screen activates *S. aureus* HssRS and displays a similar dependence on conserved sensing domain residues of HssS to that observed with heme. These results begin to clarify the mechanism of HssS activation, and point toward an indirect mechanism for heme sensing in Gram-positive bacteria.

Methods

Metalloporphyrins and XylE assays – Heme (Fluka) and metalloporphyrins (Frontier) were dissolved to 10 mM in 0.1 M NaOH. Serial dilutions were performed in 0.1 M NaOH, and metalloporphyrins were diluted into TSB. Overnight cultures of *S. aureus* harboring p*hrtAB.xylE* were subcultured into 1.5 ml snap-cap tubes containing metalloporphyrins, bacteria were grown at 37 °C with shaking for 4 hours, and XylE activity was determined as described previously (see Chapter IV Methods).

Luminescence-based reporter assays – The *S. aureus hrtAB* promoter or sortase A (*srtA*) promoter were inserted between the 5' EcoRI site and 3' BamHI sites of pXen-1 (Xenogen) (58) as described previously (See Chapter V methods).

Small molecule screen – Columns 1-22 of clear-bottom 384-well plates were loaded with 5 nmol of compound from the Vanderbilt University small molecule library. Column 24 was loaded with a standard dilution series of heme, and column 23 was left empty to prevent crossover luminescence in adjacent wells. Seventy-five µl of TSB + 10 µg/ml chloramphenicol containing exponentially growing (OD600 = 0.2) *S. aureus* harboring p*hrtAB.Lux* were added to each well. Cultures were grown for an additional 4 hours, after which luminescence readings were determined. Compounds corresponding to wells showing luminescence greater than that observed in the presence of 1 µM heme were purchased and analyzed by XylE assay as previously described (Chapter IV methods).

Construction of S. aureus HssS point mutant expression/reporter constructs – A dual reporter/complementation construct was created as follows. *S. aureus hssS-myc* was PCR amplified as described previously (See Chapter IV methods, *Complementation Constructs*) and inserted between the NdeI and BamHI sites of plasmid pOS1p*lgt*, making pOS1p*lgt.hssS-myc*. Next, the *hrtAB* promoter-*xylE* fusion described previously (see Chapter IV methods) was amplified from p*hrtAB.xylE* using a 5' primer containing

an EcoRI site and annealing to the *hrtAB* promoter, and a 3' primer also containing an EcoRI site and annealing to the 3' end of *xylE*. Amplified DNA was inserted into the EcoRI site upstream of the *lgt* promoter in pOS1p*lgt.hssS-myc*, creating p*hrt.xylE/hssS-myc*. Orientation of the *hrtAB* promoter-*xylE* fusion was confirmed by PCR and errors were ruled out by sequencing. As a template for the construction of *hssS-myc* point mutants, *S. aureus hssS-myc* was also inserted into pCR2.1 (Invitrogen). Residues were mutated by Pfu mutagenesis (176) and mutations were confirmed by sequencing. Mutant *hssS-myc* DNAs were inserted into p*hrt.xylE/hssS-myc* in place of wild type *hssS-myc*.

Immunoblotting – Immunoblotting against HssS-Myc was performed as described previously (See Chapter V methods).

Results

Toxic metalloporphyrins activate HssRS. It is possible that HssS senses heme by directly binding to it; alternatively, it is possible that HssS senses a toxic by-product of heme that accumulates within staphylococci. To determine which mode of activation is most likely, we attempted to separate heme toxicity from HssS activation. We acquired a series of non-heme metalloporphyrins, which contain first and second-series transition metals encircled by the porphyrin ring. Importantly, *S. aureus* displays differential sensitivity to these metalloporphyrins: while manganese (MnPPIX), iron (FePPIX, heme), zinc (ZnPPIX), and gallium (GaPPIX) protoporphyrin IX exert a bactericidal activity against *S. aureus* at low-micromolar concentrations, chromium (CrPPIX), cobalt (CoPPIX), nickel (NiPPIX), copper (CuPPIX), and tin (SnPPIX) protoporphyrin IX do not inhibit the growth of staphylococci (162)). Remarkably, every toxic metalloporphyrin tested activates HssS, while none of the non-toxic metalloporphyrins induce more than 1% activity in HssS (Figure 34). These data disconnect the metalloporphyrin structure from HssRS activation, and instead connect metalloporphyrin toxicity to the activation of this TCS. Based on the fact that heme-binding proteins are capable of binding even non-activating, non-toxic metalloporphyrins (27, 69, 99), these results suggest that HssS senses heme through an indirect mechanism. Importantly, only toxic metalloporphyrins and not stress-inducing antibiotics, oxidizing reagents, detergents, or adverse growth or environmental conditions activate HssRS (data not shown), suggesting that HssRS specifically responds to a cellular stress imposed by toxic metalloporphyrins.

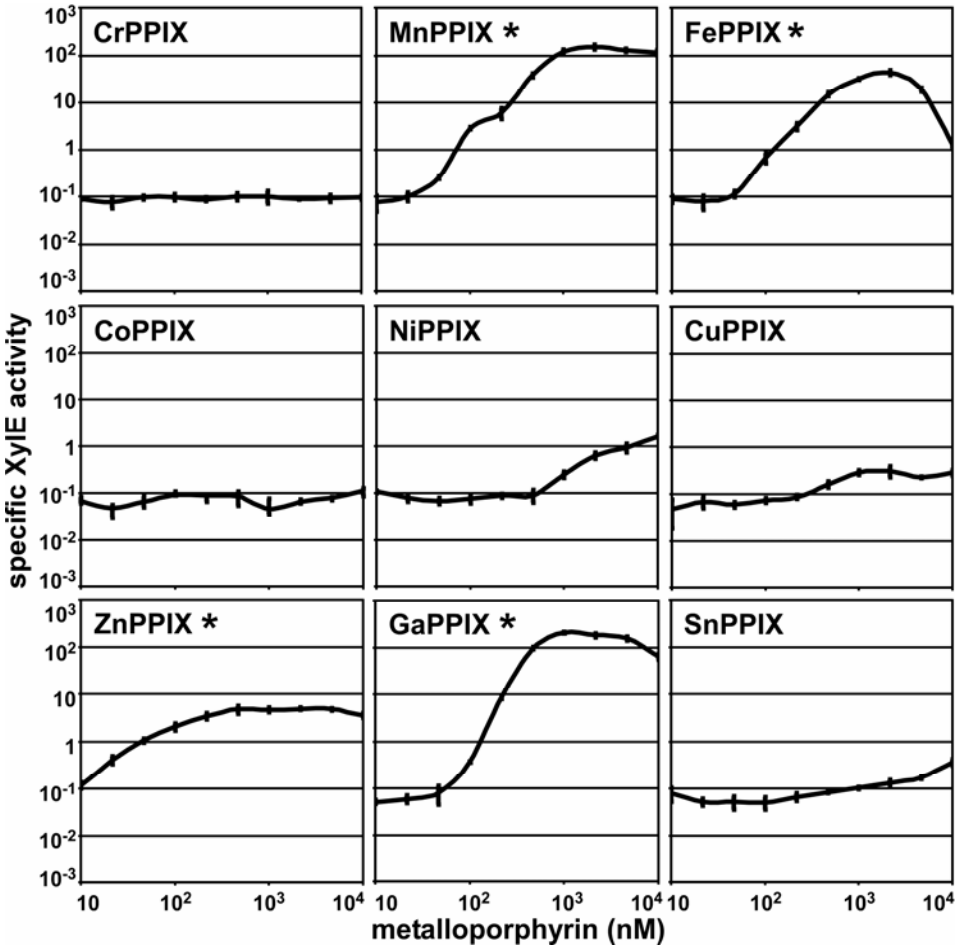

Figure 34. Toxic metalloporphyrins activate *S. aureus* HssRS. *S. aureus* harboring p*hrtAB.xylE* were grown in TSB supplemented with the indicated concentration of metalloporphyrin (FePPIX: heme) in triplicate. Reporter activity was measured. Asterisks denote metalloporphyrins that are toxic to *S. aureus* (Ref. 162).

Development of a small molecule screen to identify HssRS-activating compounds.

If HssS senses heme through binding a molecule other than heme itself, it is possible that an HssS ligand-like molecule may be present within compiled libraries of small molecules covering a broad molecular space. We therefore developed a strategy for screening such libraries for the purpose of identifying HssS-activating compounds. First, we developed a luminescence-based *hrtAB* promoter reporter. The *hrtAB* promoter appears to be the main if not only target of activated HssR in *S. aureus* (Chapter IV). Furthermore, no literature has been published demonstrating *hrtAB* promoter activation by any compound, condition, or cellular stress other than heme exposure. We therefore reasoned that *hrtAB* promoter activity is a reasonable surrogate for directly analyzing HssRS activation. Accordingly, we fused the *S. aureus hrtAB* promoter to the *luxABCDE* operon of *P. luminescens* (the same construct used to image *hrtAB* promoter activation during anthrax infection, Figure 33) and transformed *S. aureus* with this plasmid. We found that wild type *S. aureus* harboring p*hrtAB.Lux* undergoes HssRS-dependent luminescence on plates and in liquid culture following heme exposure (Figure 35). Importantly, LuxABCDE is responsible not only for the oxidation of the luciferase substrate coupled to the emission of electromagnetic radiation, but it is also responsible for the synthesis of the luciferase substrate using precursors made by *S. aureus* (58). We therefore reasoned that *S. aureus* harboring p*hrtAB.Lux* would be amenable to a simple high-throughput screen for HssRS activators, as compounds would simply need to be included in the growth medium of this strain, with the readout being luminescence of live staphylococci.

Accordingly, we were able to validate the use of this strain in a trial high-throughput screen. In this trial, heme was loaded onto 384-well plates in a checkerboard pattern, medium with growing *S. aureus* harboring p*hrtAB.Lux* were added to the plates, and luminescence was monitored. We found that such a screening method is valid, with

a large signal gap between heme-containing wells and those lacking heme. We therefore began screening a large library of compounds available at Vanderbilt University for HssRS activation. In this screen, we included a standard heme dilution series on each 384-well screening plate, along with 336 different library compounds. Potential hits were identified as compounds that activate the *hrtAB* promoter at levels equal to or higher than a specified concentration of heme.

Hits were subsequently confirmed in two independent assays. First, as HssRS-activating compounds induce expression of HrtAB, and the level of HrtAB at the time of heme exposure dictates the resistance of *S. aureus* to heme toxicity, we tested the ability of potential HssRS activators to pre-adapt *S. aureus* to heme toxicity. Second, we analyzed the ability of compounds to activate the *hrtAB* promoter in the more sensitive XylE-based reporter assay, which is also capable of sensitively assessing the HssRS dependence of *hrtAB* promoter activators.

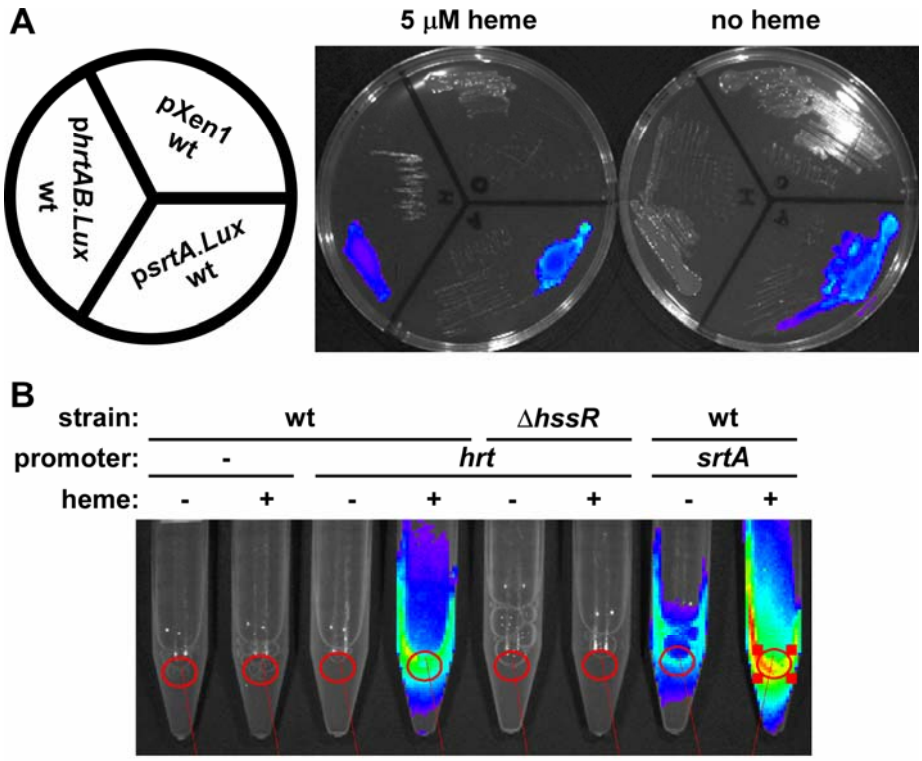

Figure 35. A luminescence-based reporter monitoring HssRS activity in *S. aureus*. ***A.*** Luminescence of *S. aureus* harboring an *hrtAB* promoter-*luxABCDE* fusion on agar plates. *S. aureus* transformed with empty vector (pXen1, upper right), a plasmid containing the *Lux* genes under the control of the constitutively expressed *srtA* promoter (p*srtA.Lux*; lower right), or a plasmid containing the *Lux* genes under the control of the *hrtAB* promoter (p*hrtAB.Lux*, left) were streaked on TSA without heme (right plate) or TSA + 5 μM heme (left plate). Plates were grown at 37 °C and were scanned by IVIS. ***B.*** Luminescence of *S. aureus* harboring an *hrtAB* promoter-*luxABCDE* fusion in liquid culture. The strains described in *A*, as well as Δ*hssR* harboring p*hrtAB.Lux*, were grown for 3 hours in TSB lacking heme (-) or containing 2 μM heme (+) and tubes were scanned by IVIS.

C3 activates the *hrtAB* promoter in an HssRS-dependent manner. One potential HssRS-activating small molecule identified in this high-throughput screen was designated compound 3, or C3. C3 is capable of pre-adapting *S. aureus* to heme toxicity (data not shown); importantly, C3 also activates the *hrtAB* promoter in a dose-dependent manner using a XylE-based assay (Figure 36A). Although an approximately 10-fold higher dose of C3 is required to activate the *hrtAB* promoter to a similar extent as heme, C3 is still capable of inducing robust XylE activity driven by the *hrtAB* promoter at mid-micromolar concentrations (Figure 36A). Importantly, C3 bears no structural resemblance to a metalloporphyrin (Figure 36B).

In a first attempt to connect C3 to HssS activation, we next tested whether activation of the *hrtAB* promoter by C3 depends on HssRS. We found that mutation of *hssRS* eliminates the ability of C3 to activate the *hrtAB* promoter at any dose tested, a further indication that treatment of staphylococci with C3 activates the histidine kinase HssS, leading to *hrtAB* promoter induction (Figure 37). Importantly, C3 is not toxic to *S. aureus* wild type or strains lacking Hss/Hrt (data not shown), a possible indication that in the case of C3, HssS is not merely sensing a by-product of growth in the presence of a toxic compound. Also, these data demonstrate that C3 fills our criteria for an HssRS-activating compound, further validating the p*hrtAB.Lux*-harboring *S. aureus* strain as a useful reagent for the detection of HssRS-activating compounds.

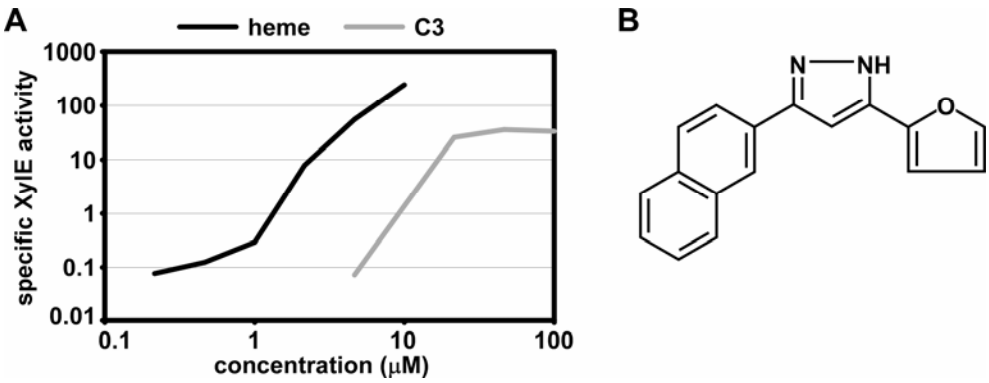

Figure 36. C3 induces *hrtAB* promoter activation in *S. aureus.* *A.* Dose-dependent *hrtAB* promoter activation by heme and C3. *S. aureus* wild type transformed with p*hrtAB.xylE* was grown in the indicated concentrations of heme (black line) or C3 (grey line) and reporter activity was measured. ***B.*** Structure of C3.

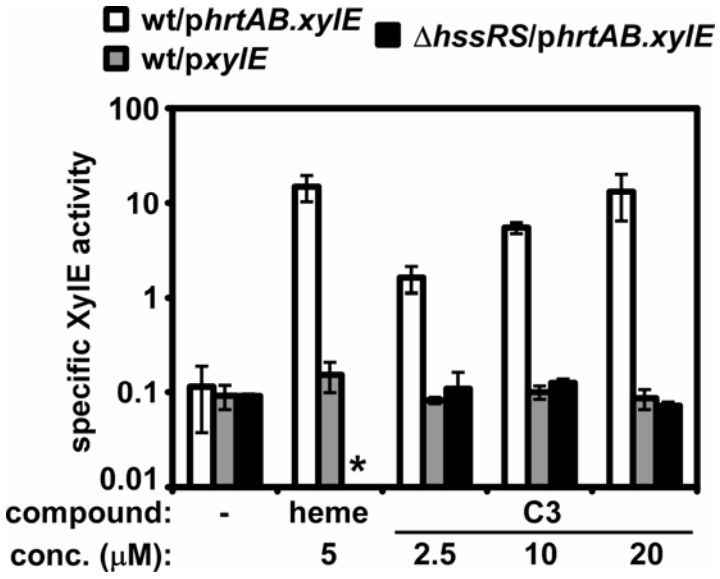

Figure 37. Activation of the *hrtAB* promoter by C3 requires HssRS. *S. aureus* wild type (wt) transformed with either p*hrtAB.xylE* (white bars), promoterless p*xylE* (grey bars), or Δ*hssRS* with p*hrtAB.xylE* (black bars) were grown in triplicate in TSB alone (-) or TSB supplemented with the indicated concentration of heme or C3. Reporter activity was measured following 5 hours of growth. Error bars correspond to one standard deviation from the mean. Asterisk denotes that Δ*hssRS* succumbed to heme toxicity in this experiment. Experiment performed by OA.

***S. aureus* HssS-Myc point mutants display signaling defects *in vivo*.** Although induction of the *hrtAB* promoter by C3 requires HssRS, it is possible that heme and C3 activate HssS by different mechanisms. In an attempt to connect the mode of HssS activation by C3 to the mode of HssS activation by heme, we returned to an HssS mutagenesis strategy. We reasoned that if mutagenesis of sensing domain residues shown to be critical for the activity of *B. anthracis* HssS is tolerated to a similar extent by heme and C3, the most likely explanation would be that both compounds activate HssS through a similar mechanism. However, such a strategy requires a reporter-based readout as opposed to a phenotypic readout. This is because subtle changes in HssS signaling need to be detectable, and because C3 is not toxic to *S. aureus*.

To assess HssS point mutant function using a reporter-based readout, we generated a dual *hrtAB* promoter reporter/complementation plasmid. This plasmid encodes the *hrtAB* promoter-*xylE* fusion joined to a divergently transcribed *lgt* promoter-*hssS-myc* fusion. Such a plasmid should complement *S. aureus* Δ*hssS*, allow for quantification of HssS-Myc abundance by anti-c-Myc immunoblotting, and be useful for XylE reporter assay-based detection of *hrtAB* promoter induction. Furthermore, mutant *hssS-myc* cassettes should be easily introduced into such a system.

Next, we generated an array of *S. aureus* HssS-Myc point mutants in the predicted sensing domain (Figure 38: residue locations can be determined by comparison to alignment presented in Figure 29, noting that *S. aureus* HssS encodes an additional N-terminal residue; for example, *B. anthracis* HssS K42 aligns with *S. aureus* HssS K43). Of the HssS point mutants that expressed (Figure 38A), most retained some function *in vivo* in terms of their ability to rescue the heme-sensitive phenotype of Δ*hssS* (Figure 38B). With the exception of HssS:K43A (which is required in *B. anthracis* but not *S. aureus*), residues dispensable for heme protection in *B. anthracis* are also dispensable for heme protection in *S. aureus* (Figure 29 & 38). Importantly,

three mutants (T125A, F128A, and R163A) fail to complement *S. aureus* Δ*hssS*; these residues are also required for the function of *B. anthracis* HssS (Figure 29 & 38).

Next, we analyzed HssS point mutant function using the more sensitive *hrtAB* promoter reporter-based assay (Figure 40). This assay revealed subtle defects in a number of HssS point mutants that were not observable using phenotypic complementation studies alone. For example, although HssS:R159A provides significant complementation to *S. aureus* Δ*hssS*, both single-dose (Figure 40A) and dose-responsive (Figure 40B) XylE assays reveal a significant signaling defect in this mutant. In fact, only those point mutants with a profound signaling defect fail to at least partially complement Δ*hssS* (Figure 40). Using reporter data, we were able to group point mutants into those that display no obvious signaling defect (K43A, S146A), those with a mild signaling defect (R94, F127, N130, R152, F159, F165), and those with a significant signaling defect (T125, F128, R163). Importantly, all HssS point mutants reduce the high basal *hrtAB* promoter activity of Δ*hssS* (Figure 40A), which presumably results from the lack of a negative regulatory activity exerted by HssS on HssR, such as trans-phosphatase activity observed for other histidine kinases (109). This is an indirect indication that these signaling-deficient point mutants are not merely misfolded, mislocalized, or generally dysfunctional.

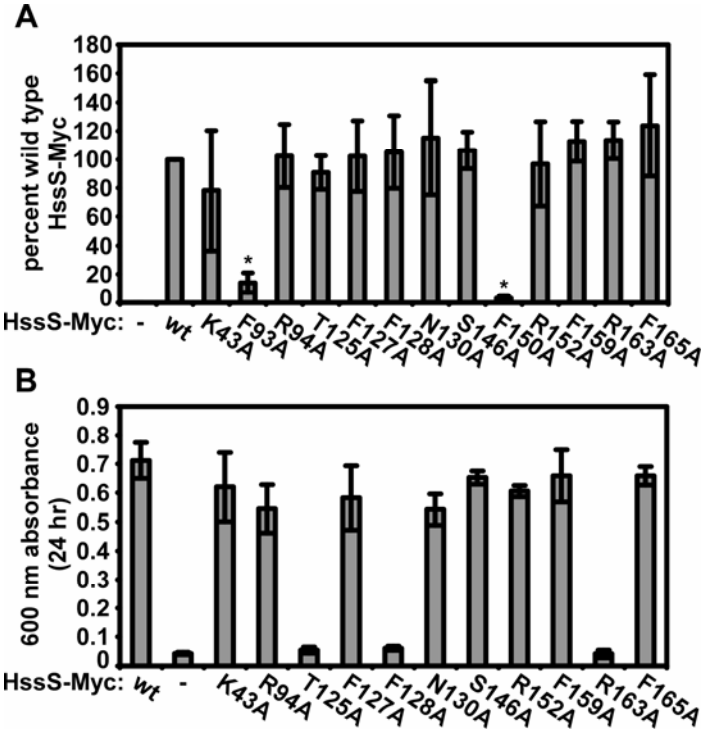

Figure 38. Expression and complementation by *S. aureus* HssS point mutants. *A.* Expression of *S. aureus* HssS-Myc point mutants. *S. aureus* Δ*hssS* was transformed with dual complementation/reporter constructs encoding either no *hssS-myc* (-), wild type *S. aureus hssS-myc* (wt), or *hssS-myc* mutated at the indicated residue. Triplicate cultures of each strain were prepared and protoplast lysates were subjected to SDS-PAGE, anti-c-Myc immunoblotting, and LiCor-based quantification of bands corresponding to HssSmyc. Band intensities were averaged and are expressed as the percent of band intensity corresponding to wild type HssS-Myc. Point mutants with significantly reduced expression compared to wild type are denoted with asterisks; these point mutant-expressing strains were omitted from subsequent analyses. ***B.*** Complementation of *S. aureus* Δ*hssS* by HssS-Myc point mutants. The strains described above were grown overnight and subcultured in triplicate into medium containing 10 μM heme. Twenty-four hours following subculture, culture densities were determined and averaged. Bars represent standard deviations.

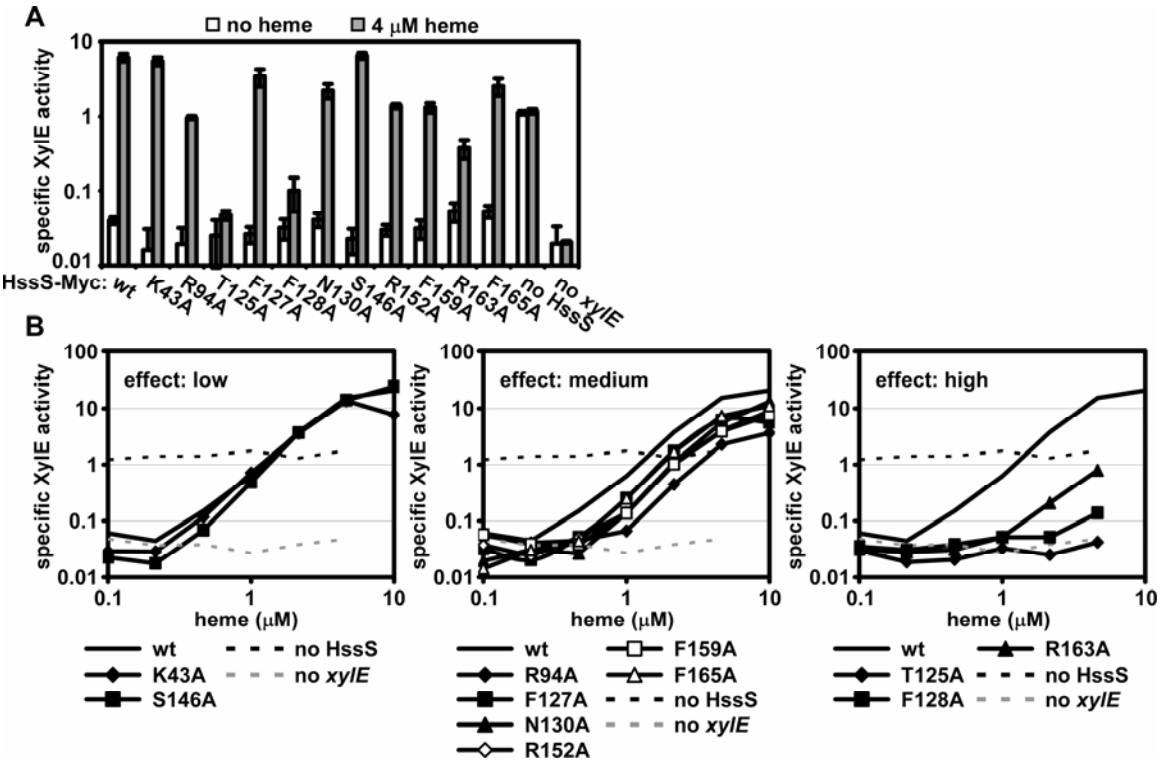

Figure 39. Regulation of *hrtAB* promoter induction by *S. aureus* HssS point mutants. ***A.*** Single-dose *hrtAB* promoter induction by HssS point mutants. *S. aureus* Δ*hssS* harboring dual complementation/*hrtAB* promoter reporter constructs encoding either wild type *hssS-myc* (wt) or *hssS-myc* mutated at the indicated residue, Δ*hssS* harboring p*hrtAB.xylE* (no HssS), and Δ*hssS* harboring pOS1 (no *xylE*) were grown in triplicate in TSB (no heme, white bars) or TSB + 4 μM heme (grey bars). Reporter activity was measured. ***B.*** Dose-dependent *hrtAB* promoter induction by HssS point mutants. The strains described in *A* were grown in the indicated concentration of heme (n = 1 per heme concentration) and reporter activity was measured. Mutants were classified according to data shown in *A*. Low: mutations with no detectable effect on heme-induced *hrtAB* promoter activity; medium: mutants that retain the ability to induce greater than 1 unit of XylE activity in response to heme; high: mutants that drive less than 1 unit of XylE activity in response to heme.

Alanine substitution point mutants connect the C3 mode of HssS activation to that of heme. Next, we compared C3- and heme-dependent *hrtAB* promoter activation controlled by wild type HssS and three HssS point mutants that display signaling perturbation to differing extents (R94A, T125A, F165A). We observed a similar trend in terns of the effect of residue mutagenesis on HssS activation by both compounds: for both C3 and heme, a slight decrease in compound responsiveness is observed for HssS:F165A, a greater decrease is observed for HssS:R94A, and a profound decrease is observed for HssS:T125A. The fact that heme and C3 depend on the same residues for HssS activation to a similar extent is a possible indication that HssS activation by both compounds occurs through a similar mechanism.

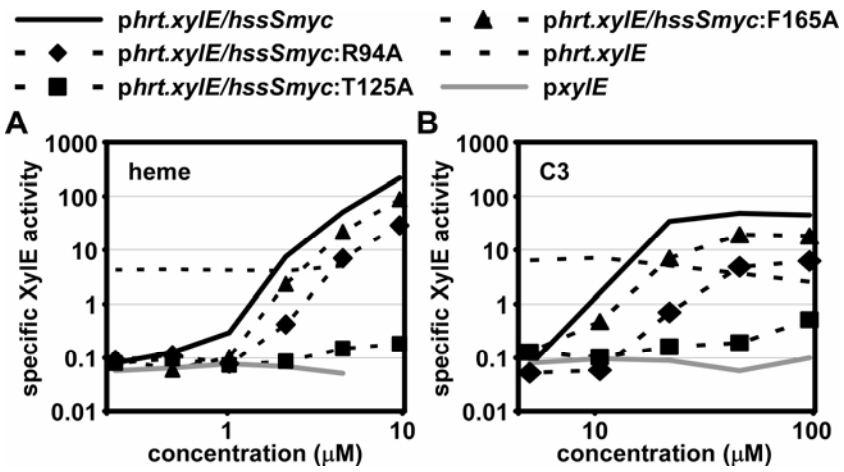

Figure 40. Heme and C3 require the same sensing domain residues for HssS activation. ***A.*** Heme dose-dependent *hrtAB* promoter activation by HssS point mutants. *S. aureus* Δ*hssS* harboring dual complementation/*hrtAB* promoter reporter constructs encoding either wild type *hssS-myc* (p*hrt.xylE/hssS-myc*) or *hssS-myc* mutated at the indicated residue, Δ*hssS* harboring p*hrtAB.xylE*, and Δ*hssS* harboring pOS1 with promoterless *xylE* (p*xylE*) were grown in TSB with the indicated heme concentration and reporter activity was measured. ***B.*** C3 dose-dependent *hrtAB* promoter activation by HssS point mutants. Strains were grown in TSB with the indicated concentration of C3 and reporter activity was measured.

Discussion

Here, we unlink metalloporphyrin structure from HssS activation. We show that only toxic metalloporphyrins activate HssS, while closely related non-toxic metalloporphyrins do not activate this histidine kinase. We also present initial results from a small molecule screen for activators of HssS. We demonstrate that one small molecule activates the *hrtAB* promoter in a manner that requires HssRS. Furthermore, we show a similar sensitivity to HssS sensing domain perturbations between this compound and heme. These results begin to clarify the mechanism of heme sensing by HssS.

Although the simplest mechanism for HssS activation would appear to be a direct interaction between heme and the sensing domain of HssS, a number of theoretical and experimental lines of evidence suggest this may not be the case. First, the sensing domain of HssS bears no resemblance to a heme-binding protein, both in terms of predicted domain structure and a lack of conserved canonical heme-coordinating residues. Second, if coordination of heme by HssS led to activation of this histidine kinase, it would be likely that all metalloporphyrins regardless of toxicity would activate HssS. Third, we have identified a non-metalloporphyrin HssS activator, further separating metalloporphyrin structure from HssS activation. Last, it is unclear that the mere presence of heme would necessitate a heme detoxification response. Susceptibility to heme toxicity is influenced by the composition of the medium bacteria are grown in as well as the overall iron abundance and degree of aerobic respiration exhibited by the bacterium (data not shown). If heme binding controlled the heme detoxification response, a similar response would be initiated regardless of the susceptibility to heme toxicity. On the other hand, if HssS were to detect heme toxicity rather than heme itself, then the extent of the heme detoxification response would be in tune with the need for cells to alleviate heme toxicity.

It is likely that the identity of the HrtAB transport substrate is closely related to the signal recognized by HssS, as is the case for other linked ABC transporter/TCS operons (137). Originally, it was thought that heme itself is recognized by HssS, and that HrtAB removes heme from the staphylococcal cytoplasm. Given the results presented herein, a more complex scheme would appear likely. We favor the hypothesis that heme perturbs a fundamental cellular process of Gram-positive bacteria, leading to the accumulation of toxic metabolites that need to be exported to alleviate heme toxicity. It is possible that HssS senses this class of metabolites, whether in the extracytoplasmic space or in the membrane, leading to HrtAB expression and the export of these metabolites leading to protection against heme toxicity.

It is unclear at this point how C3, the HssS-activating compound identified through screening a small library, leads to HssS activation. It is possible that C3 directly activates HssS. This would be consistent with the observed dependence on conserved sensing domain residues as well as the fact that C3 is not toxic to *S. aureus*. In this scenario, C3 may not activate HssS as well as the heme-induced endogenous ligand, explaining higher doses of C3 needed to activate HssS and the fact that the plateau of C3 activation is much lower than that of heme. However, it is also possible that C3 is another indirect activator of HssS, inducing the production of HssS-activating endogenous ligands. In this scenario, C3 may not be as efficient as heme at inducing the formation of such ligands, explaining its lack of toxicity and the lower *hrtAB* promoter activation plateau. Discerning which mechanism is most likely must await the development of an *in vitro* assay for directly analyzing activation of HssS (see Future Directions). Also, it is possible that identification of the HrtAB transport substrate will give important clues concerning the identity of the HssS ligand. An understanding of the mechanism for heme sensing by HssS and heme detoxification by HrtAB will significantly enhance understanding of the function of Hss/Hrt in alleviating heme

toxicity. Such a mechanism would also represent a significant advance in the understanding of bacterial TCS and ABC transporters in general.

CHAPTER VII

SUMMARY

Conclusions

The acquisition of nutrient iron from the host during infection is a fundamental process engaged in by almost all bacterial pathogens (30). Iron acquisition in bacteria is necessitated due to a dependence on critical biological processes carried out by proteins with iron or iron-containing co-factors (40). It appears that mammalian tissues take advantage of this stringent iron requirement exhibited by bacteria to prevent the proliferation of broad classes of prokaryotic pathogens. Nutritional immunity as it applies to physiologic iron concentration is an effective strategy to prevent infection, a fact highlighted by increased susceptibility to infection observed in patients with diseases leading to elevated iron levels within tissues (16).

In the important human pathogen *Staphylococcus aureus*, dependence on iron acquisition is highlighted by virulence defects observed for strains unable to efficiently amass iron or metabolize iron properly (133, 150, 168, 183). Although much attention has been given to iron acquisition in *S. aureus*, the global response of staphylococci to genetic or biochemical perturbation of iron acquisition or iron metabolism has not been elucidated. Accordingly, we have identified a subset of the *S. aureus* proteome altered in response to depletion of iron or disruption of the staphylococcal regulator of iron acquisition and metabolism, Fur (Chapter II). These studies have revealed a Fur-mediated shift to fermentative metabolism upon iron starvation. The commensurate decrease in pH of the local environment surrounding *S. aureus* cells resulting from the secretion of acidic end products of fermentative metabolism may lead to increased iron availability through release from host iron-sequestering proteins. The results presented

herein combine with those from other laboratories to highlight the remarkable metabolic elasticity of *S. aureus*, a flexibility essential for overcoming deeply conserved mechanisms of innate immunity that target fundamental biological processes of prokaryotes (135, 136, 152). It is likely that unique aspects of *S. aureus* metabolism combine with the well-studied arsenal of staphylococcal virulence factors as well the ability of this organism to acquire new virulence and resistance determinants to overwhelm mechanisms of innate immunity, adaptive immunity, and therapeutic intervention (34, 136). These are all probable contributing factors to the remarkable success of *S. aureus* as a pathogen.

During infection, *S. aureus* employs an additional and important mechanism to overcome nutritional immunity. Invasive staphylococci are able to circumvent the paucity of free iron within host tissues by tapping into the most abundant source of iron within the mammalian body, namely heme in the context of hemoglobin (134, 151). To utilize heme as an iron source, staphylococci must lyse red blood cells, bind hemoglobin, remove heme, import heme into the cytoplasm, and degrade the heme molecule to release iron for incorporation into bacterial iron-containing proteins. These processes are carried out by the staphylococcal Fur- and iron-regulated surface determinants, the Isd system (134, 151). The importance of Isd-mediated heme acquisition is highlighted by virulence defects observed for strains inactivated for Isd genes (133, 150, 168).

Although heme is a valuable source of iron for invasive staphylococci, heme is a toxic molecule capable of generating reactive oxygen species and killing bacterial cells (53, 134, 161, 162, 169). Many examples of heme acquisition systems have been well-characterized in both Gram-negative and Gram-positive bacteria; however, comparatively little attention has been devoted to mechanisms whereby bacteria that acquire heme avoid or relieve heme toxicity. Here, we demonstrate that *S. aureus* relieves heme toxicity by sensing heme and expressing a heme detoxification system,

the heme-regulated transporter HrtAB (Chapter III). The importance of HrtAB expression to the avoidance of heme toxicity is highlighted by the heightened heme sensitivity of strains inactivated for this transport system. Furthermore, *S. aureus* lacking *hrtA* display perturbed virulence in a murine model of abscess formation leading to the formation of hepatic abscesses and increased liver colonization. These virulence properties are likely due to the heme-induced secretion of virulence factors in this heme-sensitive strain. These studies have elucidated the function of a novel transport system conserved across Gram-positive bacteria that may be expressed specifically during the association of bacterial pathogens with their host. Importantly, the mechanism of increased toxin secretion in strains lacking *hrtA* may be an avenue for the identification of systems required for the regulation of immunomodulatory toxins known to be important in the host-pathogen interaction (156, 157).

We also demonstrate that HrtAB expression is regulated by a novel TCS designated the heme sensor system HssRS (Chapter IV). HssS is a heme-responsive histidine kinase that controls the phosphorylation of the response regulator HssR. Upon phosphorylation, HssR binds to a direct repeat in the *hrtAB* promoter, inducing expression of HrtAB and thereby controlling the heme detoxification response. These studies clarify the function of one of the previously uncharacterized staphylococcal two-component systems; furthermore, HssRS represents an elusive host molecule-specific TCS. It is possible that heme sensing by HssRS and subsequent heme detoxification by HrtAB expression may tailor the interaction between staphylococci and heme, allowing the amassing of heme molecules by circumventing accompanying heme toxicity.

In addition to the insight into novel biological processes of staphylococci provided by these studies, there may be important practical outcomes of the discovery of HssRS for *S. aureus* research in general. To this point, staphylococcal research has suffered from the absence of a tightly controlled inducible promoter-containing plasmid for *in vivo*

expression studies. Because of absolute dependence on HssRS-mediated induction, which is critically dependent on exogenous heme in staphylococci, the *hrtAB* promoter appears to be one of the most tightly controlled, highly inducible promoters in *S. aureus*. Therefore, it is quite likely that the *hrtAB* promoter will form the basis for an inducible expression system in *S. aureus* whereby a DNA of interest (such as an open reading frame for expression studies or an antisense RNA for knockdown experiments) is inserted in front of the *hrtAB* promoter for heme-induced expression. As heme induces *hrtAB* promoter activity in a dose-dependent manner and sub-toxic levels of heme are capable of inducing profound promoter activity, such a system may be of broad interest to the *S. aureus* research community.

Multiple Gram-positive bacteria evolutionarily related to *S. aureus* including *Bacillus anthracis* and *Listeria monocytogenes* are capable of Isd-mediated heme acquisition (23, 106, 107, 123, 148). Here, we demonstrate that Isd-mediated heme uptake may be coupled to Hss/Hrt-mediated heme detoxification in these other pathogens as well (Chapter V). Genes encoding *hssRS* and *hrtAB* are conserved in the *cereus*-group *Bacilli* and in the pathogenic and saprotrophic *Listeriae*. Furthermore, *B. anthracis*, the causative agent of anthrax and a pathogen intimately associated with host blood and heme during infection, requires Hss and Hrt for resistance to heme toxicity. In addition, members of the genus *Bacilli* may require elevated Hss/Hrt function due to the heightened heme sensitivity of such species lacking *hss* or *hrt* genes. Finally, we present evidence indicating that *B. anthracis* may experience heme stress leading to HssRS activation during association with host tissues. These studies demonstrate that heme sensing by HssRS and heme detoxification by HrtAB are not limited to *S. aureus*, and indeed may be conserved throughout the pathogenic or saprotrophic *Firmicutes*. Importantly, these studies also lay the foundation for investigation into Hss/Hrt function in other important bacterial species including *S. epidermidis, B. cereus*, *B. thuringiensis*,

and *L. monocytogenes*. It is likely that a more complete understanding of the implications behind evolutionary conservation of Hss/Hrt function across the *Firmicutes* must await the emergence of insight into the activity of these systems in other species, as well as a mechanistic understanding for heme detoxification by HrtAB and heme sensing by HssRS.

Finally, we provide initial insight into the mechanism whereby the histidine kinase HssS senses heme (Chapter VI). By unlinking metalloporphyrin structure from HssS activation and identifying a non-metalloporphyrin small molecule HssS inducer, we present evidence that HssS senses heme through an indirect mechanism. These results provide the foundation for future studies aimed at definitively identifying the HssS ligand, a step that will represent a significant advance in the understanding of Hss/Hrt function in Gram-positive bacteria and of histidine kinase activation in general.

Future Directions

An assay for directly analyzing HssS activation

Although reporter-based assays have been the basis for most of the experiments described herein and have been of immense value, such assays are limited by the fact that they are an indirect measure of HssS activity. So far, we have not been able to conclude whether a given HssS-activating compound merely perturbs the Gram-positive bacterial cell in a similar way as heme, leading to HssS activation, or whether the compound is similar enough to the HssS ligand to directly activate HssS. As a means of directly assessing HssS activation, we have made significant progress toward the development of an *in vitro* assay for HssS activation. We have been able to purify soluble epitope- and hexahistidine-tagged *S. aureus* HssS-Myc-his_8 from the membrane fraction of *E. coli* overexpressing this histidine kinase. We are in the process of attempting to incorporate this protein into proteoliposomes. HssS-containing proteoliposomes could then be loaded with potential HssS-activating small molecules (including heme, C3, and hits from our small molecule library screen), incubated with γ^{32}P-ATP, and activation of full-length HssS could be monitored by assessing its phosphorylation state. As these proteoliposomes would lack any cellular machinery that likely contributes to the heme-induced accumulation of the HssS-activating ligand, they would represent an ideal platform for separating direct HssS activators from indirect activators. Importantly, HssS sensing domain point mutants could be included in this assay as a negative control tying any *in vitro* data to the *in vivo* data presented here. Results from such an assay could significantly enhance our understanding of the mode of action of heme and non-metalloporphyrin HssS activators.

Identification of endogenous HssS ligands

If proteoliposome-based assays for direct HssS activation prove useful, they may represent a powerful platform for identification of the signal that activates HssS in *S. aureus* cells. It may be possible to grow wild type *S. aureus* in the presence of heme, prepare crude fractions from cells, apply these fractions to proteoliposomes, and analyze HssS activation. From here, it may be possible to further purify any HssS-inducing activity by HPLC and identify molecules responsible for HssS activation by high-resolution mass spectrometry. This has the potential of identify whether endogenous ligands increased in abundance or modified by heme are responsible for HssS activation. The comparison of an HssS activator identified through this scheme with HssS activators identified through screening of small molecule libraries may clarify the mechanism by which HssS is activated in staphylococci.

Identification of alternative *hrtAB* promoter-activating systems in *B. anthracis*

It is possible that in *B. anthracis, hrtAB* promoter expression is controlled by other gene regulatory systems in addition to HssRS (see Chapter V Discussion). Furthermore, newly identified small molecule activators of HssRS in *S. aureus* are able to induce significant *hrtAB* promoter activation in *B. anthracis* that occurs independent of HssRS (data not shown). Remarkably, this HssRS-independent induction requires an intact HssR binding site within the *hrtAB* promoter, suggesting that *B. anthracis* expresses an additional HssRS-like TCS that can control expression of HrtAB. As mentioned previously, a logical candidate for a system that could regulate the *hrtAB* promoter in a manner that requires the HssR binding site DR is the BAS1816/17 TCS, which contains a response regulator predicted to recognize the same DR as HssR (43). It is possible that these compounds (and possibly heme, see Figure 25) activate BAS1816/17, providing another layer of control for the heme detoxification response in

B. anthracis. Accordingly, we plan to generate mutants lacking members of this novel TCS (BAS1816/17), as well as the ABC transporter it is predicted to regulate (BAS1814/15). We will test whether BAS1814/15 plays a role in heme detoxification, whether HssRS-activating compounds induce expression of BAS1814/15 using BAS1814 reporter-based techniques, and which genes the BAS1816/17 TCS regulates in *B. anthracis* using microarray-based approaches. This line of investigation has the potential to broaden our understanding of the heme detoxification response of Gram-positive bacteria by elucidating whether HssRS signaling overlaps with that of other bacterial TCS.

APPENDIX

List of Publications

Friedman, D. B.*, Stauff, D. L.*, Pishchany, G., Whitwell, C. W., Torres, V. J., and Skaar, E. P. (2006) *Staphylococcus aureus* redirects central metabolism to increase iron availability. *PLoS Pathog* **2**(8)
*Contributed equally to authorship

Torres, V. J., Stauff, D. L., Pishchany, G., Bezbradica, J. S., Gordy, L. E., Iturregui, J., Anderson, K. L., Dunman, P., Joyce, S., and Skaar, E. P. (2007) A *Staphylococcus aureus* regulatory system that responds to host heme and modulates virulence. *Cell Host & Microbe* **1**(2), 109-119

Stauff, D. L., Torres, V. J., and Skaar, E. P. (2007) Signaling and DNA-binding activities of the *Staphylococcus aureus* HssR-HssS two-component system required for heme sensing. *J Biol Chem* **282**(36), 26111-26121

Stauff, D. L., Bagaley, D., Torres, V. J., Joyce, R., Anderson, K. L., Kuechenmeister, L., Dunman, P. M., and Skaar, E. P. (2008) *Staphylococcus aureus* HrtA Is an ATPase required for protection against heme toxicity and prevention of a transcriptional heme stress response. *J Bacteriol* **190**(10), 3588-3596

Stauff, D. L., and Skaar, E. P. (2008) The heme sensing system (HssRS) of *Staphylococcus aureus*. *Contributions to Microbiology.* **In Press**

Stauff, D.L., and Skaar, E.P. *Bacillus anthracis* HssRS signaling to HrtAB regulates heme resistance during vertebrate infection. (Manuscript in review)

BIBLIOGRAPHY

1. Book of Job, Chapter 2, v. 1-10.

2. Book of Leviticus, Chapter 13.

3. Book of Leviticus, Chapter 13 v. 24-25, King James Version.

4. 2002. Dates in Infectious Diseases. The Parthenon Publishing Group, New York.

5. **Alban, A., S. O. David, L. Bjorkesten, C. Andersson, E. Sloge, S. Lewis, and I. Currie.** 2003. A novel experimental design for comparative two-dimensional gel analysis: Two-dimensional difference gel electrophoresis incorporating a pooled internal standard. Proteomics **3:**36-44.

6. **Anderson, K. L., C. Roberts, T. Disz, V. Vonstein, K. Hwang, R. Overbeek, P. D. Olson, S. J. Projan, and P. M. Dunman.** 2006. Characterization of the *Staphylococcus aureus* heat shock, cold shock, stringent, and SOS responses and their effects on log-phase mRNA turnover. J Bacteriol **188:**6739-56.

7. **Andrews, S. C., A. K. Robinson, and F. Rodriguez-Quinones.** 2003. Bacterial iron homeostasis. FEMS Microbiol Rev **27:**215-37.

8. **Aravind, L., and C. P. Ponting.** 1999. The cytoplasmic helical linker domain of receptor histidine kinase and methyl-accepting proteins is common to many prokaryotic signaling proteins. FEMS Microbiol Lett **176:**111-6.

9. **Ascenzi, P., A. Bocedi, P. Visca, F. Altruda, E. Tolosano, T. Beringhelli, and M. Fasano.** 2005. Hemoglobin and heme scavenging. IUBMB Life **57:**749-59.

10. **Baba, T., T. Bae, O. Schneewind, F. Takeuchi, and K. Hiramatsu.** 2008. Genome sequence of *Staphylococcus aureus* strain Newman and comparative analysis of staphylococcal genomes: polymorphism and evolution of two major pathogenicity islands. J Bacteriol **190:**300-10.

11. **Bae, T., A. K. Banger, A. Wallace, E. M. Glass, F. Aslund, O. Schneewind, and D. M. Missiakas.** 2004. *Staphylococcus aureus* virulence genes identified by bursa aurealis mutagenesis and nematode killing. Proc Natl Acad Sci U S A **101:**12312-7.

12. **Bae, T., and O. Schneewind.** 2006. Allelic replacement in *Staphylococcus aureus* with inducible counter-selection. Plasmid **55:**58-63.

13. **Baichoo, N., T. Wang, R. Ye, and J. D. Helmann.** 2002. Global analysis of the *Bacillus subtilis* Fur regulon and the iron starvation stimulon. Mol Microbiol **45:**1613-29.

14. **Ban, T. A.** 2006. The role of serendipity in drug discovery. Dialogues Clin Neurosci **8:**335-44.

15. **Barrett, J. F., and J. A. Hoch.** 1998. Two-component signal transduction as a target for microbial anti-infective therapy. Antimicrob Agents Chemother **42:**1529-36.

16. **Barton, J. C., S. M. McDonnell, P. C. Adams, P. Brissot, L. W. Powell, C. Q. Edwards, J. D. Cook, and K. V. Kowdley.** 1998. Management of hemochromatosis. Hemochromatosis Management Working Group. Ann Intern Med **129:**932-9.

17. **Beier, D., and R. Gross.** 2006. Regulation of bacterial virulence by two-component systems. Curr Opin Microbiol **9:**143-52.

18. **Bernheimer, A. W., L. S. Avigad, and P. Grushoff.** 1968. Lytic effects of staphylococcal alpha-toxin and delta-hemolysin. J Bacteriol **96:**487-91.

19. **Bezkorovainy, A.** 1981. Antimicrobial properties of iron-binding proteins. Adv Exp Med Biol **135:**139-54.

20. **Bibb, L. A., N. D. King, C. A. Kunkle, and M. P. Schmitt.** 2005. Analysis of a heme-dependent signal transduction system in *Corynebacterium diphtheriae*: deletion of the *chrAS* genes results in heme sensitivity and diminished heme-dependent activation of the *hmuO* promoter. Infect Immun **73:**7406-12.

21. **Bibb, L. A., C. A. Kunkle, and M. P. Schmitt.** 2007. The ChrA-ChrS and HrrA-HrrS Signal Transduction Systems Are Required for Activation of the *hmuO* Promoter and Repression of the hemA Promoter in *Corynebacterium diphtheriae*. Infect Immun **75:**2421-31.

22. **Blanco, A. G., M. Sola, F. X. Gomis-Ruth, and M. Coll.** 2002. Tandem DNA recognition by PhoB, a two-component signal transduction transcriptional activator. Structure **10:**701-13.

23. **Borezee, E., E. Pellegrini, J. L. Beretti, and P. Berche.** 2001. SvpA, a novel surface virulence-associated protein required for intracellular survival of *Listeria monocytogenes*. Microbiology **147:**2913-23.

24. **Borst, P., and R. O. Elferink.** 2002. Mammalian ABC transporters in health and disease. Annu Rev Biochem **71:**537-92.

25. **Brickman, T. J., C. K. Vanderpool, and S. K. Armstrong.** 2006. Heme transport contributes to in vivo fitness of *Bordetella pertussis* during primary infection in mice. Infect Immun **74:**1741-4.

26. **Bronner, S., H. Monteil, and G. Prevost.** 2004. Regulation of virulence determinants in *Staphylococcus aureus*: complexity and applications. FEMS Microbiol Rev **28:**183-200.

27. **Brucker, E. A., J. S. Olson, G. N. Phillips, Jr., Y. Dou, and M. Ikeda-Saito.** 1996. High resolution crystal structures of the deoxy, oxy, and aquomet forms of cobalt myoglobin. J Biol Chem **271:**25419-22.

28. **Brunskill, E. W., and K. W. Bayles.** 1996. Identification and molecular characterization of a putative regulatory locus that affects autolysis in *Staphylococcus aureus*. J Bacteriol **178:**611-8.

29. **Bubeck Wardenburg, J., W. A. Williams, and D. Missiakas.** 2006. Host defenses against *Staphylococcus aureus* infection require recognition of bacterial lipoproteins. Proc Natl Acad Sci U S A **103:**13831-6.

30. **Bullen, J. J., and Griffiths, E.** 1999. Iron and Infection: Molecular, Physiological and Clinical Aspects. John Wiley and Sons, New York.

31. **Cassels, R., B. Oliva, and D. Knowles.** 1995. Occurrence of the regulatory nucleotides ppGpp and pppGpp following induction of the stringent response in staphylococci. J Bacteriol **177:**5161-5.

32. **Chand, H. S., M. Drysdale, J. Lovchik, T. M. Koehler, M. F. Lipscomb, and C. R. Lyons.** 2009. Discriminating virulence mechanisms among *Bacillus anthracis* strains by using a murine subcutaneous infection model. Infect Immun **77:**429-35.

33. **Chavakis, T., M. Hussain, S. M. Kanse, G. Peters, R. G. Bretzel, J. I. Flock, M. Herrmann, and K. T. Preissner.** 2002. *Staphylococcus aureus* extracellular adherence protein serves as anti-inflammatory factor by inhibiting the recruitment of host leukocytes. Nat Med **8:**687-93.

34. **Cheung, A. L., A. S. Bayer, G. Zhang, H. Gresham, and Y. Q. Xiong.** 2004. Regulation of virulence determinants *in vitro* and *in vivo* in *Staphylococcus aureus*. FEMS Immunol Med Microbiol **40:**1-9.

35. **Chien, Y., A. C. Manna, S. J. Projan, and A. L. Cheung.** 1999. SarA, a global regulator of virulence determinants in *Staphylococcus aureus*, binds to a conserved motif essential for sar-dependent gene regulation. J Biol Chem **274:**37169-76.

36. **Clausen, V. A., W. Bae, J. Throup, M. K. Burnham, M. Rosenberg, and N. G. Wallis.** 2003. Biochemical characterization of the first essential two-component signal transduction system from *Staphylococcus aureus* and *Streptococcus pneumoniae*. J Mol Microbiol Biotechnol **5:**252-60.

37. **Cohen, S., H. M. Sweeney, and F. Leitner.** 1967. Relation between iron uptake, pH of growth medium, and penicillinase formation in *Staphylococcus aureus*. J Bacteriol **93:**1227-35.

38. **Corbin, B. D., E. H. Seeley, A. Raab, J. Feldmann, M. R. Miller, V. J. Torres, K. L. Anderson, B. M. Dattilo, P. M. Dunman, R. Gerads, R. M. Caprioli, W. Nacken, W. J. Chazin, and E. P. Skaar.** 2008. Metal Chelation and Inhibition of Bacterial Growth in Tissue Abscesses. Science **319:**962-965.

39. **Cotter, P. D., and C. Hill.** 2003. Surviving the acid test: responses of gram-positive bacteria to low pH. Microbiol Mol Biol Rev **67:**429-53, table of contents.

40. **Crosa J. H., A. R. M., and S. M. Payne. .** 2004. Iron Transport in Bacteria. A.S.M. Press, Washington, D.C.

41. **Dale, S. E., A. Doherty-Kirby, G. Lajoie, and D. E. Heinrichs.** 2004. Role of siderophore biosynthesis in virulence of *Staphylococcus aureus*: identification and characterization of genes involved in production of a siderophore. Infect Immun **72:**29-37.

42. **Davis, B. M., M. Quinones, J. Pratt, Y. Ding, and M. K. Waldor.** 2005. Characterization of the small untranslated RNA RyhB and its regulon in *Vibrio cholerae*. J Bacteriol **187:**4005-14.

43. **de Been, M., M. J. Bart, T. Abee, R. J. Siezen, and C. Francke.** 2008. The identification of response regulator-specific binding sites reveals new roles of two-component systems in *Bacillus cereus* and closely related low-GC Gram-positives. Environ Microbiol **10:**2796-809.

44. **Deiss, A.** 1983. Iron metabolism in reticuloendothelial cells. Semin Hematol **20:**81-90.

45. **Delany, I., R. Rappuoli, and V. Scarlato.** 2004. Fur functions as an activator and as a repressor of putative virulence genes in *Neisseria meningitidis*. Mol Microbiol **52:**1081-90.

46. **Dixon, T. C., M. Meselson, J. Guillemin, and P. C. Hanna.** 1999. Anthrax. N Engl J Med **341:**815-26.

47. **Drysdale, M., S. Heninger, J. Hutt, Y. Chen, C. R. Lyons, and T. M. Koehler.** 2005. Capsule synthesis by *Bacillus anthracis* is required for dissemination in murine inhalation anthrax. Embo J **24:**221-7.

48. **Dubrac, S., and T. Msadek.** 2004. Identification of genes controlled by the essential YycG/YycF two-component system of *Staphylococcus aureus*. J Bacteriol **186:**1175-81.

49. **Dubrac, S., and D. Touati.** 2000. Fur positive regulation of iron superoxide dismutase in *Escherichia coli*: functional analysis of the *sodB* promoter. J Bacteriol **182:**3802-8.

50. **Duthie, E. S., and L. L. Lorenz.** 1952. Staphylococcal coagulase; mode of action and antigenicity. J Gen Microbiol **6:**95-107.

51. **Eriksen, K. R.** 1964. Methicillin-Resistance in *Staphylococcus Aureus* Apparently Developed During Treatment with Methicillin. Acta Pathol Microbiol Scand **61:**154-5.

52. **Escolar, L., J. Perez-Martin, and V. de Lorenzo.** 1999. Opening the iron box: transcriptional metalloregulation by the Fur protein. J Bacteriol **181:**6223-9.

53. **Everse, J., and N. Hsia.** 1997. The toxicities of native and modified hemoglobins. Free Radic Biol Med **22:**1075-99.

54. **Fabret, C., and J. A. Hoch.** 1998. A two-component signal transduction system essential for growth of *Bacillus subtilis*: implications for anti-infective therapy. J Bacteriol **180:**6375-83.

55. **Fillinger, S., S. Boschi-Muller, S. Azza, E. Dervyn, G. Branlant, and S. Aymerich.** 2000. Two glyceraldehyde-3-phosphate dehydrogenases with opposite physiological roles in a nonphotosynthetic bacterium. J Biol Chem **275:**14031-7.

56. **Foster, T. J.** 2005. Immune evasion by staphylococci. Nat Rev Microbiol **3:**948-58.

57. **Fournier, B., A. Klier, and G. Rapoport.** 2001. The two-component system ArlS-ArlR is a regulator of virulence gene expression in *Staphylococcus aureus*. Mol Microbiol **41:**247-61.

58. **Francis, K. P., D. Joh, C. Bellinger-Kawahara, M. J. Hawkinson, T. F. Purchio, and P. R. Contag.** 2000. Monitoring bioluminescent *Staphylococcus aureus* infections in living mice using a novel *luxABCDE* construct. Infect Immun **68:**3594-600.

59. **Fridkin, S. K., J. C. Hageman, M. Morrison, L. T. Sanza, K. Como-Sabetti, J. A. Jernigan, K. Harriman, L. H. Harrison, R. Lynfield, and M. M. Farley.** 2005. Methicillin-resistant *Staphylococcus aureus* disease in three communities. N Engl J Med **352:**1436-44.

60. **Friedman, D. B.** 2006. Quantitative Proteomics for Two-Dimensional Gels Using Difference Gel Electrophoresis (DIGE). *In* R. Matthiesen (ed.), Mass Spectrometry Data Analysis in Proteomics. The Humana Press.

61. **Friedman, D. B., D. L. Stauff, G. Pishchany, C. W. Whitwell, V. J. Torres, and E. P. Skaar.** 2006. *Staphylococcus aureus* Redirects Central Metabolism to Increase Iron Availability. PLoS Pathog **2**.

62. **Gat, O., G. Zaide, I. Inbar, H. Grosfeld, T. Chitlaru, H. Levy, and A. Shafferman.** 2008. Characterization of *Bacillus anthracis* iron-regulated surface determinant (Isd) proteins containing NEAT domains. Mol Microbiol **70:**983-99.

63. **Gerbasi, V. R., C. M. Weaver, S. Hill, D. B. Friedman, and A. J. Link.** 2004. Yeast Asc1p and Mammalian RACK1 Are Functionally Orthologous Core 40S Ribosomal Proteins That Repress Gene Expression. Mol Cell Biol **24:**8276-87.

64. **Giraudo, A. T., A. L. Cheung, and R. Nagel.** 1997. The *sae* locus of *Staphylococcus aureus* controls exoprotein synthesis at the transcriptional level. Arch Microbiol **168:**53-8.

65. **Gladstone, G. P., and E. Walton.** 1971. The effect of iron and haematin on the killing of staphylococci by rabbit polymorphs. Br J Exp Pathol **52:**452-64.

66. **Glomski, I. J., J. P. Corre, M. Mock, and P. L. Goossens.** 2007. Noncapsulated toxinogenic *Bacillus anthracis* presents a specific growth and dissemination pattern in naive and protective antigen-immune mice. Infect Immun **75:**4754-61.

67. **Gravenkemper, C. F., J. L. Brodie, and W. M. Kirby.** 1965. Resistance of Coagulase-Positive Staphylococci to Methicillin and Oxacillin. J Bacteriol **89:**1005-10.

68. **Grebe, T. W., and J. B. Stock.** 1999. The histidine protein kinase superfamily. Adv Microb Physiol **41:**139-227.

69. **Grigg, J. C., C. L. Vermeiren, D. E. Heinrichs, and M. E. Murphy.** 2007. Haem recognition by a *Staphylococcus aureus* NEAT domain. Mol Microbiol **63:**139-49.

70. **Groisman, E. A., E. Chiao, C. J. Lipps, and F. Heffron.** 1989. *Salmonella typhimurium phoP* virulence gene is a transcriptional regulator. Proc Natl Acad Sci U S A **86:**7077-81.

71. **Grundmann, H., M. Aires-de-Sousa, J. Boyce, and E. Tiemersma.** 2006. Emergence and resurgence of methicillin-resistant *Staphylococcus aureus* as a public-health threat. Lancet **368:**874-85.

72. **He, Q. Y., A. B. Mason, and R. C. Woodworth.** 1997. Iron release from recombinant N-lobe and single point Asp63 mutants of human transferrin by EDTA. Biochem J **328 (Pt 2):**439-45.

73. **Heninger, S., M. Drysdale, J. Lovchik, J. Hutt, M. F. Lipscomb, T. M. Koehler, and C. R. Lyons.** 2006. Toxin-deficient mutants of *Bacillus anthracis* are lethal in a murine model for pulmonary anthrax. Infect Immun **74:**6067-74.

74. **Herbert, S., A. Bera, C. Nerz, D. Kraus, A. Peschel, C. Goerke, M. Meehl, A. Cheung, and F. Gotz.** 2007. Molecular basis of resistance to muramidase and cationic antimicrobial peptide activity of lysozyme in staphylococci. PLoS Pathog **3:**e102.

75. **Hess, J. F., R. B. Bourret, and M. I. Simon.** 1988. Histidine phosphorylation and phosphoryl group transfer in bacterial chemotaxis. Nature **336:**139-43.

76. **Heyningen, V.** 1948. Inhibition of aerobic sporing Bacilli by Haematin. Nature **162:**114.

77. **Hiron, A., E. Borezee-Durant, J. C. Piard, and V. Juillard.** 2007. Only one of four oligopeptide transport systems mediates nitrogen nutrition in *Staphylococcus aureus*. J Bacteriol **189:**5119-29.

78. **Holland, I. B., and M. A. Blight.** 1999. ABC-ATPases, adaptable energy generators fuelling transmembrane movement of a variety of molecules in organisms from bacteria to humans. J Mol Biol **293:**381-99.

79. **Horsburgh, M. J., M. O. Clements, H. Crossley, E. Ingham, and S. J. Foster.** 2001. PerR controls oxidative stress resistance and iron storage proteins and is required for virulence in *Staphylococcus aureus*. Infect Immun **69:**3744-54.

80. **Horsburgh, M. J., E. Ingham, and S. J. Foster.** 2001. In *Staphylococcus aureus*, Fur is an interactive regulator with PerR, contributes to virulence, and is necessary for oxidative stress resistance through positive regulation of catalase and iron homeostasis. J Bacteriol **183:**468-75.

81. **Horsburgh, M. J., S. J. Wharton, A. G. Cox, E. Ingham, S. Peacock, and S. J. Foster.** 2002. MntR modulates expression of the PerR regulon and superoxide resistance in *Staphylococcus aureus* through control of manganese uptake. Mol Microbiol **44:**1269-86.

82. **Horton, R. M., Z. L. Cai, S. N. Ho, and L. R. Pease.** 1990. Gene splicing by overlap extension: tailor-made genes using the polymerase chain reaction. Biotechniques **8:**528-35.

83. **Hrycyna, C. A., M. Ramachandra, S. V. Ambudkar, Y. H. Ko, P. L. Pedersen, I. Pastan, and M. M. Gottesman.** 1998. Mechanism of action of human P-glycoprotein ATPase activity. Photochemical cleavage during a catalytic transition state using orthovanadate reveals cross-talk between the two ATP sites. J Biol Chem **273:**16631-4.

84. **Ji, G., R. C. Beavis, and R. P. Novick.** 1995. Cell density control of staphylococcal virulence mediated by an octapeptide pheromone. Proc Natl Acad Sci U S A **92:**12055-9.

85. **Jordan, A., and P. Reichard.** 1998. Ribonucleotide reductases. Annu Rev Biochem **67:**71-98.

86. **Kern, J. W., and O. Schneewind.** 2008. BslA, a pXO1-encoded adhesin of *Bacillus anthracis*. Mol Microbiol **68:**504-15.

87. **Kernodle, D. S., R. K. Voladri, B. E. Menzies, C. C. Hager, and K. M. Edwards.** 1997. Expression of an antisense *hla* fragment in *Staphylococcus aureus* reduces alpha-toxin production in vitro and attenuates lethal activity in a murine model. Infect Immun **65:**179-84.

88. **Kim, H. S., D. Sherman, F. Johnson, and A. I. Aronson.** 2004. Characterization of a major *Bacillus anthracis* spore coat protein and its role in spore inactivation. J Bacteriol **186:**2413-7.

89. **King, N. D., A. E. Kirby, and T. D. Connell.** 2005. Transcriptional control of the *rhuIR-bhuRSTUV* heme acquisition locus in *Bordetella avium*. Infect Immun **73:**1613-24.

90. **Kirby, A. E., N. D. King, and T. D. Connell.** 2004. RhuR, an extracytoplasmic function sigma factor activator, is essential for heme-dependent expression of the outer membrane heme and hemoprotein receptor of *Bordetella avium*. Infect Immun **72:**896-907.

91. **Kirby, A. E., D. J. Metzger, E. R. Murphy, and T. D. Connell.** 2001. Heme utilization in *Bordetella avium* is regulated by RhuI, a heme-responsive extracytoplasmic function sigma factor. Infect Immun **69:**6951-61.

92. **Kirby, W. M.** 1944. Extraction of a Highly Potent Penicillin Inactivator from Penicillin Resistant Staphylococci. Science **99:**452-453.

93. **Klevens, R. M., M. A. Morrison, J. Nadle, S. Petit, K. Gershman, S. Ray, L. H. Harrison, R. Lynfield, G. Dumyati, J. M. Townes, A. S. Craig, E. R. Zell, G. E. Fosheim, L. K. McDougal, R. B. Carey, and S. K. Fridkin.** 2007. Invasive methicillin-resistant *Staphylococcus aureus* infections in the United States. Jama **298:**1763-71.

94. **Krulwich, T. A., O. Lewinson, E. Padan, and E. Bibi.** 2005. Do physiological roles foster persistence of drug/multidrug-efflux transporters? A case study. Nat Rev Microbiol **3:**566-72.

95. **Kumar, S., and U. Bandyopadhyay.** 2005. Free heme toxicity and its detoxification systems in human. Toxicol Lett **157:**175-88.

96. **Lamanna, C., and L. Jones.** 1963. Lethality for Mice of Vegetative and Spore Forms of *Bacillus Cereus* and *Bacillus Cereus*-Like Insect Pathogens Injected Intraperitoneally and Subcutaneously. J Bacteriol **85:**532-5.

97. **Lee, H. W., Y. H. Choe, D. K. Kim, S. Y. Jung, and N. G. Lee.** 2004. Proteomic analysis of a ferric uptake regulator mutant of *Helicobacter pylori*: regulation of *Helicobacter pylori* gene expression by ferric uptake regulator and iron. Proteomics **4:**2014-27.

98. **Lee, L. Y., M. Hook, D. Haviland, R. A. Wetsel, E. O. Yonter, P. Syribeys, J. Vernachio, and E. L. Brown.** 2004. Inhibition of complement activation by a secreted *Staphylococcus aureus* protein. J Infect Dis **190:**571-9.

99. **Lee, W. C., M. L. Reniere, E. P. Skaar, and M. E. Murphy.** 2008. Ruffling of metalloporphyrins bound to IsdG and IsdI, two heme-degrading enzymes in *Staphylococcus aureus*. J Biol Chem **283:**30957-63.

100. **Leighton, T. J., and R. H. Doi.** 1971. The stability of messenger ribonucleic acid during sporulation in *Bacillus subtilis*. J Biol Chem **246:**3189-95.

101. **Li, M., Y. Lai, A. E. Villaruz, D. J. Cha, D. E. Sturdevant, and M. Otto.** 2007. Gram-positive three-component antimicrobial peptide-sensing system. Proc Natl Acad Sci U S A **104:**9469-74.

102. **Lindsay, J. A., and S. J. Foster.** 2001. zur: a Zn(2+)-responsive regulatory element of *Staphylococcus aureus*. Microbiology **147:**1259-66.

103. **Lindsay, J. A., and M. T. Holden.** 2004. *Staphylococcus aureus*: superbug, super genome? Trends Microbiol **12:**378-85.

104. **Lomovskaya, O., H. I. Zgurskaya, M. Totrov, and W. J. Watkins.** 2007. Waltzing transporters and 'the dance macabre' between humans and bacteria. Nat Rev Drug Discov **6:**56-65.

105. **Loo, T. W., and D. M. Clarke.** 1994. Reconstitution of drug-stimulated ATPase activity following co-expression of each half of human P-glycoprotein as separate polypeptides. J Biol Chem **269:**7750-5.

106. **Maresso, A. W., T. J. Chapa, and O. Schneewind.** 2006. Surface protein IsdC and Sortase B are required for heme-iron scavenging of *Bacillus anthracis*. J Bacteriol **188:**8145-52.

107. **Maresso, A. W., G. Garufi, and O. Schneewind.** 2008. *Bacillus anthracis* secretes proteins that mediate heme acquisition from hemoglobin. PLoS Pathog **4:**e1000132.

108. **Marraffini, L. A., and O. Schneewind.** 2006. Targeting proteins to the cell wall of sporulating *Bacillus anthracis*. Mol Microbiol **62:**1402-17.

109. **Mascher, T., J. D. Helmann, and G. Unden.** 2006. Stimulus perception in bacterial signal-transducing histidine kinases. Microbiol Mol Biol Rev **70:**910-38.

110. **Masse, E., and S. Gottesman.** 2002. A small RNA regulates the expression of genes involved in iron metabolism in *Escherichia coli*. Proc Natl Acad Sci U S A **99:**4620-5.

111. **Masse, E., C. K. Vanderpool, and S. Gottesman.** 2005. Effect of RyhB small RNA on global iron use in *Escherichia coli*. J Bacteriol **187:**6962-71.

112. **Mazmanian, S. K., E. P. Skaar, A. H. Gaspar, M. Humayun, P. Gornicki, J. Jelenska, A. Joachmiak, D. M. Missiakas, and O. Schneewind.** 2003. Passage of heme-iron across the envelope of *Staphylococcus aureus*. Science **299:**906-9.

113. **Mazmanian, S. K., H. Ton-That, K. Su, and O. Schneewind.** 2002. An iron-regulated sortase anchors a class of surface protein during *Staphylococcus aureus* pathogenesis. Proc. Natl. Acad. Sci. USA **99:**2293-8.

114. **Meehl, M., S. Herbert, F. Gotz, and A. Cheung.** 2007. Interaction of the GraRS two-component system with the VraFG ABC transporter to support vancomycin-intermediate resistance in *Staphylococcus aureus*. Antimicrob Agents Chemother **51:**2679-89.

115. **Mey, A. R., E. E. Wyckoff, V. Kanukurthy, C. R. Fisher, and S. M. Payne.** 2005. Iron and fur regulation in *Vibrio cholerae* and the role of *fur* in virulence. Infect Immun **73:**8167-78.

116. **Miller, S. I., L. R. Hoffman, and S. Sanowar.** 2007. Did bacterial sensing of host environments evolve from sensing within microbial communities? Cell Host Microbe **1:**85-7.

117. **Miller, S. I., A. M. Kukral, and J. J. Mekalanos.** 1989. A two-component regulatory system (PhoP PhoQ) controls *Salmonella typhimurium* virulence. Proc Natl Acad Sci U S A **86:**5054-8.

118. **Mizuno, T., E. T. Wurtzel, and M. Inouye.** 1982. Osmoregulation of gene expression. II. DNA sequence of the *envZ* gene of the *ompB* operon of *Escherichia coli* and characterization of its gene product. J Biol Chem **257:**13692-8.

119. **Mock, M., and A. Fouet.** 2001. Anthrax. Annu Rev Microbiol **55:**647-71.

120. **Murphy, E. R., R. E. Sacco, A. Dickenson, D. J. Metzger, Y. Hu, P. E. Orndorff, and T. D. Connell.** 2002. BhuR, a virulence-associated outer membrane protein of *Bordetella avium*, is required for the acquisition of iron from heme and hemoproteins. Infect Immun **70:**5390-403.

121. **Nakashima, K., A. Sugiura, H. Momoi, and T. Mizuno.** 1992. Phosphotransfer signal transduction between two regulatory factors involved in the osmoregulated kdp operon in *Escherichia coli*. Mol Microbiol **6:**1777-84.

122. **Neubauer, H., I. Pantel, P. E. Lindgren, and F. Gotz.** 1999. Characterization of the molybdate transport system ModABC of *Staphylococcus carnosus*. Arch Microbiol **172:**109-15.

123. **Newton, S. M., P. E. Klebba, C. Raynaud, Y. Shao, X. Jiang, I. Dubail, C. Archer, C. Frehel, and A. Charbit.** 2005. The *svpA-srtB* locus of *Listeria monocytogenes*: fur-mediated iron regulation and effect on virulence. Mol Microbiol **55:**927-40.

124. **Novick, R. P.** 1991. Methods Enzymol. **204:**587-636.

125. **Oglesby, A. G., E. R. Murphy, V. R. Iyer, and S. M. Payne.** 2005. Fur regulates acid resistance in *Shigella flexneri* via RyhB and ydeP. Mol Microbiol **58:**1354-67.

126. **Okada, S., M. D. Rossmann, and E. B. Brown.** 1978. The effect of acid pH and citrate on the release and exchange of iron on rat transferrin. Biochim Biophys Acta **543:**72-81.

127. **Pedersen, M. B., C. Garrigues, K. Tuphile, C. Brun, K. Vido, M. Bennedsen, H. Mollgaard, P. Gaudu, and A. Gruss.** 2008. Impact of aeration and heme-activated respiration on *Lactococcus lactis* gene expression: identification of a heme-responsive operon. J Bacteriol **190:**4903-11.

128. **Pichon, C., and B. Felden.** 2005. Small RNA genes expressed from *Staphylococcus aureus* genomic and pathogenicity islands with specific expression among pathogenic strains. Proc Natl Acad Sci U S A **102:**14249-54.

129. **Piddock, L. J.** 2006. Multidrug-resistance efflux pumps - not just for resistance. Nat Rev Microbiol **4:**629-36.

130. **Pohl, A., P. F. Devaux, and A. Herrmann.** 2005. Function of prokaryotic and eukaryotic ABC proteins in lipid transport. Biochim Biophys Acta **1733:**29-52.

131. **Prat, C., J. Bestebroer, C. J. de Haas, J. A. van Strijp, and K. P. van Kessel.** 2006. A new staphylococcal anti-inflammatory protein that antagonizes the formyl peptide receptor-like 1. J Immunol **177:**8017-26.

132. **Recsei, P., B. Kreiswirth, M. O'Reilly, P. Schlievert, A. Gruss, and R. P. Novick.** 1986. Regulation of exoprotein gene expression in *Staphylococcus aureus* by Agr. Mol Gen Genet **202:**58-61.

133. **Reniere, M. L., and E. P. Skaar.** 2008. *Staphylococcus aureus* haem oxygenases are differentially regulated by iron and haem. Mol Microbiol **69:**1304-15.

134. **Reniere, M. L., V. J. Torres, and E. P. Skaar.** 2007. Intracellular metalloporphyrin metabolism in *Staphylococcus aureus*. Biometals **20:**333-45.

135. **Richardson, A. R., P. M. Dunman, and F. C. Fang.** 2006. The nitrosative stress response of *Staphylococcus aureus* is required for resistance to innate immunity. Mol Microbiol **61:**927-39.

136. **Richardson, A. R., S. J. Libby, and F. C. Fang.** 2008. A nitric oxide-inducible lactate dehydrogenase enables *Staphylococcus aureus* to resist innate immunity. Science **319:**1672-6.

137. **Rietkotter, E., D. Hoyer, and T. Mascher.** 2008. Bacitracin sensing in *Bacillus subtilis*. Mol Microbiol **68:**768-85.

138. **Sambrook, J., Fritsch, E.F., and Maniatis, T.** 1989. Molecular Cloning: A laboratory Manual, 2nd ed. Cold Spring Harbor Press, Cold Spring Harbor.

139. **Schenk, S., and R. A. Laddaga.** 1992. Improved method for electroporation of *Staphylococcus aureus*. FEMS Microbiol Lett **73:**133-8.

140. **Schmitt, M. P.** 1999. Identification of a two-component signal transduction system from *Corynebacterium diphtheriae* that activates gene expression in response to the presence of heme and hemoglobin. J Bacteriol **181:**5330-40.

141. **Schmitt, M. P.** 1997. Transcription of the *Corynebacterium diphtheriae hmuO* gene is regulated by iron and heme. Infect Immun **65:**4634-41.

142. **Schmitt, M. P.** 1997. Utilization of host iron sources by *Corynebacterium diphtheriae*: identification of a gene whose product is homologous to eukaryotic heme oxygenases and is required for acquisition of iron from heme and hemoglobin. J. Bacteriol. **179:**838-45.

143. **Schneewind, O., P. Model, and V. A. Fischetti.** 1992. Sorting of protein A to the staphylococcal cell wall. Cell **70:**267-81.

144. **Schneider, E., and S. Hunke.** 1998. ATP-binding-cassette (ABC) transport systems: functional and structural aspects of the ATP-hydrolyzing subunits/domains. FEMS Microbiol Rev **22:**1-20.

145. **Sebulsky, M. T., D. Hohnstein, M. D. Hunter, and D. E. Heinrichs.** 2000. Identification and characterization of a membrane permease involved in iron-hydroxamate transport in *Staphylococcus aureus*. J Bacteriol **182:**4394-400.

146. **Senior, A. E., M. K. al-Shawi, and I. L. Urbatsch.** 1995. The catalytic cycle of P-glycoprotein. FEBS Lett **377:**285-9.

147. **Shannon, J. G., C. L. Ross, T. M. Koehler, and R. F. Rest.** 2003. Characterization of anthrolysin O, the *Bacillus anthracis* cholesterol-dependent cytolysin. Infect Immun **71:**3183-9.

148. **Skaar, E. P., A. H. Gaspar, and O. Schneewind.** 2006. *Bacillus anthracis* IsdG, a heme-degrading monooxygenase. J Bacteriol **188:**1071-80.

149. **Skaar, E. P., A. H. Gaspar, and O. Schneewind.** 2004. IsdG and IsdI, heme-degrading enzymes in the cytoplasm of *Staphylococcus aureus*. J Biol Chem **279:**436-43.

150. **Skaar, E. P., M. Humayun, T. Bae, K. L. DeBord, and O. Schneewind.** 2004. Iron-source preference of *Staphylococcus aureus* infections. Science **305:**1626-8.

151. **Skaar, E. P., and O. Schneewind.** 2004. Iron-regulated surface determinants (Isd) of *Staphylococcus aureus*: stealing iron from heme. Microbes Infect **6:**390-7.

152. **Somerville, G. A., M. S. Chaussee, C. I. Morgan, J. R. Fitzgerald, D. W. Dorward, L. J. Reitzer, and J. M. Musser.** 2002. *Staphylococcus aureus* aconitase inactivation unexpectedly inhibits post-exponential-phase growth and enhances stationary-phase survival. Infect Immun **70:**6373-82.

153. **Somerville, G. A., A. Cockayne, M. Durr, A. Peschel, M. Otto, and J. M. Musser.** 2003. Synthesis and deformylation of *Staphylococcus aureus* delta-toxin are linked to tricarboxylic acid cycle activity. J Bacteriol **185:**6686-94.

154. **Somerville, G. A., B. Said-Salim, J. M. Wickman, S. J. Raffel, B. N. Kreiswirth, and J. M. Musser.** 2003. Correlation of acetate catabolism and growth yield in *Staphylococcus aureus*: implications for host-pathogen interactions. Infect Immun **71:**4724-32.

155. **Speziali, C. D., S. E. Dale, J. A. Henderson, E. D. Vines, and D. E. Heinrichs.** 2006. Requirement of *Staphylococcus aureus* ATP-binding cassette-ATPase FhuC for iron-restricted growth and evidence that it functions with more than one iron transporter. J Bacteriol **188:**2048-55.

156. **Stauff, D. L., D. Bagaley, V. J. Torres, R. Joyce, K. L. Anderson, L. Kuechenmeister, P. M. Dunman, and E. P. Skaar.** 2008. *Staphylococcus*

aureus HrtA is an ATPase required for protection against heme toxicity and prevention of a transcriptional heme stress response. J Bacteriol **190:**3588-96.

157. **Stauff, D. L., and E. P. Skaar.** 2008. The heme sensor system (HssRS) of *Staphylococcus aureus*. Contributions to Microbiology **In Press**.

158. **Stauff, D. L., V. J. Torres, and E. P. Skaar.** 2007. Signaling and DNA-binding Activities of the *Staphylococcus aureus* HssR-HssS Two-component System Required for Heme Sensing. J Biol Chem **282:**26111-26121.

159. **Sterne, M.** 1937. Avirulent anthrax vaccine. Onderstepoort J Vet Sci Animal Ind **21:**41–43.

160. **Stock, A. M., J. M. Mottonen, J. B. Stock, and C. E. Schutt.** 1989. Three-dimensional structure of CheY, the response regulator of bacterial chemotaxis. Nature **337:**745-9.

161. **Stojiljkovic, I., B. D. Evavold, and V. Kumar.** 2001. Antimicrobial properties of porphyrins. Expert Opin. Investig. Drugs **10:**309-20.

162. **Stojiljkovic, I., V. Kumar, and N. Srinivasan.** 1999. Non-iron metalloporphyrins: potent antibacterial compounds that exploit haem/Hb uptake systems of pathogenic bacteria. Mol Microbiol **31:**429-42.

163. **Tatsumi, R., and M. Wachi.** 2008. TolC-dependent exclusion of porphyrins in *Escherichia coli*. J Bacteriol **190:**6228-33.

164. **Taylor, R. K., M. N. Hall, L. Enquist, and T. J. Silhavy.** 1981. Identification of OmpR: a positive regulatory protein controlling expression of the major outer membrane matrix porin proteins of *Escherichia coli* K-12. J Bacteriol **147:**255-8.

165. **Theodore, T. S., and A. L. Schade.** 1965. Carbohydrate metabolism of iron-rich and iron-poor *Staphylococcus aureus*. J Gen Microbiol **40:**385-95.

166. **Throup, J. P., F. Zappacosta, R. D. Lunsford, R. S. Annan, S. A. Carr, J. T. Lonsdale, A. P. Bryant, D. McDevitt, M. Rosenberg, and M. K. Burnham.** 2001. The *srhSR* gene pair from *Staphylococcus aureus*: genomic and proteomic approaches to the identification and characterization of gene function. Biochemistry **40:**10392-401.

167. **Todd, B.** 2006. Beyond MRSA: VISA and VRSA: what will ward off these pathogens in health care facilities? Am J Nurs **106:**28-30.

168. **Torres, V. J., G. Pishchany, M. Humayun, O. Schneewind, and E. P. Skaar.** 2006. *Staphylococcus aureus* IsdB is a hemoglobin receptor required for heme iron utilization. J Bacteriol **188:**8421-9.

169. **Torres, V. J., D. L. Stauff, G. Pishchany, J. S. Bezbradica, L. E. Gordy, J. Iturregui, K. L. Anderson, P. Dunman, S. Joyce, and E. P. Skaar.** 2007. A *Staphylococcus aureus* Regulatory System that Responds to Host Heme and Modulates Virulence. Cell Host & Microbe **1:**109-119.

170. **Ubukata, K., N. Itoh-Yamashita, and M. Konno.** 1989. Cloning and expression of the *norA* gene for fluoroquinolone resistance in *Staphylococcus aureus*. Antimicrob Agents Chemother **33:**1535-9.

171. **Vanderpool, C. K., and S. K. Armstrong.** 2001. The *Bordetella bhu* locus is required for heme iron utilization. J Bacteriol **183:**4278-87.

172. **Vanderpool, C. K., and S. K. Armstrong.** 2003. Heme-responsive transcriptional activation of *Bordetella bhu* genes. J Bacteriol **185:**909-17.

173. **Walderhaug, M. O., J. W. Polarek, P. Voelkner, J. M. Daniel, J. E. Hesse, K. Altendorf, and W. Epstein.** 1992. KdpD and KdpE, proteins that control expression of the *kdpABC* operon, are members of the two-component sensor-effector class of regulators. J Bacteriol **174:**2152-9.

174. **Walker, J. E., M. Saraste, M. J. Runswick, and N. J. Gay.** 1982. Distantly related sequences in the alpha- and beta-subunits of ATP synthase, myosin, kinases and other ATP-requiring enzymes and a common nucleotide binding fold. Embo J **1:**945-51.

175. **Watts, C. J., B. L. Hahn, and P. G. Sohnle.** 2009. Resistance of Athymic Nude Mice to Experimental Cutaneous *Bacillus anthracis* Infection. J Infect Dis.

176. **Weiner, M. P., G. L. Costa, W. Schoettlin, J. Cline, E. Mathur, and J. C. Bauer.** 1994. Site-directed mutagenesis of double-stranded DNA by the polymerase chain reaction. Gene **151:**119-23.

177. **Welkos, S. L., T. J. Keener, and P. H. Gibbs.** 1986. Differences in susceptibility of inbred mice to *Bacillus anthracis*. Infect Immun **51:**795-800.

178. **Wertheim, H. F., M. C. Vos, A. Ott, A. van Belkum, A. Voss, J. A. Kluytmans, P. H. van Keulen, C. M. Vandenbroucke-Grauls, M. H. Meester, and H. A. Verbrugh.** 2004. Risk and outcome of nosocomial *Staphylococcus aureus* bacteraemia in nasal carriers versus non-carriers. Lancet **364:**703-5.

179. **Wessel, D., and U. I. Flugge.** 1984. A method for the quantitative recovery of protein in dilute solution in the presence of detergents and lipids. Anal Biochem **138:**141-3.

180. **Wilderman, P. J., N. A. Sowa, D. J. FitzGerald, P. C. FitzGerald, S. Gottesman, U. A. Ochsner, and M. L. Vasil.** 2004. Identification of tandem duplicate regulatory small RNAs in *Pseudomonas aeruginosa* involved in iron homeostasis. Proc Natl Acad Sci U S A **101:**9792-7.

181. **Williams, R. J., J. M. Ward, B. Henderson, S. Poole, B. P. O'Hara, M. Wilson, and S. P. Nair.** 2000. Identification of a novel gene cluster encoding staphylococcal exotoxin-like proteins: characterization of the prototypic gene and its protein product, SET1. Infect Immun **68:**4407-15.

182. **Wu, R., E. P. Skaar, R. Zhang, G. Joachimiak, P. Gornicki, O. Schneewind, and A. Joachimiak.** 2005. *Staphylococcus aureus* IsdG and IsdI, heme-degrading enzymes with structural similarity to monooxygenases. J Biol Chem **280:**2840-6.

183. **Xiong, A., V. K. Singh, G. Cabrera, and R. K. Jayaswal.** 2000. Molecular characterization of the ferric-uptake regulator, *fur*, from *Staphylococcus aureus*. Microbiology **146 (Pt 3):**659-68.

184. **Yarwood, J. M., J. K. McCormick, and P. M. Schlievert.** 2001. Identification of a novel two-component regulatory system that acts in global regulation of virulence factors of *Staphylococcus aureus*. J Bacteriol **183:**1113-23.

185. **Yoshida, H., M. Bogaki, S. Nakamura, K. Ubukata, and M. Konno.** 1990. Nucleotide sequence and characterization of the *Staphylococcus aureus norA* gene, which confers resistance to quinolones. J Bacteriol **172:**6942-9.

186. **Young, J., and I. B. Holland.** 1999. ABC transporters: bacterial exporters-revisited five years on. Biochim Biophys Acta **1461:**177-200.

187. **Zhu, H., G. Xie, M. Liu, J. S. Olson, M. Fabian, D. M. Dooley, and B. Lei.** 2008. Pathway for heme uptake from human methemoglobin by the iron-regulated surface determinants system of *Staphylococcus aureus*. J Biol Chem **283:**18450-60.

188. **Ziegler, J., R. Linck, and D. W. Wright.** 2001. Heme Aggregation inhibitors: antimalarial drugs targeting an essential biomineralization process. Curr Med Chem **8:**171-89.